

Madeleine Anna Ehweiner, BSc

**ACTIVE SITE MODELING OF THE ENZYME
ACETYLENE HYDRATASE**
**Studies towards Complexes Employing the Tripodal Ligand
Phenyltris((methylthio)methyl)borate**

MASTERARBEIT

zur Erlangung des akademischen Grades

Master of Science

Masterstudium Chemie

eingereicht an der

Technischen Universität Graz

Betreuerin

Univ.-Prof. Dipl.-Chem. Dr.rer.nat. Nadia Carmen Mösch-Zanetti

Institut für Chemie

Bereich Anorganische Chemie

EIDESSTATTLICHE ERKLÄRUNG

Ich erkläre an Eides statt, dass ich die vorliegende Arbeit selbstständig verfasst, andere als die angegebenen Quellen/Hilfsmittel nicht benutzt, und die den benutzten Quellen wörtlich und inhaltlich entnommenen Stellen als solche kenntlich gemacht habe. Das in TUGRAZonline hochgeladene Textdokument ist mit der vorliegenden Masterarbeit identisch.

05.09.2017

Datum

A handwritten signature in blue ink, appearing to read 'G. Elmer', written above a horizontal line.

Unterschrift

Dans les champs de l'observation le hasard ne favorise que les esprits préparés.

(Louis Pasteur, 1822–1895)

ACKNOWLEDGEMENT

First of all, I would like to thank my supervisor Univ.-Prof. Dr. Mösch-Zanetti for offering me the opportunity to do my master thesis in her research group, providing me an extremely interesting, novel project, a convenient atmosphere and an excellent equipment in the lab. Most importantly, I would like to express my particular gratitude to the good-hearted head of “team tungsten”, Carina, who showed me all essential techniques in synthetic chemistry, shared nearly all her knowledge and experience with me and always had an open ear for my synthetic, chemical or personal difficulties. It surely was not always a pleasure to share a lab and even an office with me, but I am genuinely grateful for your kindness and all your efforts. Furthermore, I want to thank the temporary member of “team tungsten”, Miljan Čorovič, for always bringing good mood to the lab, making me laugh and providing me with advice and assistance not only in the field of chemistry. It was a genuine pleasure to work with you. I also want to thank Niklas for showing me lots of essential techniques and methods and teaching me how to work and think independently, and Ass.-Prof. Dr. Jörg Schachner for frequently providing me with advice and assistance and amusing me with interesting discussions. Moreover, I would like to express my gratitude to our unique lab technicians Doris, Nathalie and Alex for taking care of chemicals, solvents, glassware and NMR samples to be measured. I also want to thank Ao.Univ.-Prof. Dr. Ferdinand Belaj for solving all my crystal structures and Ing. Bernd Werner for measuring countless NMR samples. Besides, I would like to thank the other group members Stefan, Simon, Antoine, Mike, Melanie and Michi for providing me with advice and keeping me company after some long days in the lab. Furthermore, I want to thank my beloved parents and my sister for supporting me whenever and wherever they can, but especially my mum for always having an open ear for my little problems and euphorically participating in every telephone conversation on my way home from university. You really mean a lot to me. I also would like to express my gratitude to my dearest boyfriend who cares for me like no other person would ever be able to. I truly appreciate the time spent together after working in the lab or writing my thesis and enjoy our discussions about every imaginable subject. You always cheered me up when I was desperately looking for results for my project and encouraged me after a rough day in the lab. Last but not least, I want to thank my dearest friends of the “Stadtkapelle Trofaiach” for bringing loads of fun and music into my life.

ABSTRACT

The active site of the tungstoenzyme acetylene hydratase, which catalyzes the hydration of acetylene to acetaldehyde, was modeled in order to gain insight into the mechanism of this unique enzyme. A synthetic approach for a series of oxotungsten(IV) alkyne complexes employing the bioinspired scorpionate ligand phenyltris((methylthio)methyl)borate ([PhTt]) has been investigated. Therefore, two different synthetic methods – “ligand addition” and “alkyne addition” – were applied to get access to the desired complexes $[\text{WBr}(\eta^2\text{-C}_2\text{R}_2)(\text{PhTt})]$ ($\text{R} = \text{H}, \text{Me}, \text{Ph}$). For the “ligand addition” method, the tungsten(II) bis(alkyne) precursors $[\text{WBr}_2(\text{CO})(\eta^2\text{-C}_2\text{R}_2)_2(\text{NCMe})]$ ($\text{R} = \text{H}$ (**8**), Me (**9**), Ph (**10**)) were utilized. Entry point for the “alkyne addition” method was the novel complex $[\text{WBr}(\text{CO})_3(\text{PhTt})]$ (**11**). The even more sulfur-rich complex $[\text{W}(\text{CO})_2(\text{mt})(\text{PhTt})]$ (**13**) was synthesized from complex **11** and subsequently investigated regarding the coordination of the symmetric alkynes acetylene, 2-butyne and diphenylacetylene. Additionally, the novel complex $[\text{WBr}(\text{CO})_2(\eta^2\text{-CH}_2\text{SCH}_3)(\text{PhTt})]$ (**12**) could be isolated. Complexes **11**, **12** and **13** were fully characterized including NMR and IR spectroscopy and molecular structures. The synthesis of all tungsten(II) complexes started from the literature-known dimer $[\text{W}_2\text{Br}_4(\text{CO})_7]$ (**6**) which was cleaved by acetonitrile to give the monomer $[\text{WBr}_2(\text{CO})_3(\text{NCMe})_2]$ (**7**).

Synthesis via the “alkyne addition” method suffered from poor selectivity. The formation of a tungsten(II) acetylene complex was confirmed by ^1H NMR spectroscopy for both **11** and **13**, however, no complex could be isolated so far. Coordination of 2-butyne or diphenylacetylene could not be confirmed by means of NMR spectroscopy.

Synthesis of the desired complexes $[\text{WBr}(\text{CO})(\eta^2\text{-C}_2\text{R}_2)(\text{PhTt})]$ ($\text{R} = \text{H}, \text{Me}, \text{Ph}$) via the “ligand addition” route led to the isolation of $[\text{WBr}(\text{CO})(\eta^2\text{-C}_2\text{R}_2)_2(\text{PhTt-S,S'})]$ ($\text{R} = \text{Me}$ (**14**), Ph (**15**)), with the ligand phenyltris((methylthio)methyl)borate coordinated only via two sulfur atoms. After reaction of precursor **8** with [PhTt], no complex could be isolated as the reaction suffered from poor selectivity, similar to the “alkyne addition” method.

ZUSAMMENFASSUNG

Das aktive Zentrum des Wolfram-Enzyms Acetylen-Hydratase, welches die Hydratation von Acetylen zu Acetaldehyd katalysiert, wurde modelliert, um einen tieferen Einblick in den Reaktionsmechanismus dieses einzigartigen Enzyms zu bekommen. Ein Konzept zur Synthese von Oxido-Wolfram(IV)-Alkin-Komplexen, welche den bioinspirierten Skorpionat-Liganden Phenyltris((methylthio)methyl)borat ([PhTt]) enthalten, wurde untersucht. Um Zugang zu den gewünschten Verbindungen $[\text{WBr}(\eta^2\text{-C}_2\text{R}_2)(\text{PhTt})]$ ($\text{R} = \text{H}, \text{Me}, \text{Ph}$) zu bekommen, wurden die synthetischen Methoden der „Liganden-Addition“ und der „Alkin-Addition“ untersucht. Für die Methode der „Liganden-Addition“ wurden die Wolfram(II)-Komplexe $[\text{WBr}_2(\text{CO})(\eta^2\text{-C}_2\text{R}_2)_2(\text{NCMe})]$ ($\text{R} = \text{H}$ (**8**), Me (**9**), Ph (**10**)) hergestellt und verwendet. Den Eintrittspunkt für die „Alkin-Addition“ stellte der Komplex $[\text{WBr}(\text{CO})_3(\text{PhTt})]$ (**11**) dar. Der schwefelreichere, neuartige Komplex $[\text{W}(\text{CO})_2(\text{mt})(\text{PhTt})]$ (**13**) wurde durch die Reaktion von **11** mit $\text{Na}(\text{mt})$ (**4**) hergestellt und anschließend ebenfalls bezüglich der Koordination der symmetrischen Alkine Acetylen, 2-Butin und Diphenylacetylen untersucht. Außerdem konnte die Verbindung $[\text{WBr}(\text{CO})_2(\eta^2\text{-CH}_2\text{SCH}_3)(\text{PhTt})]$ (**12**) isoliert und kristallisiert werden. Die Komplexe **11**, **12** und **13** wurden vollständig charakterisiert. Die Synthese aller Wolfram(II)-Komplexe erfolgte ausgehend vom literaturbekannten Dimer $[\text{W}_2\text{Br}_4(\text{CO})_7]$ (**6**), welches mittels Acetonitril zum Monomer $[\text{WBr}_2(\text{CO})_3(\text{NCMe})_2]$ (**7**) gespalten wurde.

Die Synthese über die Methode der „Alkin-Addition“ verlief wenig selektiv. Die Bildung eines Wolfram(II)-Acetylen-Komplexes wurde zwar mit Hilfe von $^1\text{H-NMR}$ -Spektroskopie sowohl für **11** als auch **13** bestätigt, allerdings konnte bisher kein Komplex isoliert werden. Die Koordination der Alkine 2-Butin und Diphenylacetylen konnte nicht beobachtet werden.

Die Synthese der gewünschten Komplexe $[\text{WBr}(\text{CO})(\eta^2\text{-C}_2\text{R}_2)(\text{PhTt})]$ ($\text{R} = \text{H}, \text{Me}, \text{Ph}$) über den Weg der „Liganden-Addition“ führte zur Isolierung der Verbindungen $[\text{WBr}(\text{CO})(\eta^2\text{-C}_2\text{R}_2)_2(\text{PhTt-S,S'})]$ ($\text{R} = \text{Me}$ (**14**), Ph (**15**)), wobei der tridentate Ligand Phenyltris((methylthio)methyl)borat nur über zwei Schwefel-Atome an das Wolfram-Zentrum koordiniert ist. Die Reaktion von $[\text{WBr}(\text{CO})(\eta^2\text{-C}_2\text{H}_2)_2(\text{NCMe})]$ mit [PhTt] verlief wie bei der Methode der „Alkin-Addition“ wenig selektiv.

TABLE OF CONTENTS

I	INTRODUCTION.....	1
1	CLASSIFICATION OF TUNGSTOENZYMES.....	2
1.1	AOR Family	3
1.2	BCR Family.....	3
1.3	FDH Family.....	4
1.4	FMDH Family.....	5
1.5	AH Family	5
2	ACETYLENE HYDRATASE.....	6
2.1	Microorganisms Utilizing Acetylene	6
2.2	Molecular Properties of AH.....	7
2.3	Structure and Active Site of AH	8
2.4	Mechanism of AH	11
2.4.1	Second Shell Mechanism	12
2.4.2	First Shell Mechanism	12
3	MODELING CHEMISTRY OF TUNGSTEN	14
3.1	Dithiolene Ligands	15
3.1.1	Functional Models	17
3.2	Non-dithiolene Ligands	18
3.2.1	Scorpionate Ligands.....	19
3.2.1.1	Tungsten(II) Alkyne Complexes with Soft Scorpionate Ligands ...	20
3.2.2	Thioether Ligands.....	21
3.2.2.1	Tungsten(II) Alkyne Complexes with Thioether Ligands	22
3.2.3	Poly(thioether)borate Scorpionate Ligands.....	23
4	TUNGSTEN ACETYLENE COMPLEXES.....	25
4.1	Bonding Situation in Carbonyl Tungsten(II) Acetylene Complexes.....	26
4.1.1	Examples of Tungsten(II) Acetylene Complexes	28

4.2	Bonding Situation in Oxotungsten(IV) Acetylene Complexes	30
4.2.1	Examples of Tungsten(IV) Acetylene Complexes.....	31
5	OBJECTIVES.....	33
II	RESULTS AND DISCUSSION	35
1	LIGAND SYNTHESIS	35
1.1	[Bu ₄ N][PhTt].....	35
1.2	Cs[PhTt].....	37
1.3	Cs[PhTt ^{tBu}].....	37
2	PRECURSOR SYNTHESIS.....	38
2.1	[WBr ₂ (CO) ₃ (NCMe) ₂]	38
2.2	[WBr ₂ (CO)(η ² -C ₂ R ₂) ₂ (NCMe)]	39
3	COMPLEX SYNTHESIS	41
3.1	[WBr(CO) ₃ (PhTt)].....	41
3.2	[WBr(CO) ₂ (η ² -CH ₂ SCH ₃)(PhTt)].....	45
3.3	[W(CO) ₂ (mt)(PhTt)].....	48
3.4	Attempted Synthesis of [W(CO) ₃ (PhTt)(S ^{tBu})]	51
3.5	Attempted Synthesis of [WBr(CO) ₃ (PhTt ^{tBu})]	52
4	TUNGSTEN ALKYNE COMPLEXES.....	53
4.1	Ligand Addition Method	53
4.1.1	Attempted Synthesis of [WBr(CO)(η ² -C ₂ H ₂)(PhTt)].....	53
4.1.2	Attempted Synthesis of [WBr(CO)(η ² -C ₂ H ₂)(PhTt ^{tBu})].....	54
4.1.3	Synthesis of [WBr(CO)(η ² -C ₂ Me ₂) ₂ (PhTt-S,S')]	55
4.1.4	Synthesis of [WBr(CO)(η ² -C ₂ Ph ₂) ₂ (PhTt-S,S')].....	60
4.2	Alkyne Addition Method	61
4.2.1	Attempted Synthesis of [WBr(CO)(η ² -C ₂ R ₂)(PhTt)].....	61
4.2.2	Attempted Synthesis of [W(η ² -C ₂ R ₂)(mt)(PhTt)].....	63
III	CONCLUSION	64
IV	EXPERIMENTAL SECTION.....	66

1	GENERAL METHODS.....	66
2	LIGAND SYNTHESIS	67
3	PRECURSOR SYNTHESIS.....	69
4	COMPLEX SYNTHESIS.....	71
V	REFERENCES.....	74
VI	APPENDIX	80

LIST OF ABBREVIATIONS

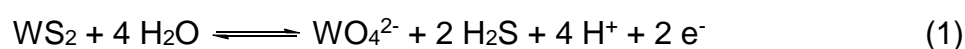
3PG	3-Phosphoglyceric acid
ADH	Aldehyde dehydrogenase
AH	Acetylene hydratase
AO	Atomic orbital
AOR	Aldehyde ferredoxin oxidoreductase
ATP	Adenosine triphosphate
ATR	Attenuated total reflection
Asp	Aspartate
bdt	1,2-Benzenedithiolate
CAR	Carboxylic acid reductase
Cys	Cysteine
DFT	Density functional theory
DMSOR	DMSO reductase
dppe	1,2-Bis(diphenylphosphino)ethane
EDG	Electron donating group
EPR	Electron paramagnetic resonance
equiv.	Equivalents
FDH	Formate dehydrogenase
FMDH	Formyl methanofuran dehydrogenase
FOR	Ferredoxin oxidoreductase
FT	Fourier transform
GAP	Glyceraldehyde 3-phosphate
GAPOR	Glyceraldehyde 3-phosphate ferredoxin oxidoreductase
GDP	Guanosine diphosphate
GMP	Guanosine monophosphate
HOMO	Highest occupied molecular orbital
HSAB	Hard and soft (Lewis) acids and bases
Ile	Isoleucine
IR	Infrared radiation
L	Ligand
LUMO	Lowest unoccupied molecular orbital
Lys	Lysine

MA	Maleic anhydride
MALDI	Matrix-assisted laser desorption/ionization
mdt	1,2-Methyl-1,2-dithiolate
MFR	Methanofuran
MCD	Molybdopterin cytosine dinucleotide
MGD	Molybdopterin guanine dinucleotide
MPT	Molybdopterin
min	Minutes
MM	Molecular mechanics
mnt	1,2-Maleonitrile-1,2-dithiolate
MO	Molecular orbital
MS	Mass spectrometry
mt	Methimazolyl
NADP(H)	Nicotinamide adenine dinucleotide phosphate
NMR	Nuclear magnetic resonance
OAT	Oxygen atom transfer
OTf	Triflate
PhTt	Phenyltris((methylthio)methyl)borate
PhTt ^{Ad}	Phenyltris(1-adamantyl(thiomethyl))borate
PhTt ^{Ph}	Phenyltris((phenylthio)methyl)borate
PhTt ^{p-Tol}	Phenyltris((4-methylphenylthio)methyl)borate
PhTt ^{tBu}	Phenyltris(<i>tert</i> -butylthio)methyl)borate
pz	Pyrazolyl
RTt	Tetra((methylthio)methyl)borate
QM	Quantum mechanics
rt	Room temperature
SO	Sulfite oxidase
S-Phoz	2-(4,4-Dimethyl-4,5-dihydrooxazol-2-yl)benzenethiol
TBHP	<i>tert</i> -Butyl hydroperoxide
TMEDA	Tetramethylethylenediamine
Tm ^{Me}	Hydrotris(methimazolyl)borate
Tn ^{Me,tBu}	Hydrotris(4-methyl-6- <i>tert</i> -butyl-3-thiopyridazinyl)borate
Tp	Hydrotris(pyrazolyl)borate
Tp'	Hydrotris(3,5-dimethyl-pyrazolyl)borate

Tr ^{Me}	Hydrotris(3-mercapto-4-methyl-1,2,4-triazolyl)borate
Trp	Tryptophane
ttmb	2,5,8-Trithia[9]- <i>m</i> -benzenophane
ttob	2,5,8-Trithia[9]- <i>o</i> -benzenophane
ttn	2,5,8-Trithianonane

I INTRODUCTION

Knowledge that the fairly heavy element tungsten would play a role in biological systems was not gained until the early 1970s, when scientists were able to show that the growth of certain microorganisms is stimulated by the addition of tungstate to their growth media.^{1,2} However, it was a decade later before NADPH-dependent formate dehydrogenase from *Clostridium thermoaceticum* – the first tungsten-containing protein – was purified and characterized.³ So far, 18 different tungstoenzymes have been isolated and purified. However, a biological function of tungsten has not yet been found in any eukaryote.⁴ With an atomic number of 74, tungsten is a very unusual biologically relevant metal, as most of the elements bearing a biological function exhibit an atomic number below 35. However, there are a few exceptions worth mentioning: Whereas molybdenum (Mo, 42) and iodine (I, 53) are fairly widespread elements in biology, strontium (Sr, 38), niobium (Nb, 41), barium (Ba, 56) and tantalum (Ta, 73) are required only by a few organisms.² In contrast to tungsten, the biological importance of the chemically similar molybdenum has been known for over 80 years. Molybdoenzymes are ubiquitous in nature and play an essential role in the global cycles of nitrogen, carbon and sulfur.⁵ Nevertheless, Mo and W have similar atomic radii and electronegativities, and their behavior in coordination chemistry is comparable. This explains why tungsten traditionally has been regarded as a potent antagonist of biologically used molybdenum. Although the chemistry of both elements is varied and complex because of the range of possible oxidation states (-II to +VI) and their moderate preference for polynuclear complexes, only mononuclear species in the oxidation states +IV, +V and +VI have been identified in biological systems so far.^{2,5,6} Both Mo and W are quite scarce, as they rank only 53rd and 54th, respectively, in the abundance of the elements on earth. Usually, sources of tungsten are oxo-rich tungstate minerals like scheelite (CaWO₄) and wolframite ((Fe,Mn)WO₄), whereas more reduced tungstenite minerals like WS₂ are fairly rare as they are readily solubilized according to Equation 1.⁷



Given the hot, anaerobic conditions under which life probably arose, tungsten might have been the first of those two similar elements to be acquired by living organisms. For example, tungsten-sulfur bonds, such as those found in all tungsten-containing

enzymes, are more stable than their molybdenum counterparts, which can be explained by the HSAB concept.^{8,9} In freshwater environments and sea water, W is generally much less abundant than Mo. However, tungsten is present in significant amounts (> 50 nM) in four types of natural waters: in groundwater associated with W-containing ore deposits, in alkaline, nitrogenous fissure-vein thermal waters of crystalline rocks, in alkaline waters of lakes in arid zones and in hot-spring waters and hydrothermal vents.^{2,8} The highest values observed are more than 0.27 mM in the highly concentrated brines of Searles Lake, California.¹⁰

1 CLASSIFICATION OF TUNGSTOENZYMES

With the exception of nitrogenase and related proteins, the active site of all tungsto- and molybdoenzymes which have been described to date, contains a pyranopterin-dithiolene cofactor in which the metal is coordinated by the dithiolene moiety.^{9,11,12} This cofactor is commonly called molybdopterin and refers to the cofactor without any molybdenum or tungsten bound. The term molybdopterin was coined before the importance of the tungstoenzymes was even realized (Figure 1).¹²

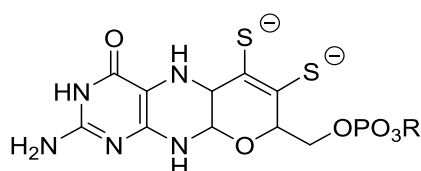


Figure 1: Structure of the molybdopterin cofactor with R being H (MPT), guanosine (MGD) or cytosine (MCD).¹¹

Generally, the active site of all tungstoenzymes harbours one tungsten atom coordinated by four sulfur atoms deriving from two molybdopterin cofactors plus oxygen and/or sulfur and/or selenium ligands.¹³ Tungstoenzymes can be classified according to their amino acid sequence, their active site structure or the reaction they catalyze. Considering their tertiary structure, tungstoenzymes can be divided into two families, which are the dimethyl sulfoxide reductase (DMSOR) family and the aldehyde ferredoxin oxidoreductase (AOR) family. The DMSOR family of tungstoenzymes includes formate dehydrogenases (FDH) from obligately anaerobic microorganisms, formyl methanofuran dehydrogenases (FMDH) and acetylene hydratase (AH) from strictly anaerobic bacteria, whereas the AOR family comprises AORs from hyperthermophilic archaea and mesophilic bacteria and the recently

identified class II benzoyl-CoA reductases (BCR) from strictly anaerobic bacteria.^{13,14,14} Members of both families differ in terms of their active site and the chemical reaction they catalyze (Figure 2).¹⁵

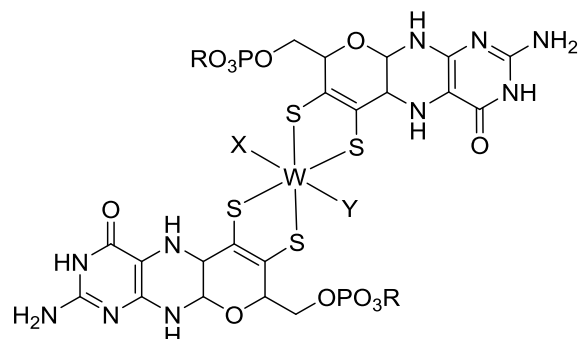
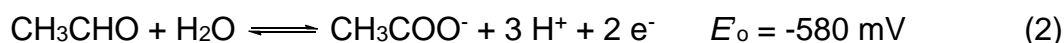


Figure 2: Active site of tungstoenzymes. DMSOR family: X = Cys-S/Cys-Se; Y = O/S; R = GMP. AOR family: X = O or Cys-S; an additional Y-ligand was not identified in AOR, but is present in BCR.¹⁴

1.1 AOR Family

The active site of the AOR family features an oxo-tungsten center bound to two molybdopterin cofactors and a [4Fe-4S] cluster. Amongst others, this family includes AOR, formaldehyde ferredoxin oxidoreductase (FOR) and glyceraldehyde-3-phosphate ferredoxin oxidoreductase (GAPOR) from thermophilic archaea, carboxylic acid reductase (CAR) from acetogens and aldehyde dehydrogenase (ADH) from sulfate-reducing bacteria. All the enzymes of this class are capable of catalyzing the oxidation of aldehydes (Equation 2).

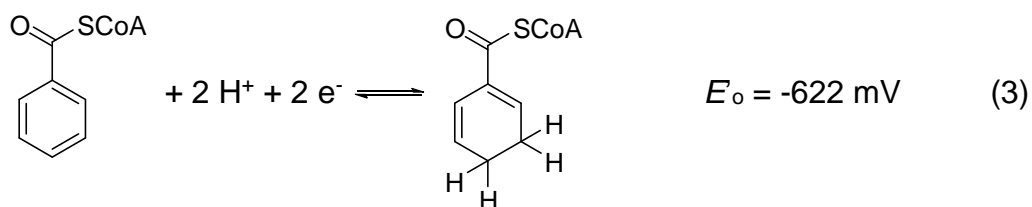


In 2015, the discovery of an unknown, phylogenetically unique and distinct member of the AOR family was reported. It was found in *Caldicellulosiruptor bescii*, a thermophilic, anaerobic cellulolytic bacteria.¹⁶

1.2 BCR Family

Tungsten is also essential for the class II benzoyl-CoA reductase of the Fe^{III}-respiring, obligately anaerobic proteobacterium *Geobacter metallireducens*. It is a key enzyme in the microbial anaerobic degradation of monocyclic aromatic compounds and

catalyzes the reduction of benzoyl-CoA to cyclohexa-1,5-diene-1-carboxyl-CoA by ferredoxin, a remarkable reaction in terms of its extremely low reduction potential (Equation 3).^{13,14}



The BCR subunit containing the active site was crystallized by Weinert *et al.* in 2015. The tungsten atom is accommodated in a highly hydrophobic pocket and octahedrally coordinated by four sulfur atoms of two molybdopterin moieties, a cysteine sulfur atom and a sixth ligand whose nature has not yet been established.¹⁷

1.3 FDH Family

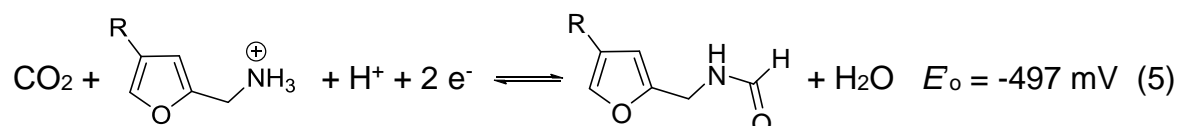
FDH was the first W-containing enzyme to be purified and characterized from *Clostridium thermoaceticum*.³ This enzyme is extremely sensitive towards oxygen and uses NADPH as the physiological electron donor. Generally, FDH catalyzes the reversible two-electron oxidation of CO₂ according to Equation 4, and together with FMDH, it contributes to CO₂ fixation.^{2,8}



The tungsten center of FDH is coordinated by the characteristic pair of molybdopterin molecules in their MGD form plus one selenocysteine and one terminal sulfur atom. The enzyme also harbours several Fe/S centers.¹³

1.4 FMDH Family

The reversible formation of *N*-formylmethanofuran from CO₂ and methanofuran (MFR) catalyzed by FMDH is the first step in CO₂ utilization performed by methanogens (Equation 5).^{2,8}



Two examples of FMDH are known, from *Methanobacterium thermoautotrophicum* and *Methanobacterium wolfei*. Remarkably, both microorganisms produce two FMDHs, a Mo-containing (FMDH I) and a W-containing (FMDH II), which differ in their response to W and Mo in their growth media. When *Methanobacterium wolfei* is grown in the presence of Mo, it exclusively expresses Mo-containing FMDH I, while in the presence of W both FMDH I and II are expressed. Interestingly, the opposite was observed for *Methanobacterium thermoautotrophicum*: Mo-grown cells produce both isoenzymes, whereas W-grown cells express only W-containing FMDH II. The catalytically active, W-substituted FMDH I isoenzyme from *Methanobacterium wolfei* and the Mo-substituted FMDH II isoenzyme from *Methanobacterium thermoautotrophicum* have both been purified and characterized separately.^{2,8,18}

1.5 AH Family

Acetylene hydratase (AH) was purified from the acetylene-utilizing anaerobe *Pelobacter acetylenicus* and catalyzes the hydration of acetylene to acetaldehyde.⁸

Since the goal of this work is to develop a structural-functional model for the active site of AH, the following chapter is fully dedicated to this unique enzyme.

2 ACETYLENE HYDRATASE

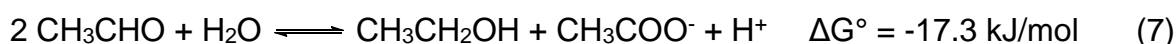
The enzyme acetylene hydratase of *Pelobacter acetylenicus* catalyzes the hydration of acetylene to acetaldehyde which is clearly a non-redox reaction. AH was purified and characterized for the first time by Rosner and Schink in 1995.¹⁹ Apart from nitrogenase, which is capable of reducing acetylene to ethylene, AH is the only enzyme known to accept acetylene as substrate.^{20,21}

2.1 Microorganisms Utilizing Acetylene

In principle, the electron-rich triple bond and the excellent solubility in water make acetylene a proper substrate for microorganisms.^{22,23} *Pelobacter acetylenicus* is the first strict anaerobe known to ferment an unsaturated hydrocarbon, and it can live on acetylene as single carbon and energy source. During growth of this strictly anaerobic bacterium, acetylene is fermented to nearly equal amounts of ethanol and acetate and only small amounts of acetaldehyde.²⁴ The initial hydration of acetylene catalyzed by AH is highly exergonic (Equation 6).²⁰



The subsequent disproportionation of acetaldehyde to ethanol and acetate yields by far less energy, but is still exergonic (Equation 7).¹⁴



In the oxidative branch of the disproportionation, acetaldehyde is transformed to acetyl phosphate via acetyl-CoA. Then, an acetate kinase transfers the phosphate group from acetyl phosphate to a molecule of ADP, thereby generating ATP and acetate. Apparently, this kinase reaction is the only energy-conserving step during fermentation of acetylene by *Pelobacter acetylenicus*.²⁴

It is rather surprising that there is an enzyme highly specific for acetylene on earth, as this gas has always been considered to be of anthropogenic origin, and traces of C₂H₂ in the atmosphere range from parts per trillion to low parts per billion.²⁴ Naturally occurring acetylene is found among other prebiotic molecules in interstellar gas clouds. In oxygen-free planetary atmospheres, photolytic decay of methane leads to the

formation of C₂H₂, hence it may have played a role in prebiotic organic chemistry.^{23,25} Therefore, it is not clear whether this tungstoenzyme arose recently as a means for microorganisms to take advantage of anthropogenic sources of acetylene, or if it represents the relict of ancestral biochemical processes.

2.2 Molecular Properties of AH

AH is a member of the DMSOR family of molybdo- and tungstoenzymes based on its amino acid sequence and its crystal structure. It was isolated, purified in both the presence and absence of air and characterized as tungsten iron-sulfur enzyme by Rosner and Schink in 1995.^{9,19} AH is a monomer with a molecular mass of 73 kDa (SDS/PAGE) or 83.5 kDa (MALDI/MS) and contains two MGD cofactors in addition to a tungsten center and a cubane-type [4Fe-4S] cluster.²⁶ Anoxically prepared AH contains 0.37 ± 0.03 mol of W and 3.69 ± 0.04 mol of Fe per mol enzyme as determined by ICP-MS.²⁷ Fluorimetric analysis of AH gave 1.3 ± 0.1 mol of MGD per mol of enzyme.²⁶ Notably, the theoretical value of two MGD ligands per mol of enzyme has not been achieved yet, however, the ratio MGD/W never fell below 2.^{26,27} EPR spectra of AH isolated under air showed an axial signal at $g_{av} = 2.01$, which is indicative for a truncated [3Fe-4S] cluster. The signal disappeared upon reduction with sodium dithionite. In contrast, AH isolated under N₂/H₂ atmosphere was EPR silent. EPR spectra of AH reduced with sodium dithionite showed the typical signal of a low potential ferredoxin-type [4Fe-4S] cluster ($g_z = 2.048$, $g_y = 1.939$, $g_x = 1.920$). Upon oxidation with one equivalent of hexacyanoferrate(III), a new rhombic EPR signal with resonances at $g_z = 2.007$, $g_y = 2.019$ and $g_x = 2.048$ ($g_{av} = 2.022$) appeared. However, the signal disappeared upon further addition of hexacyanoferrate(III). Consequently, the EPR signal with $g_{av} = 2.022$ was assigned to a W(V) center.²⁶ The [4Fe-4S] cluster showed a midpoint potential of -410 mV, although the midpoint redox potential for activation of the enzyme was at -340 mV. This finding suggests that AH was active with the tungsten center in the W(IV) state, whereas the redox state of the cluster seemed to be of less importance for the activity of AH.^{23,26} Setting the potential to ≤ -410 mV carried the cluster to the [4Fe-4S]¹⁺ state, but did not change the enzyme activity.²¹ Furthermore, model studies indicate that W(IV) participates in the catalysis of acetylene hydration, whereas the corresponding W(VI) center remained inactive.²⁸

AH activity was determined photometrically in a coupled assay with alcohol dehydrogenase and could only be measured in the presence of a strong reducing agent such as titanium(III) citrate or dithionite.¹⁹ The optimum pH of AH activity was found to be 6.0 to 6.5, and the apparent optimum temperature was 55 °C.^{19,27}

2.3 Structure and Active Site of AH

The crystal structure of AH in its active, reduced state at 1.26 Å resolution was reported by Seiffert *et al.* in 2007.^{29,30} The overall structure of this enzyme is shown in Figure 3.



Figure 3: AH from *Pelobacter acetylenicus*. Overall structure with the [4Fe-4S] cluster and W(MGD)₂ buried inside the protein; the peptide backbone is shown in dark blue at the N-terminal end and continues as light blue, cyan, green and yellow to orange at the C-terminal end.²⁷

Generally, AH is a monomer of 730 amino acids. The peptide chain folds into a tertiary structure comprising four domains that are related by an internal pseudotwofold axis and that bury all cofactors deep inside the protein. Domain I comprises residues 4–60 and holds the [4Fe-4S] cluster, while domain II (residues 65–136 and 393–542) and domain III (residues 137–327) are able to provide multiple hydrogen-bonding interactions to one of the MGD cofactors. Domain IV (residues 590–730) is mainly represented by a seven-stranded β -barrel structure.³⁰

In all known structures of the DMSOR family, the access funnel towards the active site starts at the pseudotwofold axis between domains II and III. In AH, however, the whole region connecting domains II and III is completely rearranged, resulting in a tightening of the original substrate funnel and in a shift of the loop region ranging from residues 327–337. The obvious shift of this loop region opens a new access funnel towards the active site at the intersection of domains I, II and III. This allows the substrate to approach the tungsten center from a different direction (Figure 4).^{23,30}

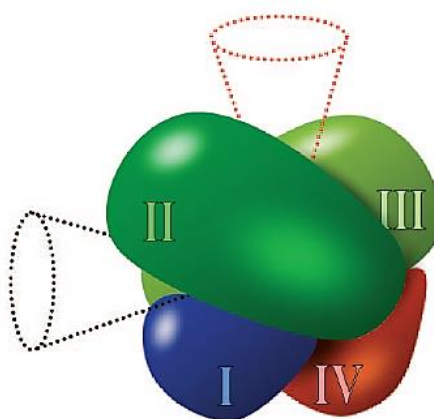


Figure 4: Schematic view of the four-domain structure typically found in members of the DMSOR family. Red cone: substrate funnel of the members of the DMSOR family. Black cone: substrate funnel of AH.³⁰

The octahedral coordination sphere of the tungsten(IV) center consists of four sulfur atoms deriving from two dithiolene moieties of two MGD cofactors (designated P_{MGD} and Q_{MGD} , considering the DMSOR nomenclature) and a thiolate contributed from Cys141. The sixth ligand position is occupied by a tightly coordinated oxygen atom at 2.04 Å distance. The W–O distance determined by X-ray diffraction analysis at 1.26 Å resolution was between the values expected for an OH-ligand (1.9–2.1 Å) and a coordinated H₂O molecule (2.0–2.3 Å). Because of the close proximity of the heavy scatterer tungsten, the distance observed in the crystal structure may be distorted by Fourier series termination effects. A simulation of this effect showed the true W–O distance to be 2.25 Å, making the ligand most likely a water molecule.^{23,30,31} The access funnel ends in a ring of six bulky hydrophobic residues – Ile14, Ile113, Ile142, Trp179, Trp293 and Trp472 – directly above the coordinated oxygen atom and the adjacent aspartate, Asp13. This Asp residue forms a strong hydrogen bond of 2.41 Å to the oxygen of the coordinated water molecule and is also a direct neighbor of the [4Fe-4S] coordinating Cys12 (Figure 5).

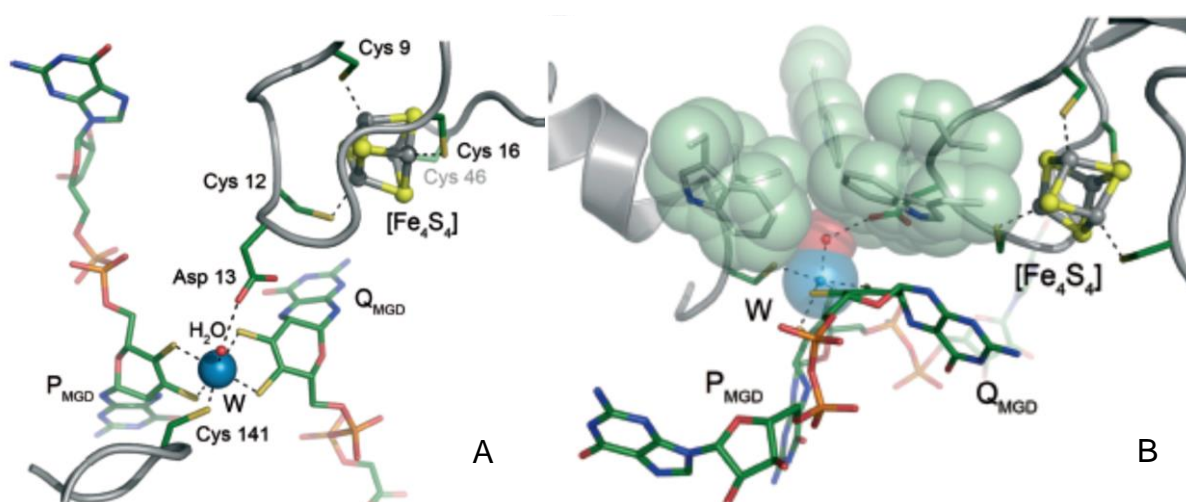


Figure 5: A: Cofactors and active site of AH. B: Active site with ring of hydrophobic amino acid residues.³⁰

The development of a successful protocol for the heterologous expression of AH in *Escherichia coli* facilitated studies on site-directed mutagenesis. The three amino acids Asp13, Lys48 and Ile142, which are close to the active site, were exchanged by site-directed mutagenesis to investigate their functional role in the mechanism of AH. Asp13 forms a hydrogen bond to the oxygen ligand of the tungsten atom and is therefore assumed to be catalytically important by activating the oxygen atom for the addition to the acetylene triple bond. The mutation of Asp13 to alanine resulted in a dramatic loss of activity, while the replacement with glutamate had only little effect. Consequently, the carboxyl group of Asp13 plays a crucial role in AH catalysis. Residue Lys48, which was found to play a critical role in electron transfer in enzymes of the DMSOR family, is located between the [4Fe-4S] cluster and the Q_{MGD} cofactor. As the hydration of acetylene does not involve a net electron transfer, the mutation of Lys48 to alanine did not influence AH activity. In contrast, the exchange of Ile142, which is part of the hydrophobic ring constituted of six bulky amino acid residues, against alanine resulted in a significant loss of catalytic activity. This is in accordance with the theoretical findings that the cavity formed by the hydrophobic amino acids might be the substrate binding site of AH.^{14,27}

2.4 Mechanism of AH

The first reaction mechanism of the conversion of acetylene to acetaldehyde was proposed by Seiffert *et al.* in 2007 after crystallization of AH.³⁰ Since then, several theoretical studies for different scenarios have been carried out using DFT approaches based on QM-only and QM/MM models. However, all these mechanisms are found to have unrealistically high energy barriers on the basis of density functional calculations, except the concept developed by Liao *et al.* (Table 1).^{32–36}

Table 1: Proposed reaction mechanisms of AH with calculated energy barriers sorted by year of proposal.

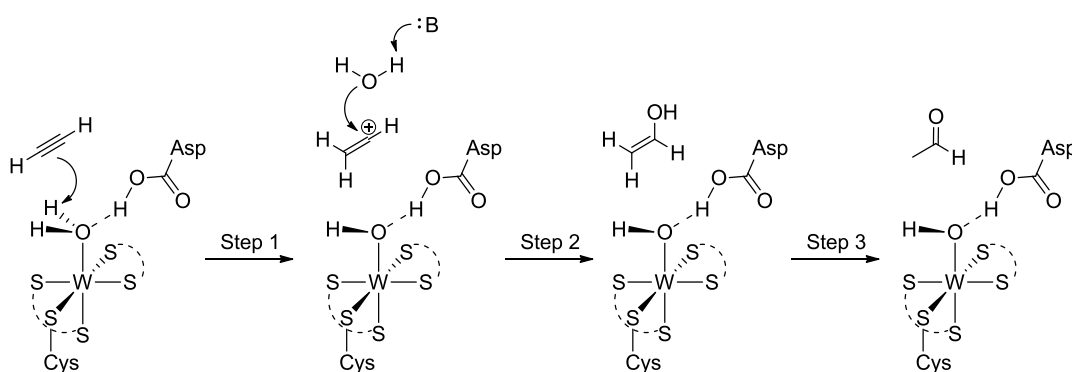
Mechanism	Year	ΔG^\ddagger (kcal/mol)
Electrophilic attack on free acetylene by coordinated water ³⁰	2007	43.9 ³³
Nucleophilic attack of water on η^2 -acetylene with the assistance of neutral Asp13 ³²	2009	41.0 ³³
Electrophilic attack on η^2 -acetylene by neutral Asp13 via a tungsten-vinylidene intermediate ³³	2010	34.0 ³³
Nucleophilic attack of water on η^2 -acetylene with the assistance of deprotonated Asp13 ³⁴	2010	16.9 ^{34a}

^a Solvation effects are included.

In principle, there are two fundamentally different mechanisms for the hydration of acetylene, a first shell and a second shell mechanism.²³ In the second shell mechanism, acetylene and all hydration intermediates are located outside of the first coordination sphere of the tungsten center. In the first shell mechanism, acetylene and all reaction intermediates are directly coordinated to the tungsten center. Only the mechanism involving a coordinated water molecule is considered to be a second shell mechanism, all others are first shell mechanisms. The following order is chosen for historical reasons.

2.4.1 Second Shell Mechanism

In this mechanism, a tungsten-coordinated water molecule gains a partially positive net charge due to hydrogen bonding interactions with the vicinal Asp13. Because of the resulting electrophilic character of the water molecule, a proton is abstracted by an uncoordinated acetylene. This addition gives rise to a vinyl cation intermediate which is in turn nucleophilically attacked by an uncoordinated water molecule in the second step. The reaction sequence is completed by tautomerization of the vinyl alcohol to acetaldehyde (Scheme 1).³⁰

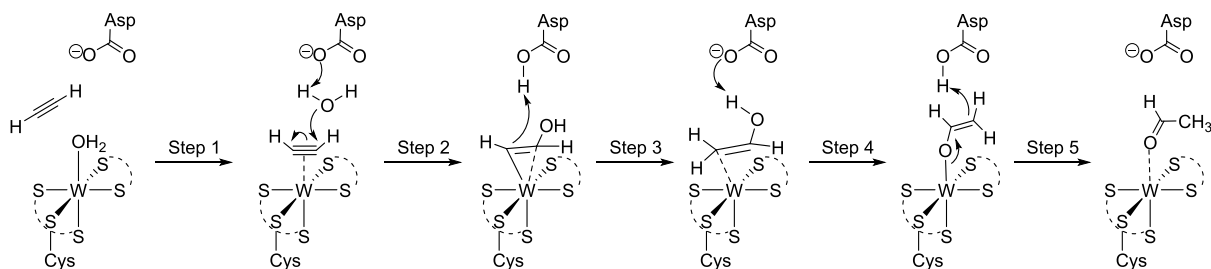


Scheme 1: Second shell mechanism proposed by Seiffert *et al.* in 2007.³⁰

Although the overall reaction was calculated to be exothermic by 21.4 kcal/mol, a rather high energy barrier of 43.9 kcal/mol makes this mechanism fairly unrealistic.³³

2.4.2 First Shell Mechanism

The only mechanism with realistic energy barriers was developed by Liao *et al.* in 2010.^{34–38} Therefore, a theoretical model of the active site of AH was designed in accordance with the crystal structure of native AH. The model comprises the tungsten(IV) center with its first-shell ligands, namely two MGD moieties, a Cys141 thiolate and a water molecule. The catalytically important Asp13 residue was modeled in its deprotonated state. In total, the model consists of 116 atoms and the overall charge is -1.^{27,30,34} The five steps of the mechanism are illustrated in Scheme 2.



Scheme 2: First shell mechanism proposed by Liao *et al.* in 2010.³⁴

This mechanism starts with a ligand exchange step, in which the coordinated water is substituted by an acetylene molecule which coordinates to the tungsten center in a η^2 -fashion. This step was calculated to be exothermic by 5.4 kcal/mol, indicating that a first shell mechanism would be more favorable from an energetic point of view.³⁴ In the second step, the coordinated acetylene is nucleophilically attacked by a free water molecule which is activated by a proton transfer to Asp13. The required energy for this step was calculated to be 16.9 kcal/mol, representing the highest energy barrier in this mechanism. The negative charge on the tungsten-coordinated carbon atom is neutralized by a subsequent proton transfer in the third step, thereby weakening the W–C bond. The reaction sequence is completed by tautomerization of the vinyl alcohol to acetaldehyde which could occur outside of the active site or with the assistance of Asp13.³⁴

In principle, acetylene acts as a four-electron donor by interaction of its two π orbitals with two empty d orbitals of tungsten(IV). In addition, π backbonding from an occupied d orbital of the metal to one unoccupied π^* orbital of acetylene is taking place, thereby weakening the C≡C bond. Interaction of two unoccupied orbitals of each tungsten and acetylene leads to the formation of a δ -like MO, which facilitates electron transfer during a nucleophilic attack on acetylene.^{34,39}

The authors also performed theoretical studies on the chemoselectivity of AH. They investigated the energies involved in the binding and subsequent hydration of propyne, ethylene and acetonitrile using the same quantum chemical cluster approach adopted for acetylene hydration. For all three molecules, the calculated barriers are higher than that for the substrate acetylene. For propyne, the binding energy to the tungsten center was found to be ~5 kcal/mol more than that for acetylene, and all further steps have an overall barrier of 35 kcal/mol. These calculations could explain, why propyne acts as a competitive inhibitor of AH. The binding energy of ethylene and acetonitrile was

found to be ~6 and 13 kcal/mol worse than acetylene binding, respectively. While a nucleophilic attack on ethylene has unrealistically high energy barriers, the overall barrier for hydration of acetonitrile is only 3 kcal/mol higher than that for acetylene. Consequently, the trend is consistent with the fact that ethylene and nitriles in general are no substrates of AH. However, the obtained energy differences are not sufficient to draw a reliable conclusion on the mechanism of AH.³⁷

Considering the architecture of the active site cavity including the ring formed by hydrophobic amino acid residues, the striking specificity for acetylene as a substrate, the results from site-directed mutagenesis and the fact, that crystallization of AH with acetylene coordinated to the tungsten center has not been possible so far, the formation of a W–acetylene bond and the probability of the proposed first shell mechanism has to be further investigated. For instance, this investigation could be performed by the development of a structural-functional model of the active site of AH.

3 MODELING CHEMISTRY OF TUNGSTEN

Bioinorganic chemistry is the study of the structures and functions of inorganic biological compounds which participate in essential biochemical processes. Thus, bioinorganic chemistry is fairly important in elucidating the implications of substrate binding and activation in nature-made enzymes.⁴⁰ Above all, the primary goal is to gain insight into the mechanism of enzymes like AH and to subsequently benefit from the knowledge of how nature performs catalysis.

Chemical approaches to investigate the mechanism of enzymes have either been biomimetic, whereby the structures of the ligand system around the metal center are as similar as possible to the active site architecture present in nature, or bioinspired, whereby the achievement of the enzymatic function under ambient conditions has clear priority, regardless of the ligand system utilized. These two approaches resulted in the formation of new terminologies in the field of modeling bioinorganic chemistry, namely “structural modeling” and “functional modeling”. A functional model does not necessarily need to mimic the exact structural features of the active site of the respective enzyme, but rather focuses on tuning the electronic properties of the model complex to achieve functional activity.^{40,41}

The outstanding role of water as an essential chemical reactant in enzymatic catalysis should always be kept in mind, as functional model compounds, that are insoluble in or even instable towards water, will probably not be too close to functional mimicry of the naturally occurring enzyme.^{40,41}

Generally, two types of ligands are outlined in the following chapters: On the one hand, dithiolene ligands, which reflect the structural modeling approach by mimicking the dithiolene moiety exhibited by the native molybdopterin cofactor, are introduced and described. On the other hand, non-dithiolene ligands, that represent the functional modeling approach, are discussed and characterized.

3.1 Dithiolene Ligands

Dithiolene complexes display unusual structural, electronic, photochemical and reactivity features. Structurally, the ligands are all based on the 1,2-ethenedithiolate unit of the molybdopterin cofactor (Figure 6).^{40,41}

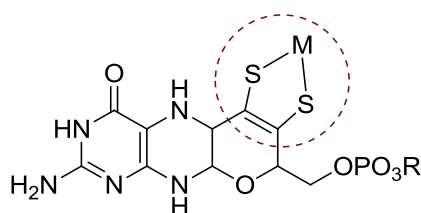


Figure 6: Metal-bound molybdopterin cofactor with the 1,2-ethenedithiolate unit labeled.

Many characteristics of dithiolene compounds can be associated with the structure and bonding of the bidentate chelate of the dithiolene ligand. Generally, they form rather rigid and roughly planar five-membered rings with enormous electronic flexibility. This electronic flexibility allows the redox state of the complex to be varied without significantly changing its basic geometry. Figure 7 shows various bonding modes of the dithiolene complex system which enables the metal center to adopt different oxidation states.⁴²

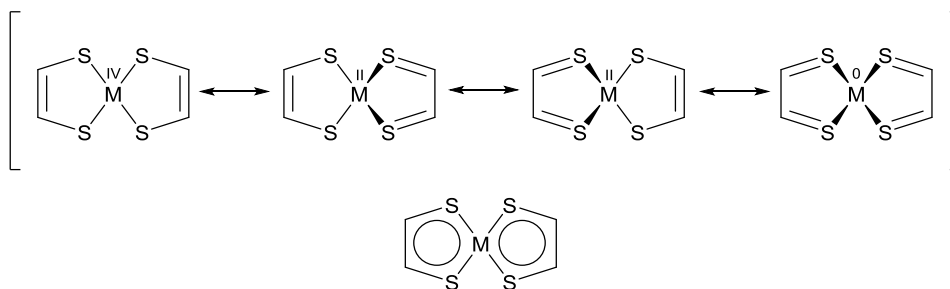


Figure 7: Possible oxidation states of dithiolene complexes.⁴²

So far, various types of dithiolenes have been used in structural modeling chemistry. Typically employed dithiolenes are substituted by simple functional groups such as methyl or cyanide or part of a ring system (Figure 8). The most frequently used ones are 1,2-methyl-1,2-dithiolate (mdt), 1,2-benzenedithiolate (bdt) and 1,2-maleonitrile-1,2-dithiolate (mnt).^{11,40,41}

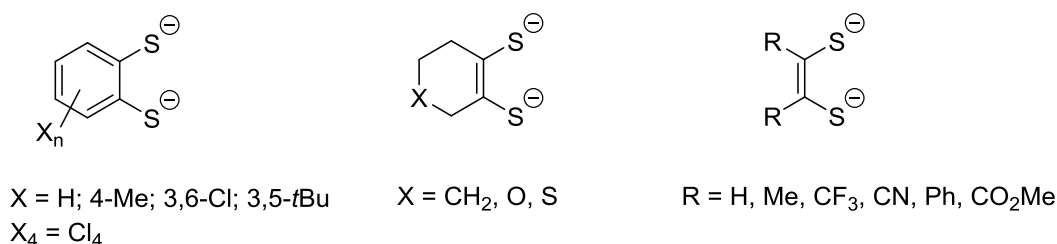


Figure 8. Selected dithiolene ligands.^{40,41}

Only a few scientists have handled the problem of linking a pterin to the dithiolene moiety to get access to both essential components of molybdopterin and therefore to a full structural mimic of the cofactor. Burgmayer *et al.*, for instance, demonstrated that a pterin dithiolene ligand can be formed in-situ by reaction of a molybdenum tetrasulfide reagent with a pterinyl arylalkyne (Figure 9).^{43,44}

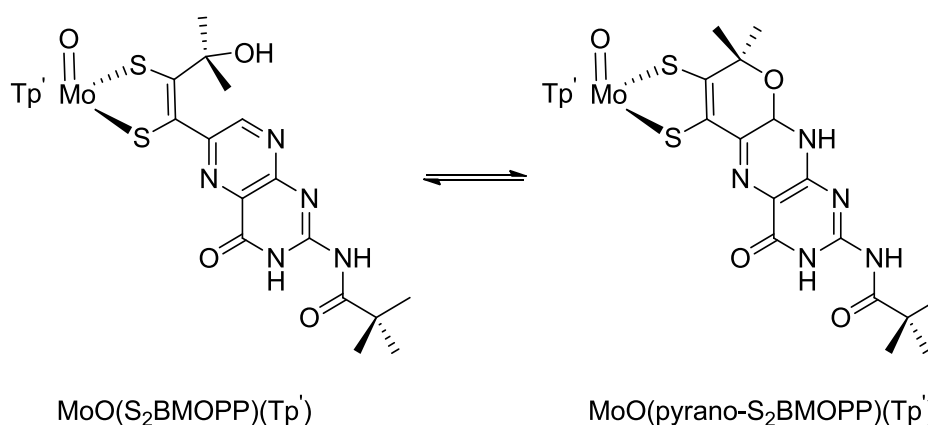


Figure 9: MoO(S₂BMOPP)(Tp'), a model complex of the molybdopterin cofactor with molybdenum(V).⁴³

However, there are a few problems associated with W-dithiolene chemistry, of which the proneness of tungsten dithiolene complexes towards hydrolysis and disulfide bond formation are the most severe.⁴¹

3.1.1 Functional Models

The functional aspects of AH have been mimicked by the tungsten(IV) complex $[\text{Et}_4\text{N}]_2[\text{WO}(\text{mnt})_2]$ which was synthesized and investigated by Sarkar *et al.* in 1996/1997 (Figure 10). This complex is the only functional model so far.^{28,45}

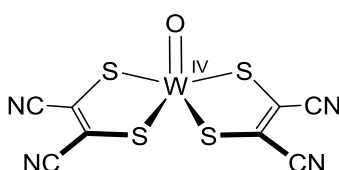


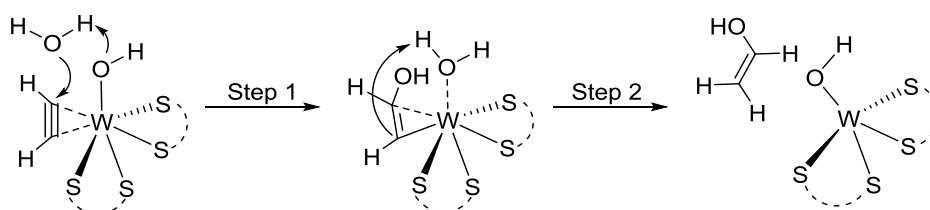
Figure 10: $[\text{WO}(\text{mnt})_2]^{2-}$, the only functional model of AH so far.

The biomimetic tungsten complex $[\text{Et}_4\text{N}]_2[\text{WO}(\text{mnt})_2]$ achieved approximately nine catalytic turnovers under the applied assay conditions. The corresponding oxidized complex, $[\text{Et}_4\text{N}]_2[\text{WO}_2(\text{mnt})_2]$, did not catalyze the hydration of acetylene, but responded equally well after reduction with excess $\text{Na}_2\text{S}_2\text{O}_4$.^{28,45} However, no tungsten-acetylene intermediate could be isolated, crystallized or observed by spectroscopic methods, thereby supporting a second shell mechanism. Theoretical investigations of the mechanism of acetylene hydration catalyzed by $[\text{WO}(\text{mnt})_2]^{2-}$ were performed by Liu *et al.* in 2011 by DFT methods.^{30,38}

At first, the uncatalyzed pathway of acetylene hydration was investigated for comparison with the efficacy of the catalyst, although no acetaldehyde formation could be observed in water at room temperature. This reaction proceeds via two steps, of which the first one – a nucleophilic attack of water on acetylene coupled with a proton transfer – is rate-limiting with a barrier of 35 kcal/mol. This high energy barrier is probably the reason for the reaction not taking place under ambient conditions.³⁸

For the reaction catalyzed by $[\text{WO}(\text{mnt})_2]^{2-}$, three different first-shell models were designed in which the tungsten-bound oxygen species is a hydroxo (model A), an aquo (model B) or an oxo (model C). Pathways based on models B and C are shown to have unrealistically high energy barriers of 38.4 and 43.8 kcal/mol, respectively.

Furthermore, it was found that $W^{IV}=O$ (model C) is a quite poor base compared to $W^{IV}-OH$ (model A). In the preferred mechanism, $W^{IV}-OH$ (model A) acts as a base by abstracting a proton from an incoming water molecule which subsequently becomes a hydroxide and is then able to perform a nucleophilic attack on the coordinated acetylene. The resulting vinyl anion is stabilized by the tungsten center until it gets protonated by the coordinated water molecule (Scheme 3). The first step was determined to be rate-limiting with a barrier of 20 kcal/mol. The isomerization of the vinyl alcohol formed in the second step can be performed with the assistance of water molecules in solution.³⁸



Scheme 3: Preferred mechanism for the conversion of acetylene to acetaldehyde catalyzed by $[WO(mnt)_2]^{2-}$, proposed and calculated by Liu *et al.* in 2011.³⁸

3.2 Non-dithiolene Ligands

Although dithiolene ligands are supposed to be the closest structural mimics of the molybdopterin cofactor, it has not yet been possible to isolate a tungsten-dithiolene complex with a coordinated acetylene molecule. Since dithiolene complexes are quite prone to hydrolysis, ligand systems, which are not even able to be hydrolyzed, ought to be further investigated.⁴¹ Furthermore, a structural-functional model of the molybdoenzyme sulfite oxidase (SO) was developed by utilizing the tridentate ligand hydrotris(methimazolyl)borate (Tm^{Me}) which coordinates the molybdenum center via three sulfur atoms which are not prone to hydrolysis. It could be demonstrated that the non-dithiolene complex shown in Figure 11 was able to transfer one of its oxygen atoms to the native enzyme's substrate HSO_3^- to form HSO_4^- .⁴⁶

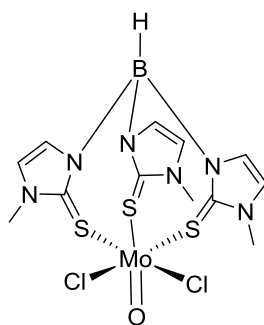


Figure 11: $[\text{MoOCl}_2(\text{Tm}^{\text{Me}})]$, an alternative functional model of the enzyme sulfite oxidase.⁴⁶

The ligand utilized in the functional model of SO belongs to the class of scorpionate ligands which is discussed in the following chapter.

3.2.1 Scorpionate Ligands

The term “scorpionate ligand” refers to a tridentate ligand which is able to coordinate to a metal in a *fac* manner. It derives from the fact that the ligand can bind to a metal with two donor sites like the pincers of a scorpion, while the third donor site reaches over the plane created by the metal and the other two donor atoms to coordinate to the metal (Figure 12).^{47,48} In the pathbreaking report by Trofimenko in 1966, a new class of chelating polypyrazolylborate ligands was created by the reaction of KBH_4 with three equivalents of pyrazole, providing the most popular class of scorpionates, the hydrotris(pyrazolyl)borate (Tp) ligands.⁴⁹

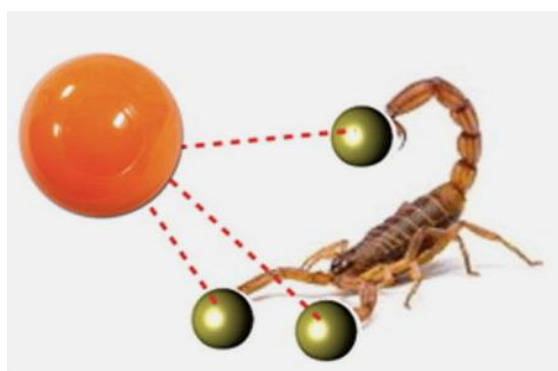


Figure 12: Schematic scorpionate complex. Orange: metal center, green: donor atoms of the ligand.⁵⁰

Depending on the donor atoms complexing the metal center, scorpionates can be considered as hard or soft ligands. According to the HSAB concept, nitrogen and oxygen donor atoms are considered as hard bases and prefer bonding to hard acids,

while phosphorus and sulfur are classified as soft bases since they exhibit contrary properties. The vast majority of hard scorpionates consists of various substituted pyrazoles, with Tp and Tp' being well-established.⁴⁸ Although hard scorpionates have been successfully used for functional modeling of molybdo- and tungstoenzymes, they are not able to provide a sulfur-rich environment present in the active site of these enzymes. Therefore, scorpionate ligands with sulfur donor atoms were introduced in the 1990s.^{51,52} Selected examples are shown in Figure 13.

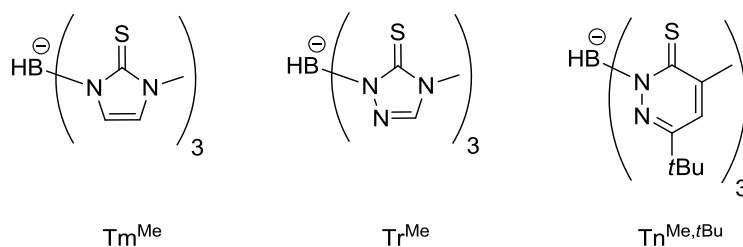


Figure 13: Selected soft scorpionates: Tm^{Me} , Tr^{Me} and $\text{Tn}^{\text{Me,tBu}}$.⁵²⁻⁵⁴

3.2.1.1 Tungsten(II) Alkyne Complexes with Soft Scorpionate Ligands

The versatile complex $[\text{Wl}_2(\text{CO})(\eta^2\text{-C}_2\text{Me}_2)_2(\text{NCMe})]$ appears to be a suitable precursor for the introduction of a hydrotris(methimazolyl)borate ligand (Tm^{Me}) to form the only literature-known tungsten(II) alkyne complex employing the tripodal ligand Tm^{Me} (Figure 14).^{55,56} So far, no crystal structure could be obtained, and $[\text{Wl}(\text{CO})(\eta^2\text{-C}_2\text{Me}_2)(\text{Tm}^{\text{Me}})]$ was only characterized by ^1H and ^{13}C NMR spectroscopy. The coordinated 2-butyne gives rise to two ^{13}C resonances ($\delta = 207.4$ and 206.9 ppm) in the region characteristic of four-electron donor alkynes.⁵⁶

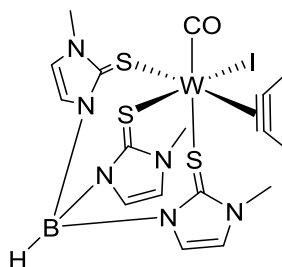


Figure 14: The only tungsten(II) alkyne complex known employing Tm^{Me} : $[\text{Wl}(\text{CO})(\eta^2\text{-C}_2\text{Me}_2)(\text{Tm}^{\text{Me}})]$.⁵⁶

3.2.2 Thioether Ligands

In general, a thioether ligand provides a soft coordination sphere for metal ions and is not prone to hydrolysis in aqueous solution. Therefore, it ought to be a suitable ligand for tungsten. Neutral chelating thioethers, like the tridentate 1,4,7-trithiacyclononane shown in Figure 15, are well-known since 1977.⁵⁷ This ligand forms complexes with many metal ions, even including those considered as hard, such as iron(II) or copper(II).⁵⁸

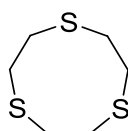


Figure 15: Structure of 1,4,7-trithiacyclononane.⁵⁷

The crown thioethers 2,5,8-trithia[9]-*o*-benzenophane (ttob) and 2,5,8-trithia[9]-*m*-benzenophane (ttmb) (Figure 16) were prepared in 1990 and intensively utilized and investigated.^{59,60}

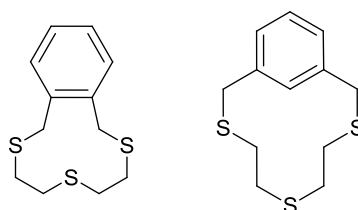


Figure 16: Structure of crown thioether ligands (ttob and ttmb).⁵⁹

In the 1990s, Baker *et al.* treated the precursors $[M_2(CO)_3(NCMe)_2]$ ($M = Mo$ or W) with neutral thioether ligands, e.g. ttob, $PhS(CH_2)_2SPh$ and $MeS(CH_2)_2S(CH_2)_2SMe$ (ttn) (Figure 17), to synthesize the corresponding complexes.^{60–63}

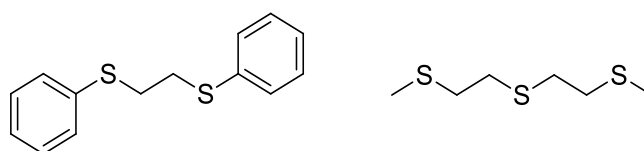


Figure 17: Structure of the dithioether ligand $PhS(CH_2)_2SPh$ and the trithioether ligand $MeS(CH_2)_2S(CH_2)_2SMe$ (ttn).^{61–63}

The first series of dioxidotungsten(VI) complexes employing thioether ligands was prepared and characterized in 2007 utilizing the rather simple ligands 1,2-bis(methylthio)ethane and 1,4-dithiane (Figure 18).⁶⁴

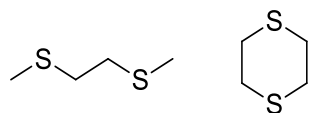


Figure 18: Structure of dithioether ligands utilized for the first preparation of dioxidotungsten(VI) complexes with thioether ligands.⁶⁴

The ligands depicted in Figure 19 reacted with molybdenum(0) and tungsten(0) precursors for approximately 15 hours to the corresponding complexes.^{65,66}

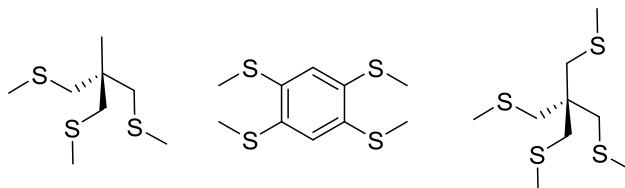


Figure 19: Structure of trithio- and tetrathioether ligands.^{65,66}

3.2.2.1 Tungsten(II) Alkyne Complexes with Thioether Ligands

Although halogenocarbonyl alkyne complexes of tungsten(II) have been extensively studied over the years, only a few examples containing neutral bi- or tridentate thioether ligands have been described so far. These complexes have generally been synthesized by the reaction of $[WX_2(CO)(\eta^2-C_2R_2)_2(NCMe)]$ ($X = Br, I; R = Me, Ph$) with *tto*b or *ttn*. By this means, the tungsten(II) alkyne complexes $[WI(CO)(\eta^2-C_2Me_2)(ttn-S, S', S'')]I$, $[WI(CO)(\eta^2-C_2Ph_2)(ttn-S, S', S'')]I$, $[WBr(CO)(\eta^2-C_2Ph_2)(ttn-S, S', S'')]Br$, $[WI_2(CO)(\eta^2-C_2Ph_2)(ttn-S, S')]I$, $[WI(CO)(\eta^2-C_2Me_2)(ttob- $S, S', S'')]I$, $[WI(CO)(\eta^2-C_2Ph_2)(ttob- $S, S', S'')]I$ and $[WBr(CO)(\eta^2-C_2Ph_2)(ttob- $S, S', S'')]Br$ (Figure 20) could be prepared in acceptable yields.⁶⁷$$$

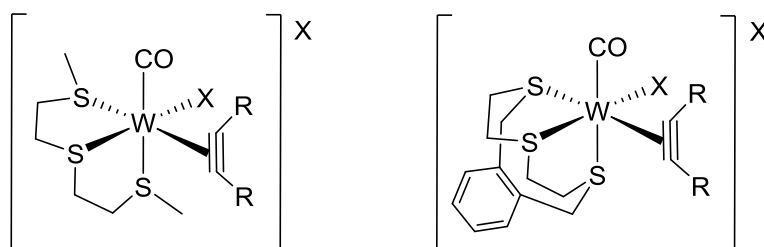


Figure 20: Tungsten(II) alkyne complexes containing thioether ligands ($X = Br, I; R = Me, Ph$).⁶⁷

All alkyne complexes prepared by Baker *et al.* contain tungsten in its oxidation state +II which is not present in naturally occurring enzymes. Besides, none of them contains

an unsubstituted acetylene molecule. Therefore, these sulfur-rich tungsten(II) complexes are no mimics of AH.

3.2.3 Poly(thioether)borate Scorpionate Ligands

The first preparation of the anionic tripodal ligand tetra((methylthio)methyl)borate, [RTt], was reported in 1994, followed by the synthesis of phenyltris((methylthio)methyl)borate, [PhTt], in 1996 (Figure 21).^{51,68} The first complex containing [RTt] was the anionic molybdenum(0) complex [Bu₄N][Mo(CO)₃(RTt)].⁵¹ The ligand [PhTt] is more established in literature, with numerous complexes of Fe(II), Co(II), Ni(II), Cu(I), Zn(II), Pd(II) and Cd(II), but none of W.^{68–70}

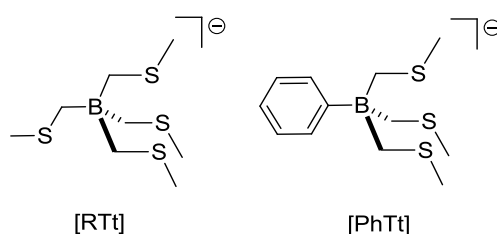


Figure 21: Structure of the first thioether scorpionate ligands, [RTt] and [PhTt], prepared by Riordan *et al.*^{51,68}

In 1999, Riordan *et al.* prepared two new borate ligands, the tridentate PhB(CH₂SCH₃)₂(pz)⁻ and the bidentate Ph₂B(CH₂SCH₃)(pz)⁻, providing mixed donor sets with sulfur and nitrogen. Coordination compounds containing Fe, Co, Ni and Zn could be synthesized in reasonable yield.

Inspired by [PhTt], Riordan *et al.* developed various anionic tripodal thioether ligands of the general form [PhTt^R], with R indicating the substituent on the sulfur donor atom (Figure 22). Significant features of the [PhTt^R] ligands include the anionic charge provided by the borate, the high polarizability of the thioether donor sites and the synthetic versatility provided by different boron and sulfur substituents.^{71–74} According to Riordan, “the Tt ligands have been developed and used in a range of contexts with studies including evaluation of their fundamental coordination characteristics and selected applications in bioinorganic and organometallic chemistry and small molecule activation by monovalent complexes of nickel and iron.”⁶⁹

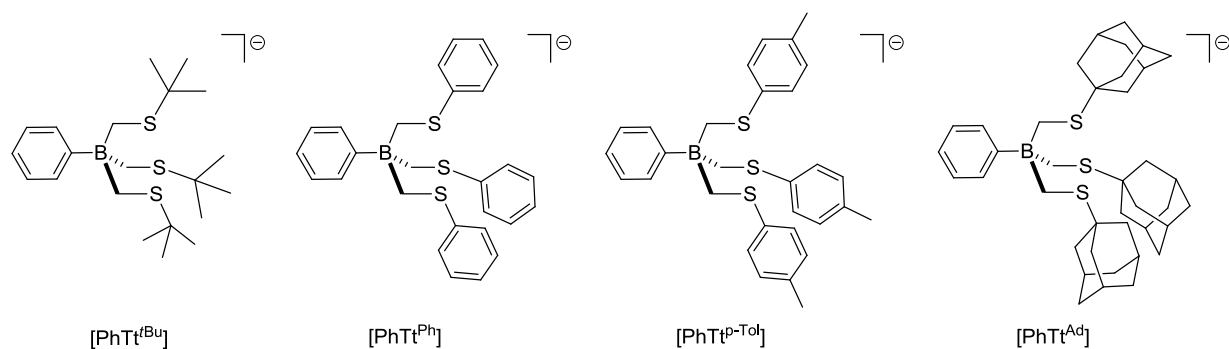


Figure 22: Structure of the tripodal thioethers prepared by Riordan *et al.*: [PhTt^{tBu}]⁷², [PhTt^{Ph}]⁷¹, [PhTt^{p-Tol}]⁷³ and [PhTt^{Ad}]⁷⁴.

The ligand [PhTt^{tBu}], for instance, was utilized in the preparation of complexes of iron in its naturally relevant monovalent oxidation state and Fe(II), Mn(II) and Co(II), thereby producing functional models of catechol dioxygenases.^{75,76} So far, there are no tungsten complexes employing poly(thioether)borate scorpionate ligands known in literature.

4 TUNGSTEN ACETYLENE COMPLEXES

Templeton *et al.* characterize acetylene as a four-electron donor interacting with the metal in a fashion similar to the Chatt-Dewar-Duncanson model which describes the chemical bonding between an alkene and a metal. In principle, acetylene is able to form a strong σ and a π bond by donating its π electrons into an empty metal orbital, whereas the metal may perform π backbonding by donating the electrons of a filled d orbital into the antibonding π^* MOs of acetylene.³⁹ The MO diagram of acetylene is depicted in Figure 23.⁷⁷

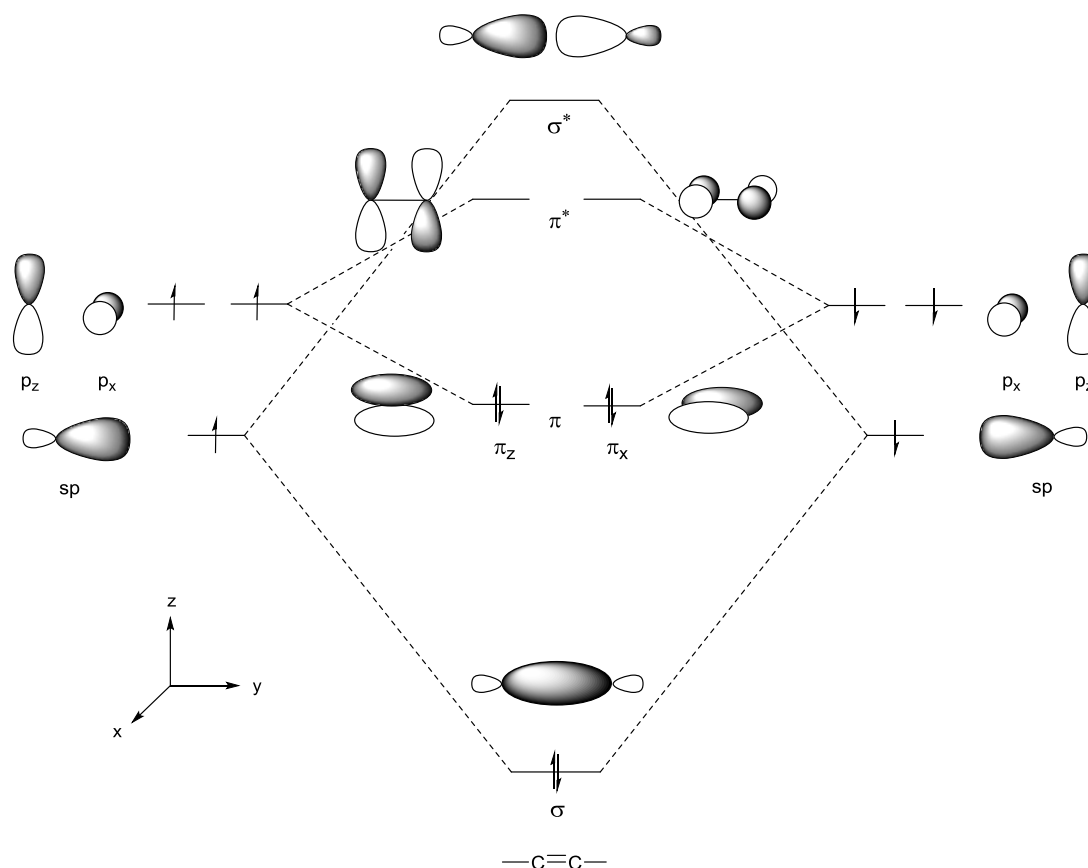


Figure 23: Schematic MO diagram of acetylene.⁷⁷

The sp hybrid orbitals of acetylene combine to a bonding (σ) and an antibonding MO (σ^*), whereas the combination of the orthogonal AOs p_x and p_z yields two bonding (π) and two antibonding MOs (π^*).

4.1 Bonding Situation in Carbonyl Tungsten(II) Acetylene Complexes

Octahedral tungsten(II) acetylene complexes bearing a CO ligand, which is also capable of π backbonding, exhibit extraordinary structural properties. Acetylene approach along the y axis (Figure 24) either selects d_{xy} or d_{yz} from the set of three d_{π} orbitals for potential overlap with one of its π^* orbitals. When acetylene is parallel to the metal carbonyl fragment ($\alpha = 0^\circ$), π^* lies in the yz plane and stabilizes the d_{yz} orbital which is filled for the d^4 configuration based on carbonyl π -acid properties. Thus, this favorable overlap creates a three-center, two-electron bond, thereby stabilizing the filled d_{yz} orbital at the expense of both CO and acetylene π -acceptor orbitals. In contrast, in the $\alpha = 90^\circ$ orientation, the corresponding parallel antibonding orbital π_y^* only stabilizes d_{xy} , but since d_{xy} houses no electrons, no net energy gain is realized.³⁹

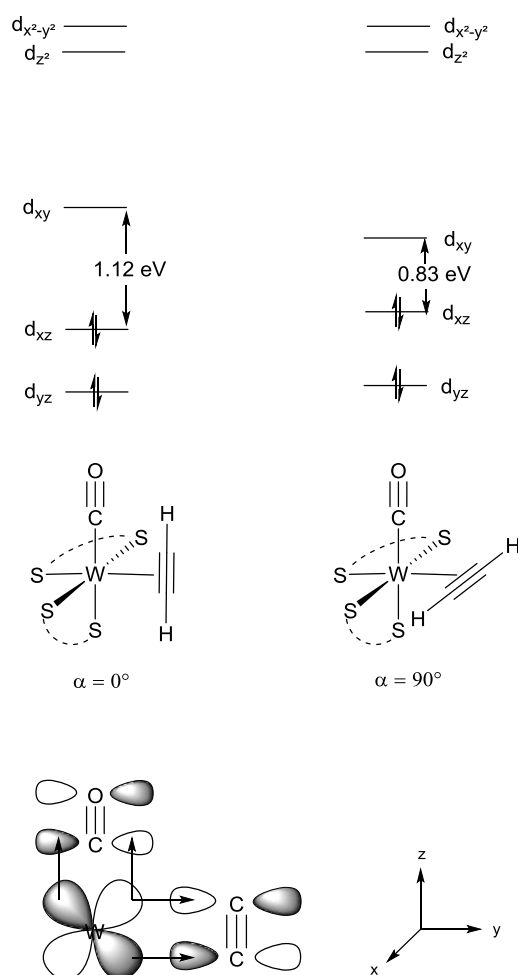


Figure 24: Relative frontier orbital energies in carbonyl tungsten(II) acetylene complexes as a function of the alkyne rotation angle and favorable orbital overlap in the structure with $\alpha = 0^\circ$.³⁹

Hence, the coordination of acetylene in carbonyl tungsten(II) acetylene complexes can be described as followed: Primary interactions take place via two ligand-metal interactions formed by σ donation from the π_y MO of acetylene to the empty $d_{x^2-y^2}$ orbital of the metal and π donation from the π_x MO of acetylene to the d_{xy} orbital of the metal, as depicted in Figure 25. As in the Chatt-Dewar-Duncanson model, π backbonding is performed from the filled d_{yz} orbital of the metal to the empty π_y^* MO. A fourth bonding interaction is δ -type between the occupied d_{xz} AO of tungsten and the π_x^* MO of acetylene. These interactions lengthen the C \equiv C bond of the coordinated acetylene, thus the better the π backbonding can be performed, the longer the C \equiv C bond becomes. As a matter of fact, d^0 metals are not able to weaken alkyne bonds since there are no electrons available for π backbonding.^{32,39}

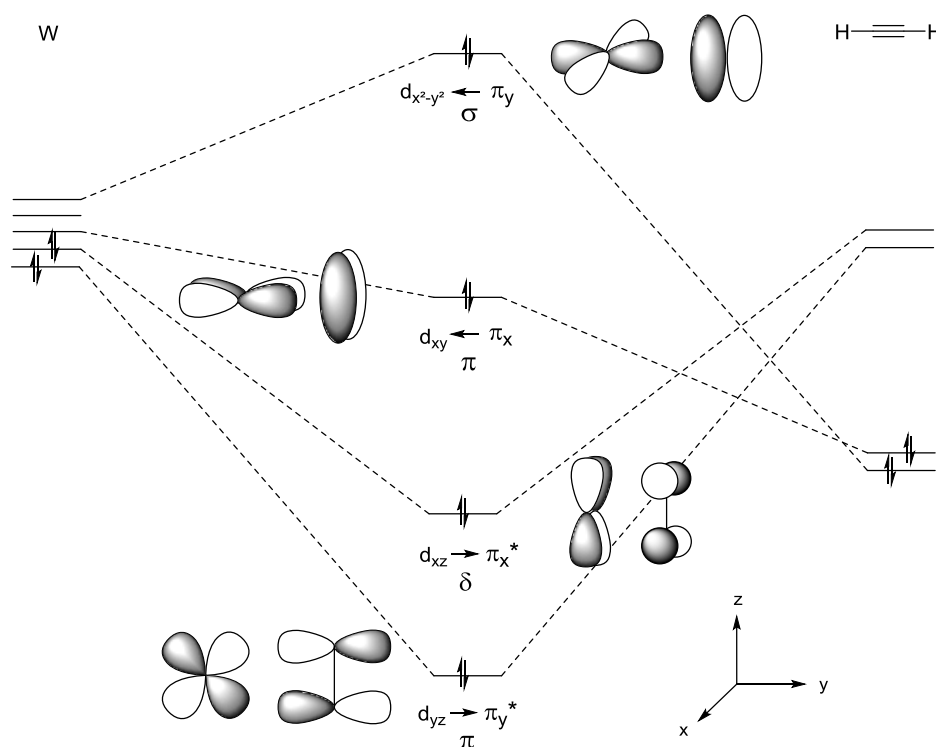
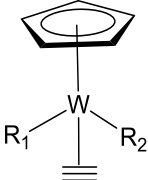
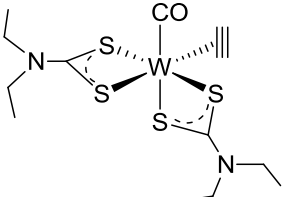
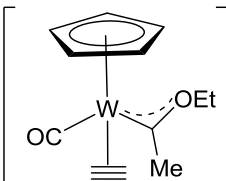
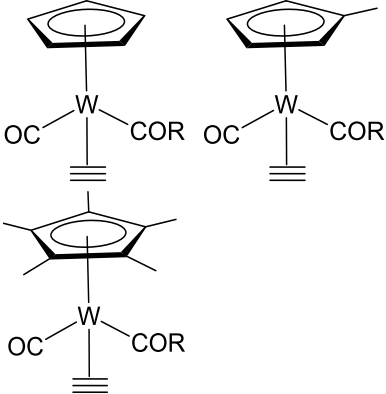


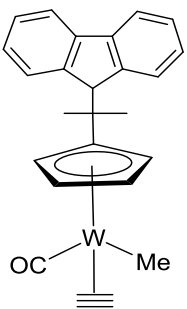
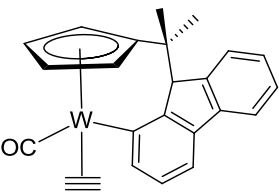
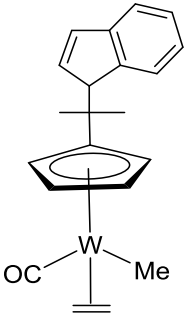
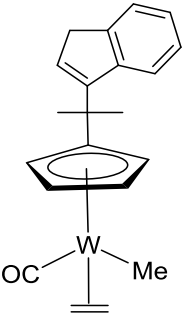
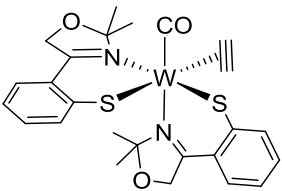
Figure 25: MO scheme for the coordination of acetylene by a d^4 metal center. The energy of the d orbitals is not considered in a quantitative manner.^{32,39}

4.1.1 Examples of Tungsten(II) Acetylene Complexes

The coordination of unsubstituted acetylene is quite challenging as this small molecule is not additionally activated by substituents like electron withdrawing carboxyl groups or electron donating methyl groups. Ricard *et al.* were the first ones to succeed in preparing and fully characterizing the first mononuclear tungsten(II) acetylene complex containing a sulfur-rich environment in 1978.⁷⁸ At present, there are several mononuclear tungsten(II) acetylene complexes known in literature, however, only five of them could be crystallized so far.^{78–80} In Table 2, all literature-known mononuclear tungsten(II) acetylene complexes are summarized sorted by year.

Table 2: Summary of all literature-known monomeric tungsten(II) acetylene complexes sorted by year.

Complex	R	Year	Reference
	$R_1 = \text{Me}; R_2 = \text{CO}$ $R_1 = \text{COMe}; R_2 = \text{CO}$ $R_1 = \text{COMe}; R_2 = \text{P(OMe)}_3$ $R_1 = \text{COMe}; R_2 = \text{PMe}_3$	1977	Alt ⁸¹
		1978	Ricard <i>et al.</i> ⁷⁸
[W(CO)(η^2 -C ₂ H ₂)(S ₂ CNMe ₂) ₂]		1980	Ward <i>et al.</i> ⁸²
[Wl ₂ (CO) ₂ (η^2 -C ₂ H ₂)R]	R = PMe ₃ , AsMe ₃	1982	Umland <i>et al.</i> ⁸³
		1983	Alt ⁸⁴
	R = Me, Et, Pr, Bu, Ph	1985	Alt ⁸⁵

$[\text{W}(\text{CO})(\eta^2\text{-C}_2\text{H}_2)(\text{MA})(\text{S}_2\text{CNEt}_2)_2]$	1985	Morrow <i>et al.</i> ⁸⁶
	1991	Alt <i>et al.</i> ⁸⁷
		
	1993	Alt <i>et al.</i> ⁸⁸
		
$[\text{W}(\text{CO})(\eta^2\text{-C}_2\text{H}_2)(\text{Tp}')]$	1997	Wells <i>et al.</i> ⁸⁹
$[\text{W}(\text{CO})_2(\eta^2\text{-C}_2\text{H}_2)(\text{Tp}')][\text{OTf}]$		
$[\text{W}(\text{CO})(\eta^2\text{-C}_2\text{H}_2)(\text{CN})(\text{Tp}')]$		
$[\text{W}(\text{CO})(\eta^2\text{-C}_2\text{H}_2)(\text{CNR})(\text{Tp}')]$	R = BF ₃	1998
$[\text{W}(\text{CO})(\eta^2\text{-C}_2\text{H}_2)(\text{CNR})(\text{Tp}')][\text{OTf}]$	R = H, Me	Frohnafel <i>et al.</i> ⁹⁰
	2015	Peschel <i>et al.</i> ⁷⁹
$[\text{W}(\text{CO})(\eta^2\text{-C}_2\text{H}_2)(\text{NCMe})(\text{Tp}')][\text{OTf}]$		
$[\text{W}(\text{CO})(\eta^2\text{-C}_2\text{H}_2)(\text{N}=\text{CHCH}_3)(\text{Tp}')]$		
$[\text{W}(\text{CO})(\eta^2\text{-C}_2\text{H}_2)(\text{NH}=\text{CHCH}_3)(\text{Tp}')][\text{BF}_4]$		
$[\text{W}(\text{CO})(\eta^2\text{-C}_2\text{H}_2)(\text{N}(\text{CH}_3)=\text{CHCH}_3)(\text{Tp}')][\text{OTf}]$	2016	Beattie <i>et al.</i> ⁸⁰
$[\text{W}(\text{CO})(\eta^2\text{-C}_2\text{H}_2)(\text{N}(\text{CH}_2\text{CH}_3)=\text{CHCH}_3)(\text{Tp}')][\text{OTf}]$		
$[\text{W}(\text{CO})(\eta^2\text{-C}_2\text{H}_2)(\text{NCH}(\text{CH}_3)\text{CPh}_3)(\text{Tp}')][\text{BF}_4]$		
$[\text{W}(\text{CO})(\eta^2\text{-C}_2\text{H}_2)(\text{NCH}(\text{CH}_3)\text{C}(\text{C}_6\text{H}_4\text{OCH}_3)\text{-Ph}_2)][\text{BF}_4]$		

4.2 Bonding Situation in Oxtungsten(IV) Acetylene Complexes

So far, eight of ten mononuclear tungsten(IV) acetylene complexes known in literature contain an oxo ligand which makes them exhibit different structural characteristics compared to the previously discussed carbonyl tungsten(II) acetylene complexes. The oxo ligand is supposed to donate two electrons from an sp hybrid orbital to form a dative metal-oxygen σ bond, while leaving the two orthogonal orbitals p_x and p_y to interact with the metal d_{xz} and d_{yz} orbitals. Given that oxygen π donation is consistent with occupation of the d_{xy} orbital with d_{yz} vacant, orientation of acetylene approaching along the y axis with $\alpha = 90^\circ$ (Figure 26) is preferred. This rotamer allows d_{xy} to donate into π_y^* , while π_z can perform π backbonding into the d_{yz} AO, both compatible with oxo π -effects. Hence, d_{yz} , the p_y orbital of oxygen and the π_z MO of acetylene produce a three-center, four-electron bond. The rotameric configuration with $\alpha = 90^\circ$ is calculated to be 17.3 kcal/mol lower in energy than the parallel configuration with $\alpha = 0^\circ$. This difference results from conflicting $d\pi$ interactions.³⁹

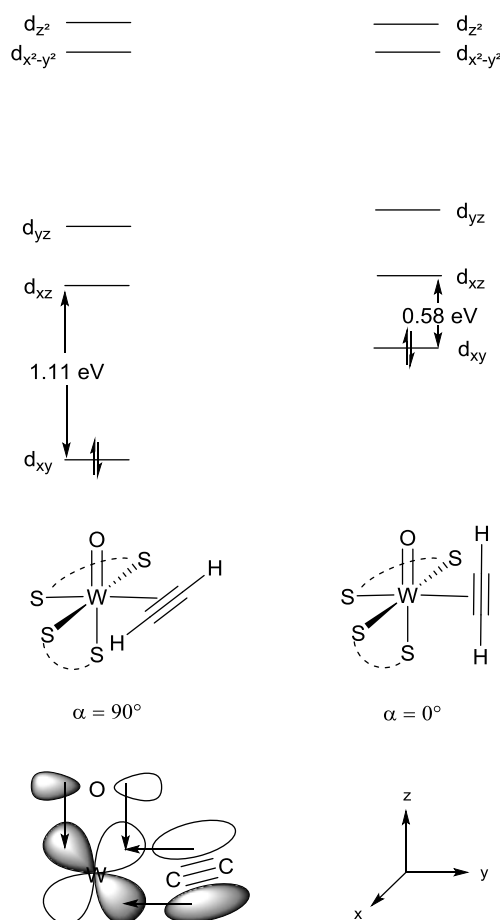


Figure 26: Relative frontier orbital energies in oxotungsten(IV) acetylene complexes as a function of the alkyne rotation angle and favorable orbital overlap in the structure with $\alpha = 90^\circ$.³⁹

The MO scheme of an oxo tungsten(IV) acetylene complex only considering the interactions of tungsten and acetylene is shown in Figure 27.

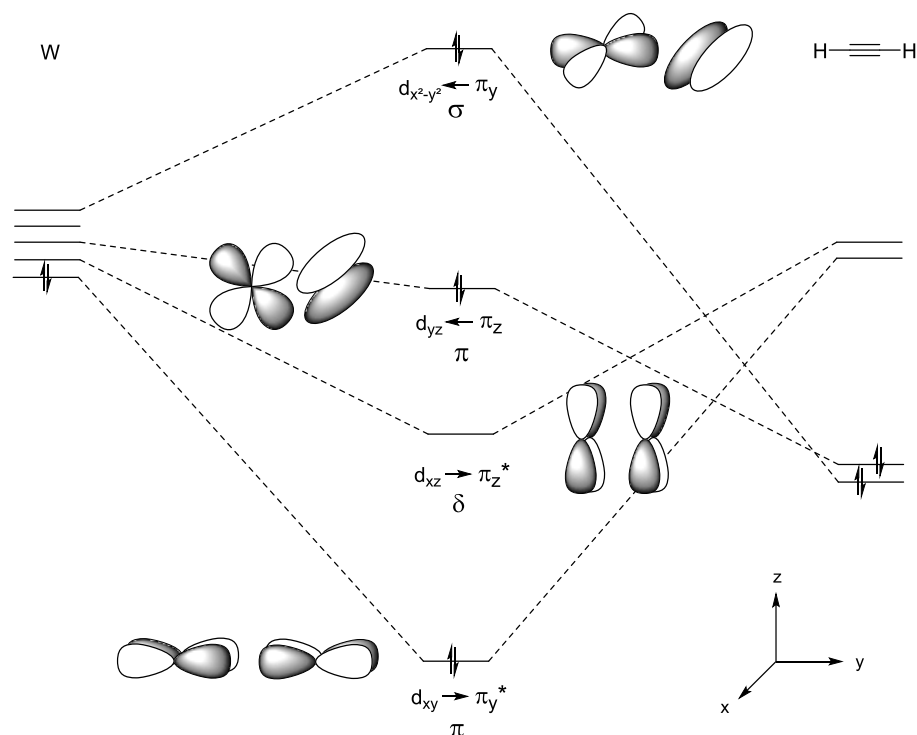


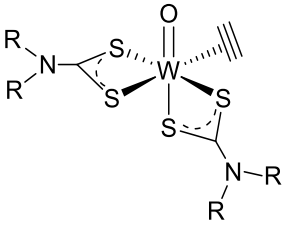
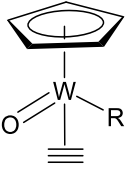
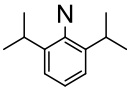
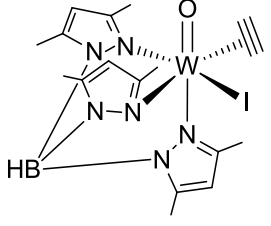
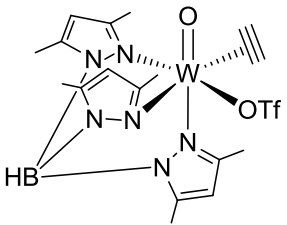
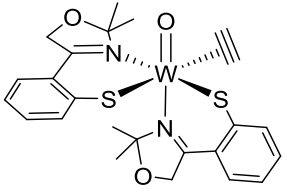
Figure 27: MO scheme for the coordination of acetylene by a d^2 metal center. The energy of the d orbitals is not considered in a quantitative manner.³⁹

4.2.1 Examples of Tungsten(IV) Acetylene Complexes

The very first synthesis of the oxotungsten(IV) acetylene complexes $[WO(\eta^2-C_2H_2)(S_2CNR_2)_2]$ ($R = Me, Et$) by controlled oxidation of $[W(CO)(\eta^2-C_2H_2)(S_2CNR_2)_2]$ with the dimeric oxygen atom transfer (OAT) reagent $[Mo_2O_3(S_2P(OEt)_2)_4]$ was reported by Templeton *et al.* in 1981.⁹¹ Tungsten(IV) acetylene complexes are genuinely scarce as the synthesis of these compounds is rather challenging because of the preference of tungsten to be in oxidation state +VI. However, another monomeric oxotungsten(IV) acetylene complex, which employs a biomimetic S,N -ligand, was successfully prepared by Peschel *et al.* in 2015. Upon exposure to visible light, the complex $[WO(\eta^2-C_2H_2)(S-Phoz)_2]$ releases its coordinated acetylene to yield the fourteen-electron species $[WO(S-Phoz)_2]$. Under exclusion of light, the formerly released acetylene can be re-coordinated by the tungsten(IV) center which makes this the first fully characterized system for the reversible activation of acetylene. Besides, $[WO(\eta^2-C_2H_2)(S-Phoz)_2]$ is the only tungsten(IV) acetylene complex which could be

crystallized so far.⁷⁹ In Table 3, all literature-known monomeric tungsten(IV) acetylene complexes are summarized sorted by year.

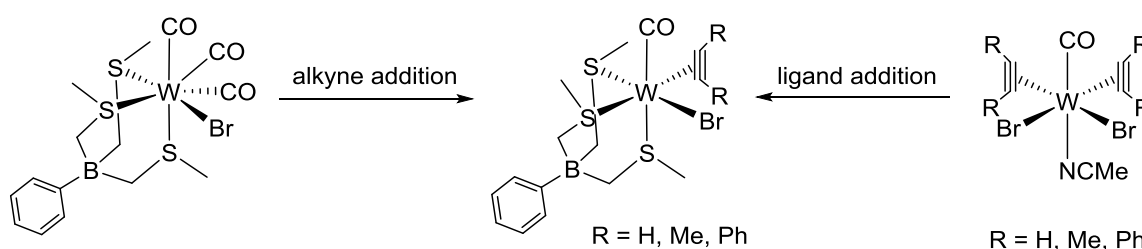
Table 3: Summary of all literature-known monomeric tungsten(IV) acetylene complexes sorted by year.

Complex	R	Year	Reference
	R = Me R = Et	1981	Templeton <i>et al.</i> ⁹¹
	R = Me R = COMe	1986	Alt <i>et al.</i> ⁹²
$[\text{WCl}_4(\eta^2\text{-C}_2\text{H}_2)(\text{Et}_2\text{O})]$		1989	Kersting <i>et al.</i> ⁹³
$[\text{W}(\eta^2\text{-C}_2\text{H}_2)(\text{PMe}_2\text{Ph})\text{R}_2]$	R = 	1993	Williams <i>et al.</i> ⁹⁴
		1999	Crane <i>et al.</i> ⁹⁵
		2000	Crane <i>et al.</i> ⁹⁶
$\left[\text{W}(\eta^2\text{-C}_2\text{H}_2)(\text{OTf})(\text{OH}_2) \right] [\text{OTf}]$			
		2015	Peschel <i>et al.</i> ⁷⁹

5 OBJECTIVES

The chemical way of gaining insight into the mechanism of acetylene hydration catalyzed by the unique enzyme acetylene hydratase, present in *Pelobacter acetylenicus*, is the development and preparation of a functional model of the tungsten-containing active site. The only functional model known so far is the oxotungsten(IV) complex $[\text{Et}_4\text{N}]_2[\text{WO}(\text{mnt})_2]$ which was synthesized and investigated by Sarkar *et al.* in 1996/1997.^{28,45}

Due to the rarity of functional models of acetylene hydratase, the main objective of this thesis is the preparation and investigation of a potential functional model of the active site of this tungstoenzyme by utilizing the bioinspired thioether scorpionate ligand [PhTt].⁶⁸ The introduction of this tripodal ligand would be favorable not only in terms of the sulfur-rich environment it is able to provide, but also with regard to the stability of the resulting complex due to the chelate effect. The ligand salt $[\text{Bu}_4\text{N}][\text{PhTt}]$ is well-known in literature and accessible in rather moderate yield via a one-pot synthesis.^{68,97} The main focus lies on the preparation of a sulfur-rich tungsten(II) complex which is able to coordinate an unsubstituted acetylene molecule. Furthermore, tungsten(II) complexes containing the symmetrically substituted alkynes 2-butyne and diphenylacetylene are of great interest because of their easier accessibility and also for comparative purposes. Therefore, two different synthetic approaches – “alkyne addition” and “ligand addition” – are to be investigated to get access to the desired complexes (Scheme 4).



Scheme 4: Different synthetic approaches to get access to a tungsten(II) acetylene complex: “alkyne addition” and “ligand addition”.

Starting from the literature-known precursor $[\text{WBr}_2(\text{CO})_3(\text{NCMe})_2]$, the complex $[\text{WBr}(\text{CO})_3(\text{PhTt})]$, which serves as entry point for the “alkyne addition” method, is prepared and investigated regarding its reactivity towards the symmetric alkynes acetylene, 2-butyne and diphenylacetylene.

The tungsten(II) alkyne precursors $[\text{WBr}_2(\text{CO})(\eta^2\text{-C}_2\text{R}_2)_2(\text{NCMe})]$ ($\text{R} = \text{H}, \text{Me}, \text{Ph}$), which serve as entry point for the “ligand addition” method, are accessible via reaction of $[\text{WBr}_2(\text{CO})_3(\text{NCMe})_2]$ with acetylene, 2-butyne or diphenylacetylene.^{55,98,99} The reaction of these precursors with the ligand $[\text{PhTt}]$ has to be investigated. In the end, both ways ought to lead to the same result, if the actual sulfur-containing complex $[\text{WBr}(\text{CO})_3(\text{PhTt})]$ is capable of coordinating the respective alkyne.

As a consequence of the chosen monoanionic, tripodal ligand, one bromo ligand remains coordinated on tungsten, thereby allowing for further fine-tuning of electronic or steric properties. This would also allow to substitute the remaining bromo ligand with a mono- or bidentate sulfur ligand in order to make the tungsten center even more sulfur-rich in case of insufficient reactivity towards alkynes.

Oxidation of the tungsten(II) alkyne complexes to the corresponding biologically relevant tungsten(IV) complexes is explored by using the OAT reagents pyridine-*N*-oxide, trimethylamine-*N*-oxide and *tert*-butyl hydroperoxide (TBHP). At this point, the remaining bromo ligand in $[\text{WOB}(\eta^2\text{-C}_2\text{R}_2)(\text{PhTt})]$ could be abstracted by addition of silver triflate, whereupon a water molecule may take its place, resulting in a cationic complex.⁹⁶

In principle, the desired complex $[\text{WOB}(\eta^2\text{-C}_2\text{R}_2)(\text{PhTt})]$ would therefore be capable of addressing both reaction mechanisms proposed for AH. Regarding the first shell mechanism investigated by Liao *et al.*, a free water molecule could perform a nucleophilic attack on the η^2 -acetylene and acetaldehyde formation is implemented with the aid of a base.³⁴ Considering the second shell mechanism proposed by Seiffert *et al.*, a coordinated water molecule could be nucleophilically attacked by a free acetylene molecule.^{30,96}

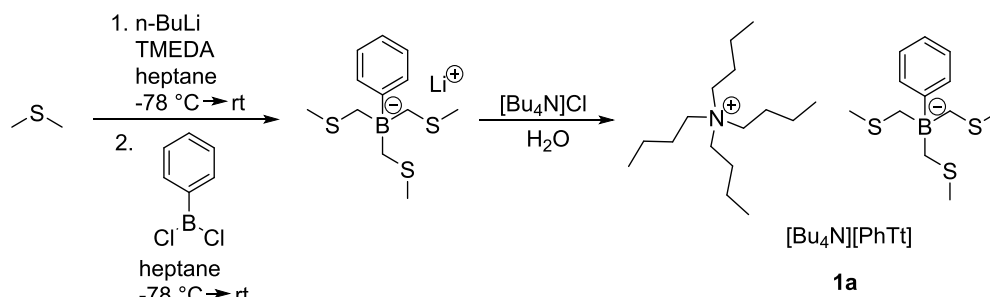
II RESULTS AND DISCUSSION

1 LIGAND SYNTHESIS

The bioinspired tris(thioether)borate ligand [PhTt] is well established in literature, with numerous complexes of Fe(II), Co(II), Ni(II), Cu(I), Zn(II), Pd(II) and Cd(II), but none of W.^{68–70} In order to prepare an active site model of the tungstoenzyme AH, the ligands [PhTt] and, to minor extend, [PhTt^{Bu}] were investigated in terms of their reactivity towards W(II) precursors with or without coordinated acetylene or other symmetric alkynes.

1.1 [Bu₄N][PhTt]

The ligand salt [Bu₄N][PhTt] (**1a**) was synthesized according to a modified literature procedure.^{68,97} Therefore, dimethyl sulfide was deprotonated by *n*-BuLi in the presence of TMEDA, and the resulting organolithium compound, LiCH₂SCH₃(TMEDA), reacted with 1 equiv. of dichlorophenylborane diluted with heptane (Scheme 5). After 48 hours, the reaction was completed and an aqueous work-up was performed. The product was precipitated by addition of aqueous [Bu₄N]Cl to the aqueous phase and isolated by filtration as white, flocculent powder in 44 % yield. The ligand salt [Bu₄N][PhTt] is soluble in chlorinated hydrocarbons, acetonitrile, THF and acetone and stable to both oxygen and moisture. ¹H NMR data were consistent with literature and showed four multiplets for Bu₄N⁺, three signals for the phenyl ring, a singlet at $\delta = 1.94$ ppm for all three SCH₃ groups and a quadruplet at $\delta = 1.80$ – 1.76 ppm for all three BCH₂ groups.⁶⁸



Scheme 5: Synthetic procedure of [Bu₄N][PhTt] (**1a**).⁶⁸

The synthesis of **1a** was quite challenging when performed according to neat literature procedures. It was found that the use of an additional solvent is crucial when carrying

out the reaction on a small scale because of the extreme reactivity and sensitivity of dichlorophenylborane. In order to optimize the ligand synthesis, the lithiation reaction was investigated separately. Therefore, a solution of heptane, TMEDA, dimethylsulfide and n-BuLi was stirred for four hours. Subsequent removal of the solvent yielded $\text{LiCH}_2\text{SCH}_3(\text{TMEDA})$ (**3**) as off-white powder in 100 % yield. The identity and purity of this compound was confirmed by comparison of obtained ^1H NMR data with literature values.¹⁰⁰ Consequently, the nucleophilic attack on the boron is the critical step of the overall reaction. The modification of the procedure includes the use of 60 mL heptane in the beginning and the addition of a solution of dichlorophenylborane in heptane instead of the pure, extremely reactive reagent. With this slightly modified procedure, the yield of Riordan *et al.* from 1996 could be reproduced.⁶⁸ Interestingly, the yield of 63 %, published by Tillmann *et al.* in 2010, could never be obtained.⁹⁷

Despite different purification attempts including flash chromatography, extraction with different solvents and filtration through Celite, the complete removal of LiCl and TMEDA and, consequently, the isolation of pure Li[PhTt] remained unsuccessful. The only reasonable way of preparing TMEDA-free Li[PhTt] is to deprotonate excess dimethylsulfide with n-BuLi in the absence of TMEDA by keeping it at reflux temperature for one week and subsequently react the resulting donor-free $\text{LiCH}_2\text{SCH}_3$ with dichlorophenylborane. This procedure was avoided for large-scale reactions because of the explosiveness of donor-free methylthiomethyl lithium when exposed to air and above temperatures of 160 °C even under argon atmosphere.^{101,102}

Since salt metathesis of **1a** leads to the formation of $[\text{Bu}_4\text{N}]\text{X}$ ($\text{X} = \text{Cl}, \text{Br}, \text{I}$), which is hard to remove from a reaction mixture because of its solubility in nearly every solvent, the introduction of a different cation was investigated. Therefore, the aqueous phase was treated with aqueous TlNO_3 or CsCl to precipitate the corresponding ligand salt. Precipitation with TlNO_3 gave a brown, sticky solid which is hardly soluble in any solvent. However, ^1H NMR signals similar to those observed for **1a** could be detected in CD_3CN . Precipitation with CsCl gave a white powder which was identified as Cs[PhTt] (**1**) by ^1H and ^{13}C NMR spectroscopy. Although both precipitation methods were successful, the use of CsCl is preferable because of the better solubility of **1** and the nontoxicity of Cs salts.

1.2 Cs[PhTt]

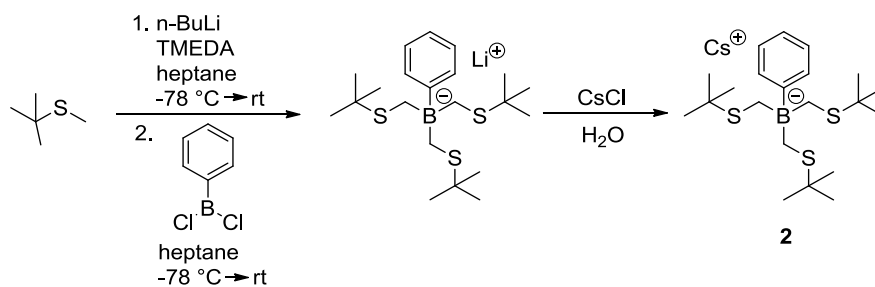
The ligand salt Cs[PhTt] was prepared in a procedure analogous to that for **1a**, but using aqueous CsCl instead of [Bu₄N]Cl in the last step. The product was isolated as white, flocculent powder in 43 % yield. Cs[PhTt] is soluble in acetonitrile, acetone and DMSO, insoluble chlorinated hydrocarbons and stable to both oxygen and moisture. ¹H NMR data of Li[PhTt](TMEDA)₂, [Bu₄N][PhTt], Cs[PhTt] and Tl[PhTt] in CD₃CN are compared in Table 4, demonstrating that the cation has no evident influence on the chemical shifts.

Table 4: Comparison of ¹H NMR data of Li[PhTt](TMEDA)₂, [Bu₄N][PhTt], Cs[PhTt] and Tl[PhTt] in CD₃CN.

δ (ppm)	Li[PhTt](TMEDA) ₂	[Bu ₄ N][PhTt]	Cs[PhTt]	Tl[PhTt]
<i>o</i> -C ₆ H ₅	7.37	7.38	7.40	7.37
<i>m</i> -C ₆ H ₅	7.00–6.95	7.01–6.96	7.07–7.03	7.00–6.96
<i>p</i> -C ₆ H ₅	6.85–6.80	6.85–6.81	6.92–6.87	6.85–6.80
SCH ₃	1.92	1.94	1.93	1.92
BCH ₂	1.79–1.75	1.80–1.76	1.79–1.75	1.79–1.75

1.3 Cs[PhTt^{tBu}]

Cs[PhTt^{tBu}] (**2**) was synthesized according to a modified published procedure.^{72,73} Therefore, *tert*-butyl methyl sulfide was deprotonated by *n*-BuLi in the presence of TMEDA, and the resulting organolithium compound reacted with 1 equiv. of dichlorophenylborane diluted with heptane (Scheme 6). As ¹H NMR data did not show reaction completion after 24 hours, the reaction was terminated after 48 hours, and an aqueous work-up was performed. The product was precipitated by addition of aqueous CsCl to the aqueous phase and collected by filtration as white powder in 2 % yield. Cs[PhTt^{tBu}] is soluble in acetonitrile, acetone, DMSO and THF, but insoluble in chlorinated hydrocarbons.



Scheme 6: Synthetic procedure of Cs[PhTt^{Bu}] (**2**).^{72,73}

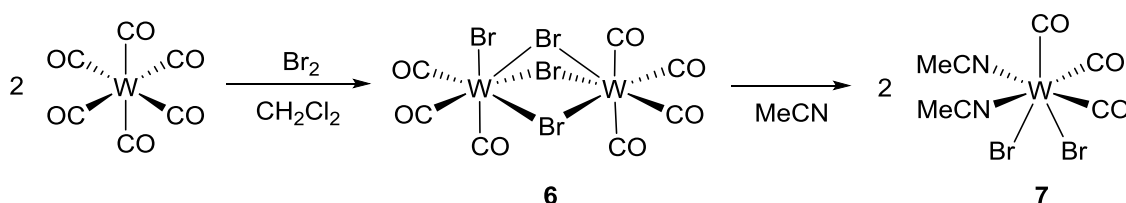
Because of the low yield obtained in the first attempt, the preparation of this ligand was not further investigated. However, the low yield can be explained by minor conversion to Li[PhTt^{Bu}], even after a reaction time of 48 hours, which was determined by ¹H NMR spectroscopy of the crude product.

It was not possible to compare the outcome of the reaction directly to the synthetic strategy developed by Riordan *et al.*, as they did not mention the yield of **2** in their publication.⁷³ They only stated the yield of the corresponding TI salt to be 22 % which is a lot in comparison to the outcome of the synthetic approach applied in this thesis.⁷²

2 PRECURSOR SYNTHESIS

2.1 [WBr₂(CO)₃(NCMe)₂]

The monomeric tungsten(II) precursor [WBr₂(CO)₃(NCMe)₂] (**7**) was prepared according to a modified literature procedure (Scheme 7).^{99,103}



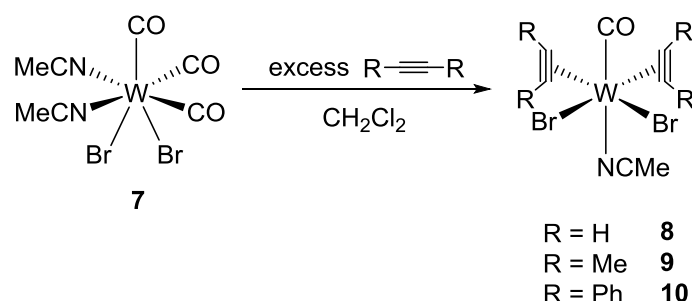
Scheme 7: Two-step synthetic procedure of [WBr₂(CO)₃(NCMe)₂] (**7**).

In the first step, the monomeric tungsten(0) complex [W(CO)₆] was oxidized with Br₂ in dichloromethane at -20 °C to give the dimeric tungsten(II) complex [W₂Br₄(CO)₇] (**6**) as orange-brown powder in 90 % yield. The identity of **6** was confirmed by IR spectroscopy with C≡O stretching vibrations at 2105, 2019, 1998, 1969, 1960, 1943 and 1924 cm⁻¹. Compound **6** is moderately soluble in chlorinated hydrocarbons. It can

be dissolved in coordinating solvents like acetonitrile or THF with concomitant formation of the corresponding monomeric $[\text{WBr}_2(\text{CO})_3]$ -solvent adduct. In the second step, **6** was therefore stirred in acetonitrile for one hour and the resulting mixture was filtrated through Celite to remove insoluble impurities. The filtrate was concentrated *in vacuo*, thereby precipitating $[\text{WBr}_2(\text{CO})_3(\text{NCMe})_2]$ (**7**) as deep red microcrystalline powder in 82 % yield. Complex **7** is soluble in acetonitrile and chlorinated hydrocarbons and instable to both air and moisture. The identity of **7** was confirmed by IR spectroscopy with $\text{C}\equiv\text{O}$ stretching vibrations at 2023, 1909 and 1896 cm^{-1} and $\text{C}\equiv\text{N}$ stretches of 2318 and 2291 cm^{-1} which are in good agreement with literature data.⁹⁹ The overall yield of the two-step synthesis is 74 % which is quite reasonable regarding the high purity of the resulting tungsten(II) precursor.

2.2 $[\text{WBr}_2(\text{CO})(\eta^2\text{-C}_2\text{R}_2)_2(\text{NCMe})]$

In order to investigate the “ligand addition” method, the tungsten(II) bis(alkyne) precursors $[\text{WBr}_2(\text{CO})(\eta^2\text{-C}_2\text{R}_2)(\text{NCMe})]$ ($\text{R} = \text{H}$ (**8**), Me (**9**), Ph (**10**)) have been prepared according to a modified literature procedure (Scheme 8).⁹⁹



Scheme 8: Synthesis of the precursors $[\text{WBr}_2(\text{CO})(\eta^2\text{-C}_2\text{R}_2)_2(\text{NCMe})]$ ($\text{R} = \text{H}$ (**8**), Me (**9**), Ph (**10**)).

The complexes $[\text{WBr}_2(\text{CO})(\eta^2\text{-C}_2\text{R}_2)(\text{NCMe})]$ ($\text{R} = \text{Me}$ (**9**), Ph (**10**)) were synthesized by adding 3 equiv. of 2-butyne and diphenylacetylene, respectively, to a stirred solution of $[\text{WBr}_2(\text{CO})_3(\text{NCMe})_2]$ (**7**) in dichloromethane at 0 °C. After stirring for 17 hours at rt, the reaction mixture was filtrated, and the filtrate was reduced to 10 mL. The product was crystallized from dichloromethane/heptane and subsequently dried *in vacuo* to give **9** as olive green crystals and **10** as yellow, needle-shaped crystals in 96 % yield.

Complex **9** displays good solubility in chlorinated hydrocarbons, acetonitrile and THF and is moderately sensitive towards air and moisture in solid state. The obtained NMR

and IR data are inconsistent with literature data.⁵⁵ Nevertheless, the identity of **9** could be confirmed by comparison of NMR and IR data obtained within the working group which were verified by the first crystal structure of **9**.¹⁰⁴ A comparison of ¹H NMR data in CDCl₃ and IR data obtained in the course of this work and by Baker *et al.* is shown in Table 5.⁵⁵ Interestingly, a difference in chemical shifts of 1 ppm can be observed for the protons of one methyl substituent on the alkyne, although those of the other substituent display the same chemical shift. A significant difference in chemical shifts could also be found for the protons of the coordinated acetonitrile. As a chemical shift of 2.02 ppm in CDCl₃ is indicative for uncoordinated acetonitrile, Baker *et al.* probably mixed the signals since the signal resulting from the coordinated acetonitrile sometimes overlaps with the signal of the protons of 2-butyne at 2.83 ppm. The frequencies of the C≡N stretching vibrations are nearly identical, whereas those of the C≡O stretching vibrations display a difference of 35 cm⁻¹.

Table 5: Comparison of ¹H NMR data in CDCl₃ and IR data of **9**.

	This work	Baker <i>et al.</i> ⁵⁵
δ (\equiv -CH ₃) (ppm)	2.89	3.91
δ (CH ₃ CN) (ppm)	2.85	2.02
δ (\equiv -CH ₃) (ppm)	2.83	2.84
ν (C≡N) (cm ⁻¹)	2326	2322
ν (C≡N) (cm ⁻¹)	2298	2296
ν (C≡O) (cm ⁻¹)	2035	2070

Complex **10** is well soluble in chlorinated hydrocarbons and THF, but only to a minor extent in acetonitrile. IR spectroscopy revealed one C≡O stretching vibration at 2099 cm⁻¹. The identity of **10** was confirmed by both NMR and IR spectroscopy.⁵⁵

The electronic properties of the complexes [WBr₂(CO)(η^2 -C₂R₂)₂(NCMe)] (R = H (**8**), Me (**9**), Ph (**10**)) can be compared regarding the stretching frequencies of the respective carbonyl ligand (Table 6). Since a methyl group is considered as an EDG, the σ and π donation of 2-butyne to the tungsten center in **9** is stronger than the σ donation of acetylene in **8**. Hence, the tungsten center of [WBr₂(CO)(η^2 -C₂Me₂)₂(NCMe)] can provide more electron density and therefore perform a stronger π backbonding to the CO ligand. By filling an anti-bonding orbital of CO, the C≡O bond

is weakened, leading to the decrease of the C≡O stretching frequency and making the carbon atom more electrophilic. The electrophilic character of the carbon atom can be identified by means of ^{13}C NMR spectroscopy. The opposite effect is observed in complex **10** due to the electron withdrawing character of the phenyl groups attached to the coordinated alkyne.^{99,104}

Table 6: Comparison of IR and ^{13}C NMR data in CD_2Cl_2 of the carbonyl ligands of complexes **8–10**.

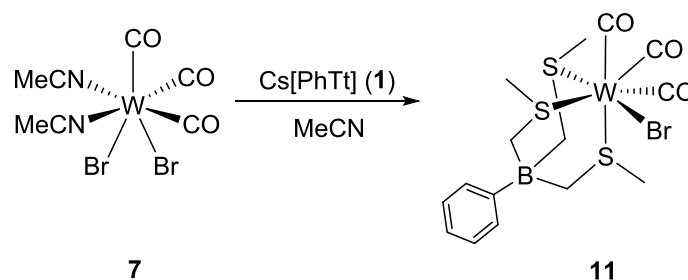
Complex	$\nu(\text{C}\equiv\text{O})$ (cm^{-1})	$\delta(\text{C}\equiv\text{O})$ (ppm)
$[\text{WBr}_2(\text{CO})(\eta^2\text{-C}_2\text{H}_2)(\text{NCMe})]$ (8) ¹⁰⁴	2069	a
$[\text{WBr}_2(\text{CO})(\eta^2\text{-C}_2\text{Me}_2)(\text{NCMe})]$ (9)	2034	207.73
$[\text{WBr}_2(\text{CO})(\eta^2\text{-C}_2\text{Ph}_2)(\text{NCMe})]$ (10)	2099	201.57

^a Complex **8** is badly soluble in every solvent.

3 COMPLEX SYNTHESIS

3.1 $[\text{WBr}(\text{CO})_3(\text{PhTt})]$

In order to investigate the “alkyne addition” method for the preparation of $[\text{W}(\text{CO})(\eta^2\text{-C}_2\text{R}_2)\text{L}(\text{PhTt})]$, the precursor complex $[\text{WBr}(\text{CO})_3(\text{PhTt})]$ (**11**) was synthesized in the first place (Scheme 9). Therefore, a solution of $\text{Cs}[\text{PhTt}]$ (**1**) was slowly added to a solution of $[\text{WBr}_2(\text{CO})_3(\text{NCMe})]$ (**7**) in acetonitrile. At the end of the addition, the formation of CsBr and crystallization of **11** could be observed. After an overall reaction time of one hour, the reaction mixture was concentrated and finally filtrated. Then, the solid was suspended in dichloromethane and filtrated through Celite to remove CsBr . The product was recrystallized by addition of acetonitrile and subsequent slow evaporation to dryness. The obtained orange crystals were washed with acetonitrile to give **11** in 89 % yield.



Scheme 9: Synthetic procedure of $[\text{WBr}(\text{CO})_3(\text{PhTt})]$ (**11**).

Complex [WBr(CO)₃(PhTt)] is soluble in chlorinated hydrocarbons, benzene, toluene and THF, badly soluble in acetonitrile and Et₂O, insoluble in heptane and water, and stable to both moisture and air in solid state.

As expected, IR spectroscopy revealed three different C≡O stretching frequencies at 2026, 1940 and 1908 cm⁻¹. ¹H NMR spectra recorded in different solvents show only one sharp singlet for the protons of all three CH₃ groups and one broad signal for those of all three CH₂ groups which is in accordance with the ¹³C NMR spectrum. Besides, only one weak singlet at δ = 223.23 ppm was observed for all three CO ligands in the ¹³C NMR spectrum which is indicative for rather shielded carbonyl carbons. The equivalence of the signals is ascribed to the fluxionality of the complex in solution which is a typical property of seven-coordinate triscarbonyl tungsten(II) complexes.¹⁰⁴

A comparison of the chemical shifts observed in ¹H NMR spectra recorded in various solvents is given in Table 7. As expected, the proton shifts in benzene-d₆ are fairly different to those observed in the other solvents. Furthermore, the solvent stability of **11** was tested by pursuing the change of the corresponding ¹H NMR spectrum in a Young tube over a few days. However, decomposition of **11** does not lead to the emergence of a well-defined species, but rather to the disappearance of all signals in every solvent tested, accompanied by a color change from orange to dark brown and the formation of a white precipitate.

Table 7: Comparison of ¹H NMR data and stability of **11** in different solvents.

δ (ppm)	CD ₂ Cl ₂	CDCl ₃	CD ₃ CN	C ₆ D ₆
PhH	7.19–7.15 (m, 4H)	7.24–7.22 (m, 4H)	7.18–7.11 (m, 4H)	7.43–7.38 (m, 2H)
	7.07–7.01 (m, 1H)	7.15–7.07 (m, 1H)	7.02–6.98 (tt, 1H)	7.29–7.24 (m, 3H)
CH₃	2.79	2.79	2.78	2.15
CH₂	2.19–2.18	2.21	2.16–2.15	1.90
Stability	decomposition after 48 hours	decomposition after 48 hours	decomposition after 24 hours	decomposition after 5 days

The stability of [WBr(CO)₃(PhTt)] towards higher temperatures was investigated by means of in-situ IR spectroscopy. Therefore, a concentrated solution of **11** in toluene was continuously heated with an oil bath, thereby monitoring an intensity decrease of

the C≡O absorption bands. The complex solution was held at each temperature for at least 15 min. As shown in Figure 28, full decomposition of complex **11** was observed at 70 °C.

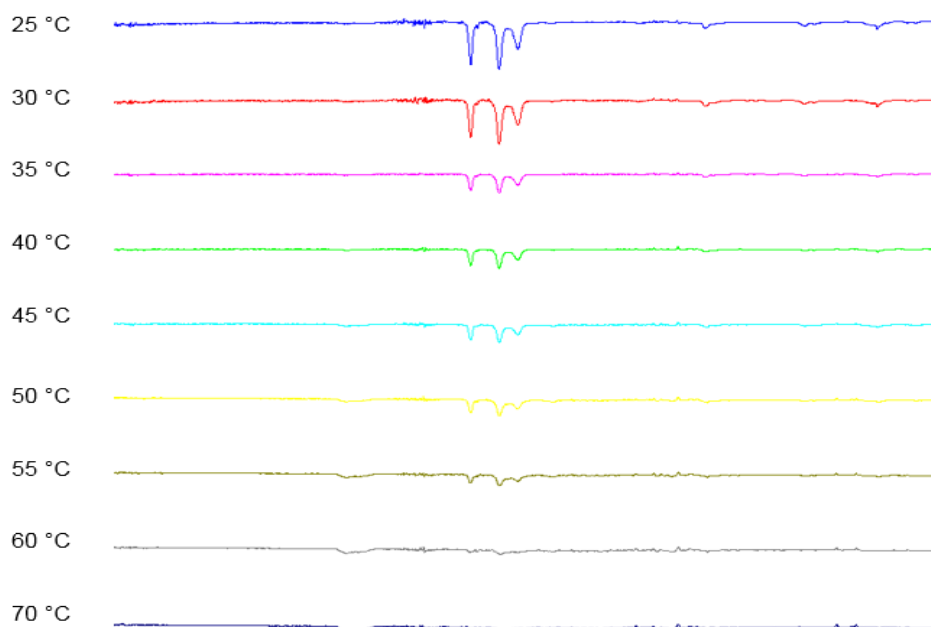


Figure 28: In-situ IR spectrum of **11** in toluene as a function of the temperature.

Complex **11** was found to be unstable towards higher temperatures probably because of the simultaneous dissociation of all carbonyl ligands due to thermal excitation and subsequent decomposition.¹⁰⁴ The dark brown decomposition product was divided into a soluble and an insoluble fraction. The soluble compound bears three different carbonyl ligands at 2030, 1907 and 1839 cm^{-1} , but its concentration in toluene was probably too low to be recognized by in-situ IR spectroscopy. ^1H NMR spectroscopy revealed no conclusive signals. The insoluble species bears no CO ligands and could neither be identified by ^1H NMR spectroscopy.

A comparison of the C≡O stretching frequencies of **11** to those of literature-known tricarbonyl tungsten(II) complexes containing either the scorpionate ligand Tm^{Me} or thioether ligands is given in Table 8. Complex **11** displays C≡O stretching frequencies similar to the thioether complexes, whereas $[\text{WBr}(\text{CO})_3(\text{Tm}^{\text{Me}})]$ contains CO ligands of lower stretching frequencies. Consequently, the electronic properties of **11** are more similar to those of the thioether complexes which are less electron-rich than $[\text{WBr}(\text{CO})_3(\text{Tm}^{\text{Me}})]$. This finding can be explained by different hybridization of the sulfur

donor atoms (sp^3 or sp^2) and different electronic properties due to the substituents on the sulfur atoms.

Table 8: Comparison of the C≡O stretching frequencies of $[W(CO)_3L_2]$.

Complex	ν (C≡O) (cm^{-1})
$[WBr(CO)_3(PhTt)]$ (11)	2026, 1940, 1908
$[WBr(CO)_3(Tm^{Me})]^{104}$	1996, 1902, 1882
$[WBr_2(CO)_3\{PhS(CH_2)_2SPh-S,S'\}]^{62}$	2035, 1965, 1908
$[WBr(CO)_3\{PhS(CH_2)_2SPh-S'\}\{PhS(CH_2)_2SPh-S,S'\}]Br^{62}$	2043, 1960, 1896
$[WBr_2(CO)_3\{MeS(CH_2)_2S(CH_2)_2SMe-S,S'\}]^{62}$	2036, 1950, 1905

Comparison of the C≡O stretching frequencies of **11** to those of carbonyl tungsten(II) complexes capable of acetylene coordination reveals significant differences (Table 9). The complexes $[W(CO)_2(PPh_3)(S_2CNMe_2)_2]$ and $[W(CO)_2(S-Phoz)_2]$ contain a more electron-rich tungsten center which is capable of strong π backbonding and consequent acetylene activation.

Table 9: Comparison of the C≡O stretching frequencies of **11** to C_2H_2 activating carbonyl tungsten(II) complexes.

Complex	ν (C≡O) (cm^{-1})
$[WBr(CO)_3(PhTt)]$ (11)	2026, 1940, 1908
$[W(CO)_2(PPh_3)(S_2CNMe_2)_2]^{105}$	1910, 1820
$[W(CO)_2(S-Phoz)_2]^{103}$	1917, 1807

Single crystals suitable for X-ray diffraction analysis were obtained by crystallization from acetonitrile at rt. A molecular view is depicted in Figure 29, a full list of bond lengths and angles is given in Table 16 (Appendix). Crystallographic data are summarized in Table 13 (Appendix).

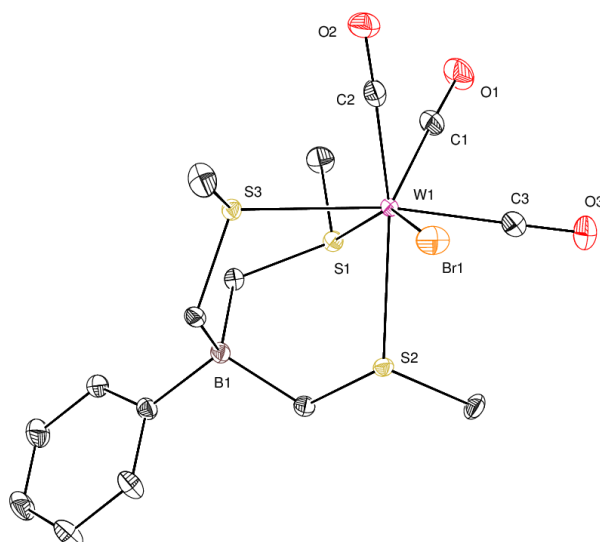


Figure 29: ORTEP¹⁰⁶ plot of **11** showing the atomic numbering scheme. The probability ellipsoids are drawn at the 50 % probability level. H atoms are omitted for clarity.

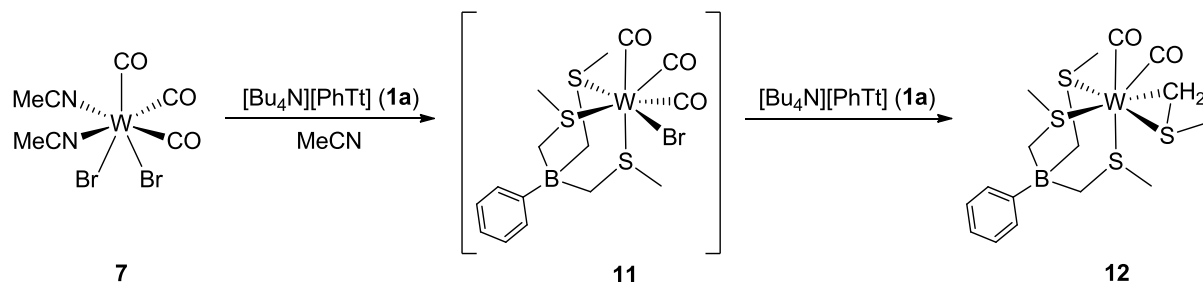
X-ray analysis of **11** shows a capped octahedral structure for the seven-coordinate tungsten(II) complex. The W–S bonds (2.5420(6)–2.5654(5) Å) of the tripodal ligand enclose rather small angles (S–W–S 75.837(18)°–87.232(19)°). In contrast to [WBr(CO)₃(Tm^{Me})], there is no CO ligand opposite the boron atom which was determined by comparison of crystallographic data.¹⁰⁴ The W–CO bonds are in the range of 1.972(3)–2.009(3) Å, and the W–Br bond length is 2.6517(3) Å.

The W–S bond lengths of **11** are similar to those of the thioether complex [WBr₂(CO)₃{PhS(CH₂)₂SPh-S,S}] (2.557(7) and 2.573(7) Å) and also to those found in [WBr(CO)₃(Tm^{Me})] (2.5361(10)–2.5913(11) Å), although the W–S bond lengths of the latter vary significantly due to the *trans* influence of the carbonyl ligand.^{62,104}

3.2 [WBr(CO)₂(η²-CH₂SCH₃)(PhTt)]

The novel tungsten(II) complex [WBr(CO)₂(η²-CH₂SCH₃)(PhTt)] (**12**) was formed as a side product by reaction of [WBr₂(CO)₃(NCMe)₂] with 1.3 equiv. of [Bu₄N][PhTt] in acetonitrile for at least four hours (Scheme 10). In order to isolate **12**, the dark brown, sticky crude product was dissolved in dichloromethane. The solution was saturated with heptane, and upon slow evaporation of dichloromethane, a brown, sticky solid was precipitated. The yellow supernatant solution was isolated by filtration and evaporated to dryness to give pure, but small amounts of a yellow powder, which could

be crystallized from acetonitrile and subsequently identified as **12** by X-ray diffraction analysis.



Scheme 10: Formation of complex **12** by reaction of **7** with excess $[\text{Bu}_4\text{N}][\text{PhTt}]$ (**1a**) in acetonitrile for at least four hours.

Complex **12** is soluble in chlorinated hydrocarbons, acetonitrile, benzene, toluene and THF, and crystals of **12** are stable to both moisture and air. The complex was found to be stable in dichloromethane solution at rt for a week. IR spectroscopy of the orange crystals revealed two $\text{C}\equiv\text{O}$ stretching vibrations at 1925 and 1810 cm^{-1} , indicative for an electron-rich tungsten center.

Single crystals suitable for X-ray diffraction analysis were obtained by crystallization from acetonitrile at rt. A molecular view is provided in Figure 30, a full list of bond lengths and angles is given in Table 17 (Appendix). Crystallographic data are summarized in Table 13 (Appendix).

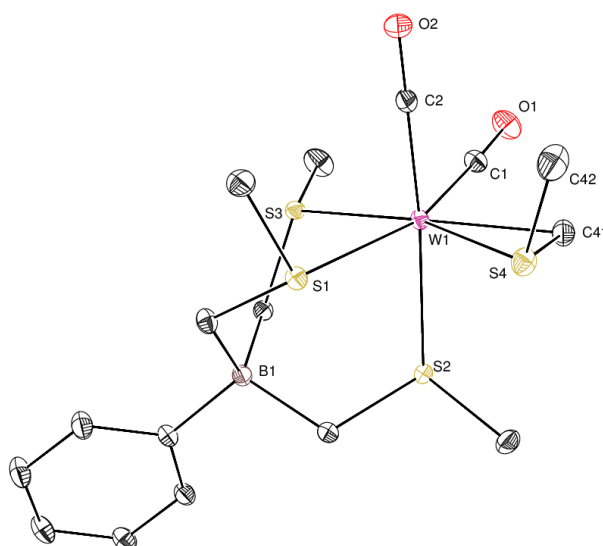


Figure 30: ORTEP¹⁰⁶ plot of **12** showing the atomic numbering scheme. The probability ellipsoids are drawn at the 50 % probability level. H atoms are omitted for clarity.

The octahedral coordination sphere of the tungsten center consists of the *fac* tripodal ligand (W1–S1 2.5528(3) Å, W1–S2 2.5804(3) Å, W1–S3 2.4999(3) Å), two CO ligands (W1–C1 1.9824(14) Å, C1–W1–S1 161.30(4)°; W1–C2 1.9267(14) Å, C2–W1–S2 175.03(4)°) and the side-on coordinated (methylthio)methyl ligand (S4–C41 1.7611(15) Å, W1–C41 2.2184(14) Å, W1–S4 2.4561(4) Å; S3–W1–S4 162.3A18(12)°, S3–W1–C41 150.47(4)°). The sulfur atoms S2 and S4 are practically orthogonal to each other (S4–W1–S2 89.237(12)°). The three-membered ring formed by tungsten and the bidentate (methylthio)methyl ligand is by its angles (C41–W1–S4 43.90(4)°, C41–S4–W1 60.86(5)° and S4–C41–W1 75.24(5)°) defined as an acute triangle.

Complex **12** was also characterized by ^1H NMR spectroscopy which revealed interesting features of the novel complex. For instance, the two protons on the (methylthio)methanide carbon atom coordinated to tungsten are diastereotopic. Hence, the corresponding ^1H NMR spectrum measured in dichloromethane- d_2 shows two symmetric doublets with a distinctive roof effect at $\delta = 3.31\text{--}3.29$ and $3.01\text{--}2.98$ ppm. Interestingly, the proton resonating at $\delta = 3.31\text{--}3.29$ ppm displays a weak coupling with the NMR active ^{183}W . The two protons of the CH_2 groups bound to the boron atom are also diastereotopic. They display two broad signals at $\delta = 2.20$ and 1.95 ppm integrating for three protons each, whereas the protons of the methyl groups of [PhTt] and the protons of the methyl group of (methylthio)methanide are equivalent, respectively. The protons of the methyl groups of [PhTt] resonate at $\delta = 2.66$ ppm, those of the methyl group of the (methylthio)methyl ligand at $\delta = 2.39$ ppm. A listing of all chemical shifts is given in Table 10.

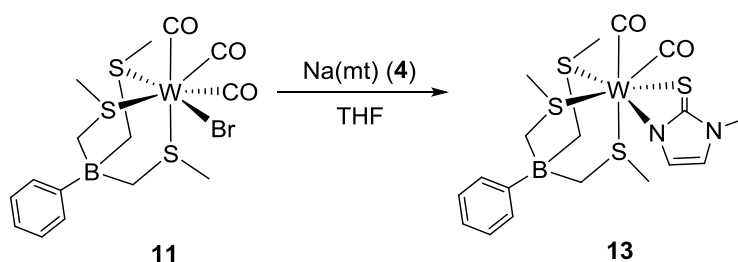
Table 10: Proton shifts of **12** displayed in dichloromethane- d_2 and acetonitrile- d_3 .

δ (ppm)	CD_2Cl_2	CD_3CN
	7.20 (m, 2H)	7.18 (m, 2H)
PhH	7.15–7.10 (t, 2H)	7.13–7.08 (t, 2H)
	7.00–6.96 (tt, 1H)	6.98–6.93 (tt, 1H)
WCH₂	3.31–3.29 (d, 1H)	3.34–3.31 (d, 1H)
	3.01–2.98 (d, 1H)	3.06–3.04 (d, 1H)
CH₃	2.66 (bs, 9H)	2.66 (bs, 9H)
CH₃	2.39 (s, 3H)	2.40 (s, 3H)
BCH₂	2.20 (m, 3H)	2.15 (m, 3H)
	1.95 (m, 3H)	1.91 (m, 3H)

Because of its favorable electronic and structural properties, the selective synthesis of **12** was attempted by reaction of **11** with $\text{LiCH}_2\text{SCH}_3(\text{TMEDA})$ (**3**) in toluene at rt. However, no formation of compound **12** or the tricarbonyl complex $[\text{W}(\text{CO})_3(\text{CH}_2\text{SCH}_3)(\text{PhTt})]$, with (methylthio)methanide end-on coordinated, could be observed by ^1H NMR spectroscopy. IR spectroscopy of the crude product revealed at least six different $\text{C}=\text{O}$ absorption bands ranging from $2018\text{--}1709\text{ cm}^{-1}$. Considering the low energies of the $\text{C}=\text{O}$ stretching vibrations (1793 , 1777 , 1719 and 1709 cm^{-1}), (methylthio)methanide probably performs a nucleophilic attack on the electrophilic carbonyl carbon atoms in addition to a substitution of the bromo ligand in a simple salt metathesis reaction. The formation of a tungsten-TMEDA complex can be excluded as the protons of all four methyl groups and both CH_2 groups of TMEDA were found to be chemically equivalent by means of NMR spectroscopy.¹⁰⁷

3.3 $[\text{W}(\text{CO})_2(\text{mt})(\text{PhTt})]$

Complex $[\text{WBr}(\text{CO})_3(\text{PhTt})]$ was investigated towards substitution of the bromo ligand with the bidentate *S,N*-ligand methimazole (mt) as the utilization of such ligands has previously been proven to be advantageous in terms of acetylene activation.^{79,108} The sulfur-rich complex $[\text{W}(\text{CO})_2(\text{mt})(\text{PhTt})]$ (**13**) could be isolated as major species from the reaction of **11** with $\text{Na}(\text{mt})$ (**4**).



Scheme 11: Synthesis of $[\text{W}(\text{CO})_2(\text{mt})(\text{PhTt})]$ (**13**).

For the synthesis of **13**, a solution of **4** was added dropwise to a stirred solution of $[\text{WBr}(\text{CO})_3(\text{PhTt})]$ in THF. The flask was equipped with a bubbler, and the dark orange reaction mixture was stirred until no further gas evolution could be observed. The reaction was terminated by evaporation to dryness, and the resulting solid was suspended in acetonitrile and filtrated through Celite which was washed with THF afterwards. The desired product was crystallized by slow evaporation of the filtrate,

washed with acetonitrile and subsequently dried *in vacuo* to give **13** as dark orange crystals in 51 % yield.

Complex **13** is soluble in chlorinated hydrocarbons and THF, badly soluble in acetonitrile and toluene, insoluble in hydrocarbons and water, and stable to both moisture and air in solid state. $[\text{W}(\text{CO})_2(\text{mt})(\text{PhTt})]$ was found to be stable in dichloromethane solution at rt for several days. IR spectroscopy revealed two $\text{C}\equiv\text{O}$ stretching vibrations at 1922 and 1826 cm^{-1} , indicative for an electron-rich tungsten center.

The novel complex **13** was characterized by ^1H and ^{13}C NMR spectroscopy which revealed interesting features. In contrast to the expected asymmetric split-up of the signals due to coordination of a different ligand *trans* to every sulfur donor atom of [PhTt], the ^1H NMR spectrum recorded in dichloromethane- d_2 shows only one sharp singlet for the protons of all three CH_3 groups of [PhTt] at $\delta = 2.46$ ppm and one broad signal for those of all three CH_2 groups at $\delta = 2.17$ ppm. The aliphatic protons of mt resonate at $\delta = 3.34$ ppm and the protons of the five-membered ring at $\delta = 7.18$ – 7.17 and 6.60 ppm. The ^{13}C NMR spectrum displays a quadruplet at $\delta = 161.56$ – 159.46 ppm resulting from the coupling of the boron atom with the quaternary carbon bound to it. The quaternary carbon of the mt ligand resonates at $\delta = 152.43$ ppm. Probably due to an extremely fast exchange of the two CO ligands, the carbonyl carbons could never be detected by ^{13}C NMR spectroscopy.

Single crystals suitable for X-ray diffraction analysis were obtained by crystallization from acetonitrile at rt. A molecular view is provided in Figure 31, a full list of bond lengths and angles is given in Table 20 (Appendix). Crystallographic data are summarized in Table 15 (Appendix).

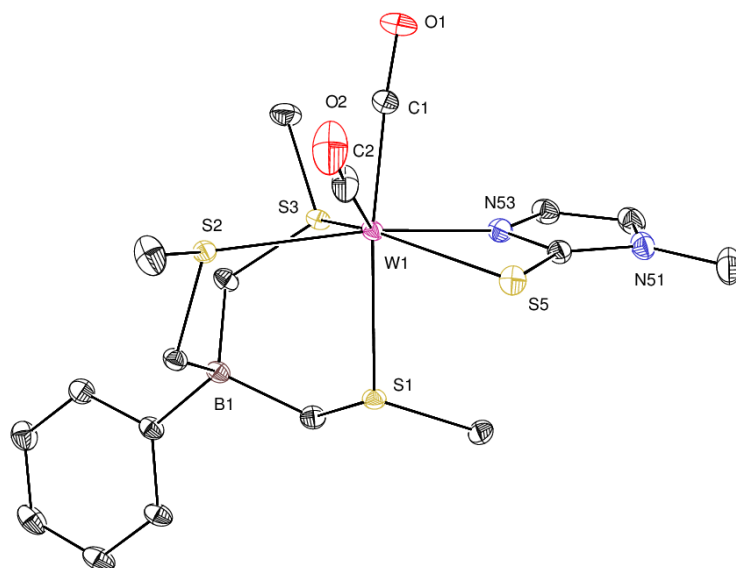


Figure 31: ORTEP¹⁰⁶ plot of **13** showing the atomic numbering scheme. The probability ellipsoids are drawn at the 50 % probability level. H atoms are omitted for clarity.

The W–S bonds (2.5068(5)–2.5920(5) Å) of the tridentate ligand enclose rather small angles (S–W–S 75.746(16)–85.107(17)°). The coordination of the tungsten center is completed by two carbonyl ligands (W1–C1 1.934(2) Å, W1–C2 1.967(2) Å; C1–W1–C2 73.14(11)°) and the bidentate methimazolyl ligand (W1–N53 2.1862(18) Å, W1–S5 2.6098(6) Å).

The carbonyl ligands of the biscarbonyl complexes **12** and **13** display similar stretching frequencies, whereas those of the tricarbonyl complex **11** show higher stretching frequencies. A comparison is shown in Table 11. Hence, the sulfur-containing, bidentate ligands (methylthio)methanide and methimazole provide more electron density to the tungsten center than an electron withdrawing bromo and a π acidic carbonyl ligand. The C≡O stretching frequencies of the carbonyl ligands of **12** and **13** are rather similar to those of the complexes [W(CO)₂(PPh₃)(S₂CNMe₂)₂] and [W(CO)₂(S-Phoz)₂] which were found to activate acetylene.^{103,105}

Table 11: Comparison of the C≡O stretching frequencies of complexes **11**–**13**.

Complex	ν (C≡O) (cm ⁻¹)
[WBr(CO) ₃ (PhTt)] (11)	2026, 1940, 1908
[WBr(CO) ₂ (η^2 -CH ₂ SCH ₃)(PhTt)] (12)	1925, 1810
[W(CO) ₂ (mt)(PhTt)] (13)	1922, 1826

Interestingly, the W–S bond lengths of complexes **12** and **13** vary significantly among themselves, while those of compound **11** lie within a rather small range (Table 12). This finding can be explained by the enormous *trans* influence of a carbonyl ligand.¹⁰⁹ In [WBr(CO)₃(PhTt)], no sulfur donor atom adopts the position *trans* to a carbonyl ligand. Therefore, no W–S bond is weakened due to carbonyl π acidity, and all the bond lengths lie within a small range. In [W(CO)₂(η^2 -CH₂SCH₃)(PhTt)], however, one carbonyl ligand occupies the position *trans* to a sulfur donor atom (C2–W1–S2 175.03(4)°) and weakens the W–S2 bond opposite the CO ligand significantly. The W–S1 bond is also slightly stretched, although the sulfur atom and the opposite carbonyl carbon enclose an angle smaller than 180° (C1–W1–S1 161.30(4)°). A similar scenario is observed in complex [W(CO)₂(mt)(PhTt)]: Although the sulfur and carbonyl opposite of each other enclose an angle different from 180° (C1–W1–S1 167.11(7)°), the W–S bond *trans* to the carbonyl ligand is remarkably stretched in comparison to the other W–S bonds.

Table 12: Comparison of W–S bond lengths present in complexes **11**–**13**.

	11	12	13
W–S1 (Å)	2.5420(6)	2.5528(3)	2.5920(5)
W–S2 (Å)	2.5654(5)	2.5804(3)	2.5279(5)
W–S3 (Å)	2.5526(6)	2.4999(3)	2.5068(5)

3.4 Attempted Synthesis of [W(CO)₃(PhTt)(S*t*Bu)]

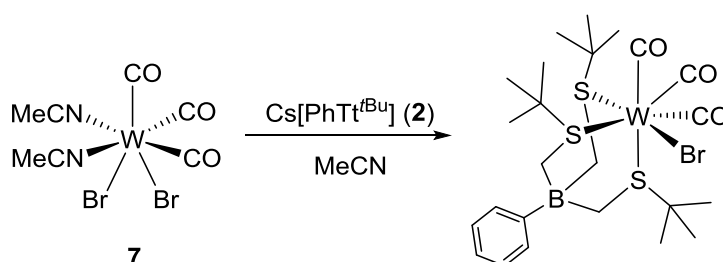
Complex [WBr(CO)₃(PhTt)] was also investigated towards substitution of the bromo ligand with the monodentate *tert*-butyl thiolate. On the one hand, this ligand should make the first coordination sphere more sulfur-rich and therefore more similar to the active site of AH, and on the other hand, the electron donating *tert*-butyl group should increase the electron density on the tungsten center. This would be beneficial in terms of acetylene coordination.

For the synthesis of [W(CO)₃(PhTt)(S*t*Bu)], a solution of NaS*t*Bu (**5**) was added dropwise to a solution of **11** in THF. The reaction was terminated after 40 min by evaporation to dryness. The solid was suspended in THF and the resulting mixture was filtrated through Celite to remove generated NaBr. After evaporation to dryness, the crude product was isolated as dark green-brown, sticky solid. ¹H NMR

spectroscopy did not show any conclusive signals. IR spectroscopy revealed at least seven C≡O absorption bands ranging from 2034–1736 cm⁻¹. As for the attempted selective synthesis of **12**, C≡O stretching frequencies of 1775 and 1736 cm⁻¹ could be indicative for a nucleophilic attack on the carbonyl carbon leading to a product mixture.

3.5 Attempted Synthesis of [WBr(CO)₃(PhTt^tBu)]

In order to investigate the electronic influence of a *tert*-butyl group on the sulfur donor atom, the synthesis of [WBr(CO)₃(PhTt^tBu)] was attempted according to Scheme 12.



Scheme 12: Synthetic approach for the attempted synthesis of [WBr(CO)₃(PhTt^tBu)].

Because of small quantities of **2**, two equal NMR experiments and one experiment on preparative scale were performed. For the NMR experiments, a solution of Cs[PhTt^tBu] (**2**) was slowly added to a solution of **7** in acetonitrile-d₃. Immediate formation of CsBr and a color change from dark brown to dark yellow could be observed. However, ¹H NMR spectra recorded after 30 min and three hours did neither show a major species nor other conclusive signals. For the experiment on preparative scale, the reaction was performed in acetonitrile and terminated after 20 min by evaporation to dryness. After five hours, the solid was suspended in dichloromethane and filtrated through Celite. The resulting dark green solution was evaporated to dryness. IR spectroscopy of the green-black solid revealed three C≡O stretching frequencies at 2011, 1919 (broad) and 1814 cm⁻¹. ¹H NMR spectra recorded in acetonitrile-d₃ were similar to those of the NMR experiments. The color of the putative product is rather unreasonable, as tricarbonyl tungsten(II) complexes were found to be usually orange or red.

Originally expected recrystallization from acetonitrile was not successful which is contrary to complexes **11**, **12** and **13**, as these compounds crystallize readily from acetonitrile.

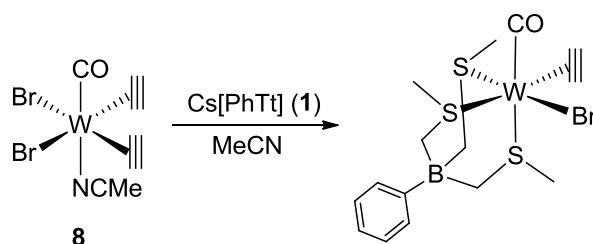
4 TUNGSTEN ALKYNE COMPLEXES

In order to prepare tungsten(II) alkyne complexes employing the tripodal, sulfur-rich ligand [PhTt], two different synthetic approaches were investigated: For the “ligand addition” method, the salt metathesis reaction of the tungsten(II) alkyne precursors **8**–**10** with [PhTt] was investigated, whereas for the “alkyne addition” method, the ability of **11** and **13** to coordinate the symmetric alkynes acetylene, 2-butyne and diphenylacetylene was tested.

4.1 Ligand Addition Method

4.1.1 Attempted Synthesis of $[\text{WBr}(\text{CO})(\eta^2\text{-C}_2\text{H}_2)(\text{PhTt})]$

Reaction of $[\text{WBr}_2(\text{CO})(\eta^2\text{-C}_2\text{H}_2)_2(\text{NCMe})]$ with **1** ought to yield the complex $[\text{WBr}(\text{CO})(\eta^2\text{-C}_2\text{H}_2)(\text{PhTt})]$ according to Scheme 13. Therefore, one bromo ligand, one acetylene molecule and the coordinated acetonitrile must be replaced by the scorpionate ligand.



Scheme 13: Synthetic approach for the attempted synthesis of $[\text{WBr}(\text{CO})(\eta^2\text{-C}_2\text{H}_2)(\text{PhTt})]$.

A solution of **1** was added dropwise to a suspension of **8** in acetonitrile. At the end of the addition, formation of CsBr and a color change from olive green to deep violet was observed. After an overall reaction time of 30 min and no further visible changes, the reaction was terminated by evaporation to dryness. The violet solid was suspended in dichloromethane and filtrated through Celite. Subsequent evaporation of the filtrate gave the crude product as deep violet solid.

The crude product is soluble in chlorinated hydrocarbons, acetonitrile and THF, yet insoluble in benzene and toluene.

IR spectroscopy revealed one intensive C≡O stretching vibration at 1938 cm⁻¹. ¹H NMR data of the crude product confirmed the presence of coordinated acetylene with protons resonating at $\delta = 13.29$ and 12.64 ppm. However, the signals do not match with those of the aromatic or aliphatic protons. Purification via flash chromatography or extraction with dichloromethane/toluene has not been successful so far.

When the reaction of complex **8** with **1** and all further steps are performed at -15 °C, the macroscopic properties of the crude product are identical to those of the product obtained in the reaction at rt. Interestingly, ¹H NMR spectroscopy showed two signal sets of coordinated acetylenes, two doublets at $\delta = 12.73$ and 11.85 ppm and two singlets at $\delta = 11.82$ and 11.51 ppm. The doublets can probably be ascribed to the tungsten(II) bis(alkyne) complex [WBr(CO)(η^2 -C₂H₂)₂(PhTt-S,S')], with the ligand coordinated only via two sulfur atoms (see point 4.1.3). However, the signals do not match with those of the aromatic or aliphatic protons.

The crude product changes its color when stored in solid state at rt for one hour and was therefore long-term stored at -35 °C. However, no obvious molecular changes could be detected by means of NMR or IR spectroscopy when storing it at rt. Even after leaving a solution at rt for a week, the corresponding ¹H NMR spectrum did not change significantly. These observations give rise to the assumption that the desired complex [WBr(CO)(η^2 -C₂H₂)(PhTt)] is either formed only in small amounts or not at all. Instead, the formation of a species bearing one carbonyl ligand with a stretching frequency of 1938 cm⁻¹ and other compounds seems to be realistic.

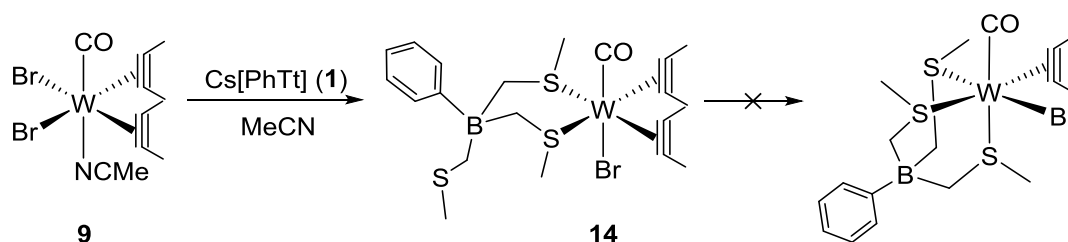
4.1.2 Attempted Synthesis of [WBr(CO)(η^2 -C₂H₂)(PhTt^{tBu})]

The reaction of **8** with Cs[PhTt^{tBu}] (**2**) was performed once as an NMR experiment. Therefore, a solution of **2** was added to a solution of **8** in acetonitrile-d₃, whereupon the color of the solution changed to dark blue. ¹H NMR spectra were recorded 30 min and three hours after ligand addition. Both spectra displayed two signal sets indicative for the protons of a coordinated acetylene: one at $\delta = 13.54$ and 13.46 ppm and the other at $\delta = 13.19$ and 12.20 ppm. However, the intensity of these signals did not match with the intensity of the signals resulting from the aromatic and aliphatic protons.

Consequently, the synthesis of $[\text{WBr}(\text{CO})(\eta^2\text{-C}_2\text{H}_2)(\text{PhTt}^{\text{tBu}})]$ was not found to be promising and was therefore not further investigated.

4.1.3 Synthesis of $[\text{WBr}(\text{CO})(\eta^2\text{-C}_2\text{Me}_2)_2(\text{PhTt-S,S'})]$

In order to synthesize $[\text{WBr}(\text{CO})(\eta^2\text{-C}_2\text{Me}_2)(\text{PhTt})]$, complex **9** was reacted with **1**. However, NMR spectroscopy and X-ray diffraction analysis revealed the formation of $[\text{WBr}(\text{CO})(\eta^2\text{-C}_2\text{Me}_2)_2(\text{PhTt-S,S'})]$ (**14**) as the major species. The desired complex $[\text{WBr}(\text{CO})(\eta^2\text{-C}_2\text{Me}_2)(\text{PhTt})]$, with only one 2-butyne and three sulfur atoms coordinated to the tungsten(II) center, could not be isolated (Scheme 14).



Scheme 14: Synthetic approach for the preparation of $[\text{WBr}(\text{CO})(\eta^2\text{-C}_2\text{Me}_2)(\text{PhTt})]$.

For the preparation of **14**, a solution of **1** was added to a solution of **9** in acetonitrile at rt. After addition, the formation of CsBr and a color change from olive green to yellow-green could be observed. The reaction mixture was allowed to stir at $-15\text{ }^\circ\text{C}$ for 30 min. Then, the reaction was terminated by evaporation to dryness. The dark yellow solid was suspended in dichloromethane and filtrated through Celite at $-15\text{ }^\circ\text{C}$. The dark yellow filtrate was evaporated to dryness which gave the crude product as yellow ocher solid in 100 % yield. The crude product was purified by recrystallization from dichloromethane/heptane at $-35\text{ }^\circ\text{C}$ which yielded **14** as yellow crystals suitable for X-ray diffraction analysis in 50 % yield.

Compound **14** is soluble in chlorinated hydrocarbons, benzene, toluene, THF and acetonitrile. The crude product is a yellow ocher powder which ought to be stored at $-35\text{ }^\circ\text{C}$, as it decomposes at rt. Thereby, its color changes to magenta. The resulting powder can be separated into a magenta-colored, soluble and a white, insoluble fraction. IR spectroscopy revealed that the decomposition products are, to a small extent, always present in the raw product. The desired complex can only be separated from those products by recrystallization from dichloromethane/heptane at $-35\text{ }^\circ\text{C}$. In

contrast to the crude product, the obtained crystals are stable at rt for several days, even under ambient conditions. Compound **14** is generally instable in solution at rt. Thereby, the color of the solutions changes from yellow to magenta, and a white precipitate is formed after a few hours. ^1H NMR data revealed the formation of benzene and the presence of free 2-butyne, indicative for the total decomposition of $[\text{WBr}(\text{CO})(\eta^2\text{-C}_2\text{Me}_2)_2(\text{PhTt})]$. Solutions stored at $-35\text{ }^\circ\text{C}$ are found to be stable for several days.

IR spectroscopy of complex **14** revealed one $\text{C}\equiv\text{O}$ stretching vibration at 2038 cm^{-1} which is nearly identical to that of the starting complex (2035 cm^{-1}). The magenta-colored decomposition product contains one carbonyl ligand displaying a $\text{C}\equiv\text{O}$ stretching frequency of 1940 cm^{-1} .

Crystallization of $[\text{WBr}(\text{CO})(\eta^2\text{-C}_2\text{Me}_2)_2(\text{PhTt-S,S'})]$ from dichloromethane/heptane gave many different types of yellow crystals of which blocks and rhombs were characterized by X-ray diffraction analysis. This analysis confirmed the existence of two isomers concerning the six-membered ring formed by the tungsten center and the two coordinating arms of the ligand. A molecular view of isomer 1 (**14a**), which crystallizes as block, is depicted in Figure 32. A full list of bond lengths and angles is given in Table 18 (Appendix). Crystallographic data are summarized in Table 14 (Appendix).

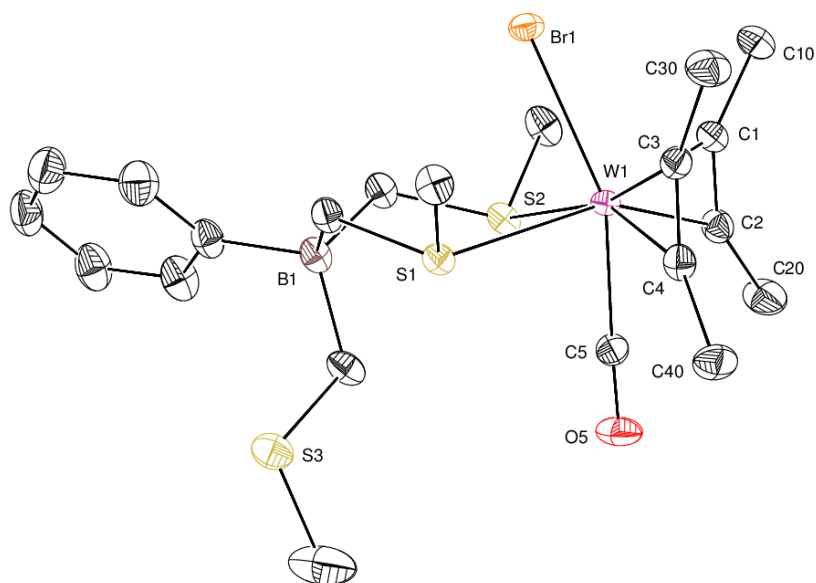


Figure 32: ORTEP¹⁰⁶ plot of **14a** showing the atomic numbering scheme. The probability ellipsoids are drawn at the 50 % probability level. H atoms are omitted for clarity.

The distorted octahedral coordination sphere of the tungsten center in **14a** consists of a carbonyl ligand (W1–C5 2.019(3) Å) *trans* to the bromo ligand (W1–Br1 2.6073(4) Å; C5–W1–Br1 157.99(8)°) and of the two 2-butyne ligands (C1–C2 1.281(4) Å, W1–C2 1.985(3) Å; C3–C4 1.282(4) Å, W1–C2 1.990(3) Å) in *trans* positions to two of the three sulfur atoms of the borate ligand (W1–S1 2.6500(7) Å, W1–S2 2.6533(7) Å). The 2-butyne C≡C bonds are parallel to the C≡O bond, as in the precursor [WBr₂(CO)(η²-C₂Me₂)₂(NCMe)]. The C≡C–C angles are in the range of 143.2(3)°–145.5(3)°. The central six-membered ring adopts a chair conformation with the non-coordinating (methylthio)methyl chain almost *cis* to the carbonyl ligand.

A molecular view of isomer 2 (**14b**) is depicted in Figure 33, a full list of bond lengths and angles is given in Table 19 (Appendix). Crystallographic data are summarized in Table 14 (Appendix).

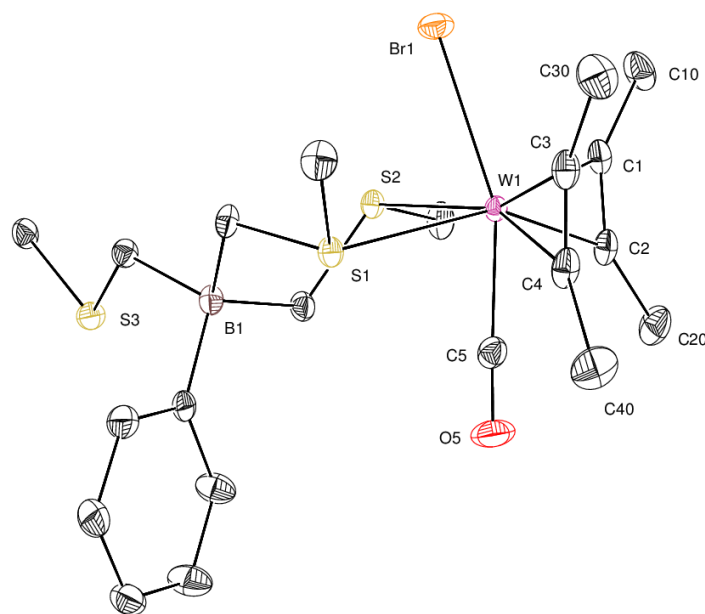


Figure 33: ORTEP¹⁰⁶ plot of **14b** showing the atomic numbering scheme. The probability ellipsoids are drawn at the 50 % probability level. H atoms are omitted for clarity.

Bond lengths and angles of **14b** are similar to **14a**. However, the central six-membered ring adopts a distorted boat conformation with the phenyl ring almost *cis* to the carbonyl ligand.

Different single crystals were dissolved in various solvents to characterize both isomers by ¹H and ¹³C NMR spectroscopy. Surprisingly, ¹H NMR spectra recorded within one hour after dissolution in different solvents always showed both isomers in a

3:2 ratio. After a few hours, both isomers were present in a 1:1 ratio in both dichloromethane- d_2 and chloroform- d which means that one isomer either decomposes faster or converts to the other. In benzene- d_6 , the ratio changes to 1:2 within 12 hours because one isomer decomposes while the other does not. Consequently, one isomer must be more stable. As a chair conformation is generally more favorable than a boat conformation, it is assumed that isomer **14a** is the more stable one. The protons of the methyl groups of the two coordinated 2-butyne in isomer 1 (**14a**) resonate at $\delta = 3.10$ and 2.89 ppm and the corresponding carbon atoms at $\delta = 18.92$ and 18.31 ppm. In contrast, the protons of the methyl groups of the two coordinated 2-butyne in isomer 2 (**14b**) resonate at $\delta = 3.13$ and 3.00 ppm and the corresponding carbon atoms at $\delta = 18.98$ and 18.34 ppm. The carbonyl carbons resonate at $\delta = 208.74$ and 208.71 ppm, respectively. This closeness explains, why IR spectroscopy shows only one strong absorption band: The carbonyl ligands are too similar to be distinguished by IR spectroscopy.

In order to synthesize the complex $[\text{WBr}(\text{CO})(\eta^2\text{-C}_2\text{Me}_2)(\text{PhTt})]$ from the reaction of **9** with **1**, one bromo ligand is substituted by one sulfur atom of $[\text{PhTt}]$. This is performed in the course of a fast and simple salt metathesis reaction. Additionally, the coordinated acetonitrile and one 2-butyne must be substituted by one sulfur atom each. However, the ligand is only capable of replacing the solvent molecule which is indicative for the rather weak donor ability of the third sulfur atom. This finding is contradictory to the reaction of $[\text{WX}_2(\text{CO})(\eta^2\text{-C}_2\text{Me}_2)_2(\text{NCMe})]$ ($X = \text{Br}, \text{I}$) with the soft scorpionate ligand Tm^{Me} which yields the tungsten(II) alkyne complex $[\text{WX}(\text{CO})(\eta^2\text{-C}_2\text{Me}_2)(\text{Tm}^{\text{Me}})]$.¹⁰⁴ The W–S bond lengths found in $[\text{WBr}(\text{CO})(\eta^2\text{-C}_2\text{Me}_2)(\text{Tm}^{\text{Me}})]$ (2.4043(13), 2.5936(12) and 2.6330(13) Å) vary significantly among themselves, but in general, they are all much shorter than the W–S bonds present in **14** (2.6500(7) and 2.6533(7) Å).¹⁰⁴ The fairly long W–S bonds found in **14** are probably the reason for the instability of the complex in solution at rt.

Usually, tungsten(II) bis(alkyne) complexes are synthesized by reaction of a tungsten(II) bis(alkyne) precursor with an anionic, bidentate ligand. For instance, the first tungsten(II) bis(alkyne) complexes employing a sulfur ligand were prepared by reaction of the binuclear precursor $[\{\text{W}(\mu\text{-Br})\text{Br}(\text{CO})(\eta^2\text{-C}_2\text{Me}_2)_2\}_2]$ with 1 equiv. of $\text{Na}(\text{S}_2\text{PMe}_2)$ and $\text{Na}(\text{S}_2\text{CNMe}_2)$, respectively, yielding the complexes $[\text{WBr}(\text{CO})(\eta^2\text{-C}_2\text{Me}_2)_2(\text{L})]$ ($\text{L} = \text{S}_2\text{PMe}_2, \text{S}_2\text{CNMe}_2$).¹¹⁰ In 1990, the tungsten(II) bis(alkyne) complexes

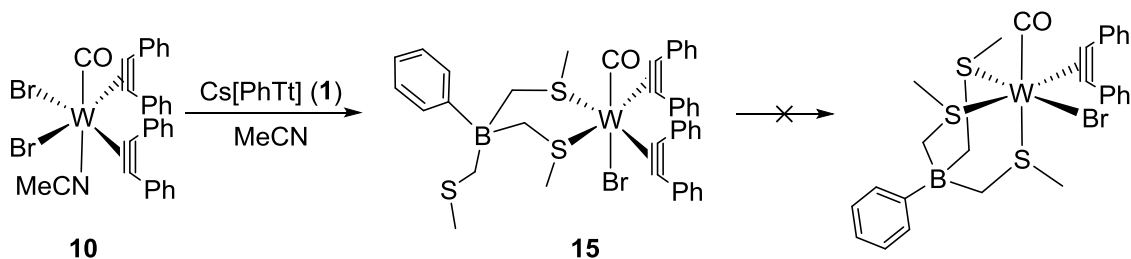
$[\text{W}(\text{CO})(\text{C}_2\text{Me}_2)_2(\text{L})]$ ($\text{L} = \text{S}_2\text{CNMe}_2, \text{S}_2\text{CNEt}_2, \text{S}_2\text{CN}(\text{CH}_2\text{Ph})_2, \text{S}_2\text{COEt}, \text{S}_2\text{CNC}_4\text{H}_8, \text{S}_2\text{CNC}_5\text{H}_{10}$) were isolated by reaction of the precursor complex $[\text{Wl}_2(\text{CO})(\eta^2\text{-C}_2\text{Me}_2)_2(\text{NCMe})]$ with the corresponding bidentate sulfur ligands.¹¹¹ Consequently, the tridentate ligand [PhTt] behaves like a bidentate ligand as it only coordinates via two sulfur atoms.

Baker *et al.* performed reactions of the precursor $[\text{Wl}_2(\text{CO})(\eta^2\text{-C}_2\text{Me}_2)_2(\text{NCMe})]$ with the tridentate thioether ligands ttn and ttoc. After a reaction time of 72 hours, the complexes $[\text{W}(\text{CO})(\eta^2\text{-C}_2\text{Me}_2)(\text{L-S,S}',\text{S}'')]_2$ ($\text{L} = \text{ttn}, \text{ttoc}$) could be crystallized. In contrast to [PhTt], the tridentate ligands ttn and ttoc are capable of substituting one 2-butyne. Consequently, they are able to coordinate the tungsten center via all three sulfur atoms.⁶⁷ A common method to remove coordinated alkynes is heat. If complex **14** was heated to reflux, though, it probably would lose both 2-butyne in a short time and subsequently decompose completely, as it already decomposes at rt.

Altogether, the attempted synthesis of the tungsten(II) alkyne complex $[\text{WBr}(\text{CO})(\eta^2\text{-C}_2\text{Me}_2)(\text{PhTt})]$ led to the isolation of complex **14**. In this complex, the tungsten center is coordinated only by two of the three sulfur atoms of the tripodal ligand [PhTt]. Because of the general instability of $[\text{WBr}(\text{CO})(\eta^2\text{-C}_2\text{Me}_2)_2(\text{PhTt-S,S}')]_2$ at rt, no further experiments are planned.

4.1.4 Synthesis of $[\text{WBr}(\text{CO})(\eta^2\text{-C}_2\text{Ph}_2)_2(\text{PhTt-S,S'})]$

In order to synthesize the complex $[\text{WBr}(\text{CO})(\eta^2\text{-C}_2\text{Ph}_2)(\text{PhTt})]$, compound **10** was reacted with **1**. X-ray diffraction analysis revealed the formation of $[\text{WBr}(\text{CO})(\eta^2\text{-C}_2\text{Ph}_2)_2(\text{PhTt-S,S'})]$ (**15**) amongst other species. The desired complex $[\text{WBr}(\text{CO})(\eta^2\text{-C}_2\text{Ph}_2)(\text{PhTt})]$, with only one diphenylacetylene and three sulfur atoms coordinated to the tungsten(II) center, could not be isolated (Scheme 15).



Scheme 15: Synthetic approach for the preparation of $[\text{WBr}(\text{CO})(\eta^2\text{-C}_2\text{Ph}_2)(\text{PhTt})]$.

For the preparation of **15**, a solution of **1** was added dropwise to a solution of **10** in acetonitrile. After addition, the formation of CsBr could be observed, and the resulting reaction mixture was allowed to stir for 30 min. Then, the reaction was terminated by evaporation to dryness. The resulting solid was suspended in dichloromethane and filtrated through Celite at $-15\text{ }^\circ\text{C}$. The green-brown filtrate was evaporated to dryness to yield the crude product as green ocher solid. Recrystallization from dichloromethane/heptane at $-35\text{ }^\circ\text{C}$ gave **15** as yellow-green crystals. The development of an experimental procedure for the synthesis of pure **15** has not been possible so far as the reaction is fairly unselective. Probably due to dislocation of the incorporated heptane, crystallization of **15** has been unsuccessful on a larger scale. Further purification methods have to be investigated.

Compound **15** is soluble in chlorinated hydrocarbons, acetonitrile and THF. IR spectroscopy of the crystals revealed one $\text{C}\equiv\text{O}$ stretching vibration at 2074 cm^{-1} .

Single crystals suitable for X-ray diffraction analysis were obtained by crystallization from dichloromethane/heptane at $-35\text{ }^\circ\text{C}$. A molecular view of complex **15** is depicted in Figure 34, selected bond lengths and angles are given in Table 21. Crystallographic data are summarized in Table 15 (Appendix).

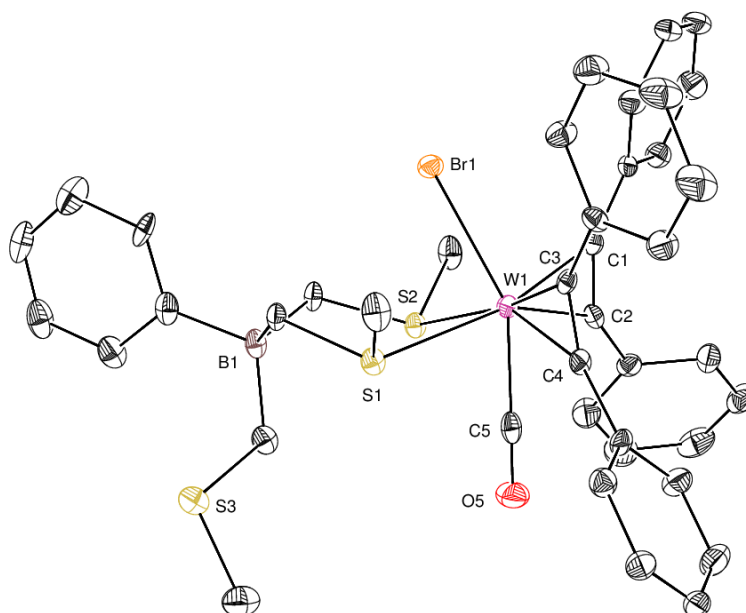


Figure 34: ORTEP¹⁰⁶ plot of **15** showing the atomic numbering scheme. The probability ellipsoids are drawn at the 50 % probability level. H atoms are omitted for clarity.

The octahedral coordination sphere of the tungsten atom consists of the two η^2 -diphenylacetylene ligands (C1–C2 1.303(6) Å, W1–C₂ 1.989(5) Å; C3–C4 1.313(6) Å, W1–C₂ 1.979(4) Å) *trans* to the sulfur atoms of two branches of the fundamentally tridentate borate ligand (W1–S1 2.6532(12) Å, W1–S2 2.6501(10) Å), and a carbonyl ligand (W1–C1 2.035(5) Å) in *trans* position to the bromo ligand (W1–Br1 2.6047(5) Å; C5–W1–Br1 151.99(12)°). The C≡C–C angles are in the range of 137.0(4)–144.5(4)°.

As expected, the W–S bonds present in **14a** (2.6500(7) and 2.6533(7) Å) and **15** (2.6532(12) and 2.6501(10) Å) exhibit the same length. Due to a strong *trans* influence of the coordinated alkynes, the bonds are relatively long and therefore, the complexes are quite prone to decomposition.

4.2 Alkyne Addition Method

4.2.1 Attempted Synthesis of [WBr(CO)(η^2 -C₂R₂)(PhTt)]

In order to prepare the tungsten(II) acetylene complex [WBr(CO)(η^2 -C₂H₂)(PhTt)] via the “alkyne addition” method, the reaction of [WBr(CO)₃(PhTt)] with acetylene was closely investigated with respect to different reaction conditions. Therefore, **11** was dissolved in dichloromethane or toluene, and the solution was purged with acetylene

under heavy stirring for one hour. Reactions in dichloromethane were performed for 16 hours, either at rt or by heating to reflux. Reactions in toluene or toluene/acetonitrile 9+1 were performed for 1, 2.5, 3 or 15 hours either without or under the influence of a daylight lamp to facilitate the dissociation of two carbonyl ligands.¹¹² The reactions performed under light irradiation were cooled with a water bath to avoid warming. Formation of fine, black polyacetylene was observed under all applied conditions. Coordination of acetylene under all conditions, except heating at reflux for 16 hours in dichloromethane, was confirmed by ¹H NMR spectroscopy which showed the presence of two singlets at $\delta = 13.29$ and 12.64 ppm, characteristic of tungsten(II) acetylene complexes. These signals are also present in ¹H NMR spectra of the crude product obtained by the "ligand addition" method. However, in both cases, the intensity of the signals is rather low compared to the signals of aromatic or aliphatic protons. Consequently, the reaction suffered from poor selectivity. Purification attempts including flash chromatography remained unsuccessful so far.

The coordination of 2-butyne in order to prepare the complex $[\text{WBr}(\text{CO})(\eta^2\text{-C}_2\text{Me}_2)(\text{PhTt})]$ was investigated by performing two experiments. In the first experiment, 2-butyne was added to a solution of $[\text{WBr}(\text{CO})_3(\text{PhTt})]$ in dichloromethane and the solution was heated to reflux for 16 hours. The second experiment was carried out in toluene/acetonitrile 9+1 under the influence of a daylight lamp for 3 hours. ¹H NMR spectroscopy revealed the full conversion of **11** under both conditions, yet did not indicate the coordination of a 2-butyne molecule. Instead, it showed a rather vast number of resonance signals. IR spectroscopy revealed an intensive absorption band at 1940 cm^{-1} which is identical to the stretching vibration of the carbonyl ligand present in the decomposition product of complex **14**. Similar to the reaction of **11** with acetylene, the synthesis of $[\text{WBr}(\text{CO})(\eta^2\text{-C}_2\text{Me}_2)(\text{PhTt})]$ suffered from poor selectivity.

The reaction of $[\text{WBr}(\text{CO})_3(\text{PhTt})]$ with diphenylacetylene to yield the complex $[\text{WBr}(\text{CO})(\eta^2\text{-C}_2\text{Ph}_2)(\text{PhTt})]$ was performed twice, too. In the first experiment, 5 equiv. of diphenylacetylene were added to a solution of **11** in dichloromethane and the solution was allowed to stir for 16 hours. ¹H NMR and IR spectroscopy of the crude product revealed the presence of the starting material. Consequently, complex **11** does not react with diphenylacetylene at rt. The second experiment was carried out in toluene for 3 hours under the influence of a daylight lamp. The color of the reaction solution changed from orange to dark red-brown after 30 min, however, ¹H NMR

spectroscopy revealed only partial conversion of the starting material and three new signals of different intensity resulting from aliphatic protons, but no indications of coordinated diphenylacetylene. IR spectroscopy showed the appearance of a new $\text{C}\equiv\text{O}$ stretching vibration at 1848 cm^{-1} .

4.2.2 Attempted Synthesis of $[\text{W}(\eta^2\text{-C}_2\text{R}_2)(\text{mt})(\text{PhTt})]$

As the reaction of **11** with acetylene, 2-butyne and diphenylacetylene suffered from poor selectivity, the reactivity of $[\text{W}(\text{CO})_2(\text{mt})(\text{PhTt})]$ towards these symmetric alkynes was investigated. Generally, **13** is more reactive towards acetylene because polyacetylene is formed at rt without the use of a daylight lamp. However, the reaction of **13** with acetylene in toluene for eight hours or three days was not too promising so far. In contrast, ^1H NMR spectroscopy confirmed the formation of a tungsten acetylene complex showing a singlet at $\delta = 12.92\text{ ppm}$ (CDCl_3) for the product obtained from the reaction of **13** with acetylene in dichloromethane for 20 hours.

Furthermore, complex **13** does not react quantitatively with 2-butyne in toluene at rt in 24 hours. ^1H NMR data showed only partial conversion of **13** and no coordinated 2-butyne molecules. Due to time limitations, further experiments have not been performed yet.

III CONCLUSION

The chemical way of gaining insight into the mechanism of acetylene hydration catalyzed by the enzyme acetylene hydratase is the development and preparation of a functional model of the tungsten-containing active site. The only structural-functional model known so far is the oxotungsten(IV) complex $[\text{Et}_4\text{N}]_2[\text{WO}(\text{mnt})_2]$ which was synthesized and investigated by Sarkar *et al.* in 1996/1997.^{28,45} Tungsten(IV) complexes capable of acetylene activation are genuinely scarce. In order to extend this rather limited range, the bioinspired thioether scorpionate ligand $[\text{PhTt}]$ and, to a minor extent, the variant $[\text{PhTt}^{\text{tBu}}]$ were employed to synthesize novel tungsten acetylene complexes with the potential to serve as functional model compound of acetylene hydratase.

The synthesis of all tungsten(II) complexes started from the literature-known dimer $[\text{W}_2\text{Br}_4(\text{CO})_7]$ (**6**) which was cleaved by acetonitrile to give the monomer $[\text{WBr}_2(\text{CO})_3(\text{NCMe})_2]$ (**7**). For the “alkyne addition” method, the novel complex $[\text{WBr}(\text{CO})_3(\text{PhTt})]$ (**11**), which was successfully synthesized in good yield by reaction of **7** with $\text{Cs}[\text{PhTt}]$ (**1**), served as entry point. Furthermore, the complex $[\text{W}(\text{CO})_2(\eta^2\text{-CH}_2\text{SCH}_3)(\text{PhTt})]$ (**12**) was isolated and crystallized as a side product of the reaction of **7** with an excess of $[\text{Bu}_4\text{N}][\text{PhTt}]$ (**1a**). The selective synthesis of **12** by reaction of complex **11** with $\text{LiCH}_2\text{SCH}_3(\text{TMEDA})$ (**3**) has not been successful. In order to make the first coordination sphere of compound **11** more sulfur-rich, the complex $[\text{W}(\text{CO})_2(\text{mt})(\text{PhTt})]$ (**13**) was prepared by reaction of **11** with $\text{Na}(\text{mt})$ (**4**) in reasonable yield. The carbonyl ligands of the two biscarbonyl complexes **12** and **13** display similar stretching frequencies, whereas those of the triscarbonyl complex **11** show higher stretching frequencies. Consequently, the sulfur-containing, bidentate ligands (methylthio)methanide and mt provide more electron density to the tungsten center than a bromo and a carbonyl ligand, which is beneficial in terms of alkyne activation. The preparation of the sulfur-rich compound $[\text{W}(\text{CO})_3(\text{PhTt})(\text{S}^t\text{Bu})]$ by reaction of complex **11** with NaS^tBu (**5**) has not been successful so far. Employing the ligand $[\text{PhTt}^{\text{tBu}}]$, the formation of the desired complex $[\text{WBr}(\text{CO})_3(\text{PhTt}^{\text{tBu}})]$ by reaction of **7** with $\text{Cs}[\text{PhTt}^{\text{tBu}}]$ (**2**) could not be confirmed by means of NMR spectroscopy.

For the “alkyne addition” method, the novel, sulfur-rich complexes $[\text{WBr}(\text{CO})_3(\text{PhTt})]$ and $[\text{W}(\text{CO})_2(\text{mt})(\text{PhTt})]$ were investigated regarding their reactivity towards the

coordination of the symmetric alkynes acetylene, 2-butyne and diphenylacetylene. Coordination of acetylene could be confirmed for both complexes by ^1H NMR spectroscopy, however, the reaction suffered from poor selectivity and therefore, no tungsten acetylene complexes could be isolated so far. Coordination of 2-butyne or diphenylacetylene could not be confirmed by NMR spectroscopy.

In order to investigate the “ligand addition” method, the well-established tungsten(II) bis(alkyne) precursors $[\text{WBr}_2(\text{CO})(\eta^2\text{-C}_2\text{R}_2)_2(\text{NCMe})]$ ($\text{R} = \text{Me}$ (**9**), Ph (**10**)) were synthesized in excellent yield by reaction of **7** with the respective alkyne. The synthesis of the desired complexes $[\text{WBr}(\text{CO})(\eta^2\text{-C}_2\text{R}_2)(\text{PhTt})]$ ($\text{R} = \text{H}$, Me , Ph) was not straightforward: The reaction of $[\text{WBr}_2(\text{CO})(\eta^2\text{-C}_2\text{H}_2)_2(\text{NCMe})]$ (**8**) with **1** suffered from poor selectivity, although ^1H NMR spectroscopy revealed signals characteristic of protons belonging to a coordinated acetylene. However, it has not been possible to isolate this complex so far. After reaction of **9** and **10** with $\text{Cs}[\text{PhTt}]$, the complexes $[\text{WBr}(\text{CO})(\text{C}_2\text{R}_2)_2(\eta^2\text{-PhTt-S,S'})]$ ($\text{R} = \text{Me}$ (**14**), Ph (**15**)), with the ligand coordinated via two sulfur atoms, were isolated. It was found that complex **14** forms two isomers differing in the conformation of the six-membered ring formed by the tungsten center and the two coordinated arms of the ligand $[\text{PhTt}]$. The W-S bonds present in complexes **14** and **15** exhibit the same length. Due to a strong *trans* influence of the coordinated alkynes, the bonds are relatively long and therefore, these compounds are quite prone to decomposition at rt.

IV EXPERIMENTAL SECTION

1 GENERAL METHODS

All experiments were carried out under N₂ atmosphere employing standard Schlenk and glovebox techniques. All chemicals were purchased from commercial sources and with the exception of acetylene, diphenylacetylene, trimethylamine-*N*-oxide and pyridine-*N*-oxide, all were used without further purification. Acetylene 2.6 was purified by bubbling it through water and conc. H₂SO₄ and subsequently dried by passing it through CaCl₂ and KOH. Diphenylacetylene was recrystallized from ethanol, and trimethylamine-*N*-oxide and pyridine-*N*-oxide were purified by sublimation. Celite was dried at 100 °C prior to use. All solvents were purified via a Pure Solv Solvent Purification System. Reactions supported by a daylight lamp were carried out with a TV Das Original 770 Tageslichtleuchte Day Light bought from Amazon.

NMR spectra were recorded on a Bruker Avance III 300 MHz spectrometer at 25 °C. ¹H NMR spectra were recorded at 300.13 MHz and ¹³C NMR spectra at 75.48 MHz. The chemical shifts δ are given in ppm. The multiplicity of peaks is denoted as broad singlet (bs), singlet (s), doublet (d), triplet (t), triplet of triplets (tt), quadruplet (q), quintuplet (qt), sextet (sx), multiplet (m) or broad multiplet (bm). NMR solvents were stored over molecular sieve. Solid state IR spectra were measured on a Bruker ALPHA ATR-FT-IR spectrometer at a resolution of 2 cm⁻¹. The relative intensity of signals is declared as strong (s), medium (m) and weak (w). In-situ IR measurements were performed under N₂ atmosphere from 2800–750 cm⁻¹ using a Bruker MATRIX-MF FT-IR spectrometer equipped with a IN350-T diamond ATR probe operating at a resolution of 1 cm⁻¹.

All crystal structures were determined with a Bruker AXS SMART APEX-II CCD diffractometer using monochromated Mo-K α radiation (0.71073 Å) at 100 K. Structures were solved by direct methods (SHELXS-97)¹¹³ and Full-matrix least-squares on F² was employed as refinement method. Elemental analyses (C, H, S) were performed at the Department of Inorganic Chemistry at the University of Technology in Graz using a Heraeus Vario Elementar automatic analyzer. All values for elemental analyses are given as percentages.

Na(mt) (**4**)¹¹⁴, NaSfBu (**5**)¹¹⁴ and [WBr₂(CO)(η²-C₂H₂)(NCMe)] (**8**)¹⁰⁴ were synthesized according to literature and provided by Carina Vidovič, MSc.

Cs[PhTt] (**1**)⁶⁸, [Bu₄N][PhTt] (**1a**)⁶⁸ and Cs[PhTt^{tBu}] (**2**)^{72,73} were synthesized according to modified published procedures.

[W₂Br₄(CO)₇] (**6**)¹⁰³, WBr₂(CO)₃(NCMe)₂] (**7**)⁹⁹, [WBr₂(CO)(η²-C₂Me₂)₂(NCMe)] (**9**)⁹⁹ and [WBr₂(CO)(η²-C₂Ph₂)(NCMe)] (**10**)⁹⁹ were prepared according to established procedures.

2 LIGAND SYNTHESIS

Cs[PhTt] (**1**)

In an inert 250 mL Schlenk flask, 60 mL heptane, 21 mL TMEDA (5.5 equiv., 138 mmol) and 18 mL (CH₃)₂S (10.0 equiv., 250 mmol) were combined. Subsequently, 42 mL n-BuLi (2.5 M in hexane, 4.2 equiv., 105 mmol) were added at -78 °C over 15 min. The resulting solution was allowed to warm to rt and was then stirred for three hours. Excess (CH₃)₂S was subsequently removed *in vacuo* for 15 min. The resulting light yellow, cloudy solution was again cooled to -78 °C and a solution of 3.3 mL PhBCl₂ (1 equiv., 25.0 mmol) in 12 mL heptane was added dropwise via syringe. The resulting white, cloudy mixture was allowed to warm to rt and was then stirred for 48 hours. The supernatant solution was removed, and the remaining solid was subsequently dried *in vacuo*. The resulting white residue was treated with 130 mL H₂O and 20 mL CH₂Cl₂. The aqueous phase was filtered, and the product was precipitated by adding aqueous CsCl and then leaving the cloudy solution at -10 °C overnight. The white, flocculent product was isolated by filtration, washed with H₂O (1x 4 mL) and Et₂O (3x 4 mL) and subsequently dried *in vacuo*.

Yield: 43 % (4.30 g, 10.6 mmol).

¹H NMR (CD₃CN): δ 7.40 (bm, 2H, *o*-C₆H₅), 7.07–7.03 (t, 2H, *m*-C₆H₅), 6.92–6.87 (tt, 1H, *p*-C₆H₅), 1.93 (s, 9H, CH₃), 1.79–1.75 (q, ²J_{BH} = 4.1 Hz, 6H, BCH₂).

¹³C NMR (CD₃CN): δ 165.29–163.29 (q, ¹J_{BC} = 50.4 Hz, BC_q), 134.06 (d, *o*-C₆H₅), 127.15–127.05 (q, *m*-C₆H₅), 123.70 (s, *p*-C₆H₅), 36.94–35.31 (q, ¹J_{BC} = 41.1 Hz, BCH₂), 20.35–20.22 (q, ³J_{BC} = 3.4 Hz, CH₃).

[Bu₄N][PhTt] (1a)

[Bu₄N][PhTt] was prepared in a procedure analogous to that for **1**. The product was precipitated by addition of aqueous [Bu₄N]Cl and isolated by filtration. The white, flocculent powder was washed with Et₂O (3x 3 mL) and subsequently dried *in vacuo*.

Yield: 44 % (5.65 g, 11.0 mmol).

¹H NMR (CD₃CN): δ 7.38 (bm, 2H, *o*-C₆H₅), 7.01–6.96 (t, 2H, *m*-C₆H₅), 6.85–6.81 (tt, 1H, *p*-C₆H₅), 3.09–3.03 (m, 8H, NCH₂), 1.92 (s, 9H, SCH₃), 1.80–1.76 (q, ²J_{BH} = 4.1 Hz, 6H, BCH₂), 1.64–1.54 (m, 8H, CH₂), 1.41–1.29 (sx, 8H, CH₂), 0.99–0.95 (t, 12H, CH₃).

Cs[PhTt^{tBu}] (2)

In an inert 250 mL Schlenk flask, 60 mL heptane, 14 mL TMEDA (3.8 equiv., 94 mmol) and 9.8 mL (CH₃)₃CSCCH₃ (3.0 equiv., 75 mmol) were combined. Subsequently, 30 mL n-BuLi (2.5 M in hexane, 3.0 equiv., 75 mmol) were added at -78 °C over 15 min. The solution was allowed to warm to rt and was then stirred for three hours. The resulting light yellow solution was again cooled to -78 °C and a solution of 3.3 mL PhBCl₂ (1 equiv., 25 mmol) in 12 mL heptane was added dropwise via syringe. The resulting white, cloudy mixture was allowed to warm to rt and was then stirred for 48 hours. The reaction mixture was extracted with H₂O (4x 50 mL), and the combined aqueous phases were then washed with CH₂Cl₂ (1x 20 mL). Aqueous CsCl was added to the aqueous phase which was then left at -10 °C overnight. The white, flocculent precipitate was isolated by filtration, washed with H₂O (1x 2 mL) and Et₂O (4x 2 mL) and dried *in vacuo*.

Yield: 2 % (280 mg, 0.53 mmol).

¹H NMR (CD₃CN): δ 7.42 (m, 2H, *o*-C₆H₅), 7.03–6.98 (t, 2H, *m*-C₆H₅), 6.88–6.83 (tt, 1H, *p*-C₆H₅), 1.20 (s, 27H, C(CH₃)₃), 1.74–1.70 (q, ²J_{BH} = 4.5 Hz, 6H, BCH₂).

LiCH₂SCH₃(TMEDA) (3)

In an inert 25 mL Schlenk flask, 10 mL heptane, 2.5 mL TMEDA (1.5 equiv., 16.5 mmol) and 1.9 mL (CH₃)₂S (2.4 equiv., 26.4 mmol) were combined. Then, 4.4 mL n-BuLi

(2.5 M in hexane, 1 equiv., 11.0 mmol) were added dropwise at -78 °C. The resulting solution was allowed to warm to rt and was then stirred for three hours. Subsequently, the solvent was evaporated *in vacuo* to give the product as off-white powder.

Yield: 100 % (2.03 g, 11.0 mmol).

¹H NMR (C₆D₆): δ 2.35 (s, 3H, SCH₃), 2.24 (s, 12H, NCH₃), 2.02 (s, 4H, NCH₂), 0.82 (s, 2H, SCH₂).

3 PRECURSOR SYNTHESIS

[W₂Br₄(CO)₇] (6)

A solution of 6.30 g Br₂ (1 equiv., 39.4 mmol) in 40 mL CH₂Cl₂ was added dropwise to a suspension of 15.26 g [W(CO)₆] (1.1 equiv., 43.36 mmol) in 100 mL CH₂Cl₂ at -20 °C. The resulting brown mixture was then stirred for 30 min at -20 °C and another two hours at rt. After no further gas evolution was observed, two thirds of the solvent were evaporated *in vacuo*. The orange-brown precipitate was isolated by filtration, washed with 6 mL CH₂Cl₂ and dried *in vacuo*. The resulting orange-brown powder was purified by fractionated sublimation (52 °C, 0.40 mbar).

Yield: 90 % (15.62 g, 17.68 mmol).

IR (cm⁻¹): ν (C≡O): 2105 (s), 2019 (s), 1998 (s), 1969 (s), 1960 (m), 1943 (s), 1924 (s).

[WBr₂(CO)₃(NCMe)₂] (7)

In a 250 mL Schlenk flask, 15.50 g [W₂Br₄(CO)₇] (6) (1 equiv., 17.55 mmol) were combined with 180 mL MeCN at 0 °C. Then, the ice bath was removed, and the mixture was allowed to stir for one hour at rt until complete dissolution. The solution was filtrated through Celite which was subsequently washed with 50 mL MeCN. Then, the red-brown reaction solution was reduced to 20 mL. The deep red precipitate was isolated by filtration, washed with 6 mL MeCN and dried *in vacuo*.

Yield: 82 % (14.66 g, 28.76 mmol).

IR (cm⁻¹): ν (C≡N): 2318 (w), 2291 (w); ν (C≡O): 2023 (s), 1909 (s), 1896 (s).

[WBr₂(CO)(η²-C₂Me₂)₂(NCMe)] (9)

To a solution of 2.55 g [WBr₂(CO)₃(NCMe)₂] (**7**) (1 equiv., 5.00 mmol) in 35 mL CH₂Cl₂, 1.2 mL 2-butyne (3.1 equiv., 15 mmol) were added dropwise at 0 °C. The flask was equipped with a bubbler, and the dark violet solution was stirred for 45 min at 0 °C. Then, the ice bath was removed, and the solution was allowed to stir at rt for 17 hours. The dark green reaction mixture was filtrated, and the filtrate was reduced to 10 mL. The product was recrystallized from CH₂Cl₂/heptane, and the obtained olive green crystals were subsequently dried *in vacuo*.

Yield: 96 % (2.37 g, 4.55 mmol).

¹H NMR (CD₂Cl₂): 2.88 (s, 6H, ≡-CH₃), 2.85 (s, 3H, CH₃CN), 2.83 (s, 6H, ≡-CH₃).

¹³C NMR (CD₂Cl₂): δ 207.73 (d, ¹J_{WC} = 105.1 Hz, CO), 167.90 (d, J_{WC} = 32.1 Hz, C≡C), 157.73 (d, J_{WC} = 13.9 Hz, C≡C), 126.01 (s, CN), 19.75 (s, ≡-CH₃), 16.64 (s, ≡-CH₃), 5.04 (s, CH₃CN).

IR (cm⁻¹): ν (C≡N): 2326 (w), 2298 (w); ν (C≡O): 2035 (s).

[WBr₂(CO)(η²-C₂Ph₂)₂(NCMe)] (10)

In an inert 100 mL Schlenk flask, 2.87 g [WBr₂(CO)₃(NCMe)₂] (**7**) (1 equiv., 6.83 mmol) were dissolved in 50 mL CH₂Cl₂ and cooled to 0 °C with an ice bath. Then, 3.66 g diphenylacetylene (3.0 equiv., 20.5 mmol) were added portionwise, and the mixture was allowed to stir for 15 min at 0 °C with an attached bubbler. The ice bath was removed, and the mixture was allowed to stir for 17 hours at rt. The resulting reaction mixture was filtrated, and the filtrate was reduced to 10 mL. The product was recrystallized from CH₂Cl₂/heptane, and the obtained yellow, needle-shaped crystals were washed with heptane (1x 10 mL).

Yield: 96 % (5.03 g, 6.53 mmol).

¹H NMR (CD₂Cl₂): 7.50–7.30 (m, 20H, C₆H₅), 2.27 (s, 3H, CH₃CN).

¹³C NMR (CD₂Cl₂): δ 201.57 (d, ¹J_{WC} = 100.6 Hz, CO), 176.22 (d, J_{WC} = 30.8 Hz, C≡C), 166.40 (d, J_{WC} = 16.9 Hz, C≡C), 138.19 (s, C_q), 136.51 (s, C_q), 130.17 (s, C₆H₅), 129.64

(s, C₆H₅), 129.21 (s, 2 C, C₆H₅), 128.98 (s, 2 C, C₆H₅), 128.20 (s, 2 C, C₆H₅), 128.11 (s, 2 C, C₆H₅), 126.84 (s, CN), 4.63 (s, CH₃CN).

IR (cm⁻¹): ν (C≡N): 2328 (w), 2301 (w); ν (C≡O): 2099 (s).

4 COMPLEX SYNTHESIS

[WBr(CO)₃(PhTt)] (11)

A solution of 3.33 g Cs[PhTt] (**1**) (1.1 equiv., 8.25 mmol) in 35 mL MeCN was slowly added to a stirred solution of 3.82 g [WBr₂(CO)₃(NCMe)₂] (**7**) (1 equiv., 7.50 mmol) in 30 mL MeCN. After one hour, the resulting mixture was reduced to 5 mL. The supernatant solution was removed, and the precipitate was subsequently dried *in vacuo*. Then, the residue was suspended in 50 mL CH₂Cl₂ and filtrated through Celite. The desired product was recrystallized by addition of 30 mL MeCN and subsequent slow evaporation. The obtained orange crystals were washed with 10 mL MeCN and dried *in vacuo*. These crystals were suitable for X-ray diffraction analysis.

Yield: 89 % (3.97 g, 6.41 mmol).

¹H NMR (CD₂Cl₂): δ 7.19–7.15 (m, 4H, C₆H₅), 7.07–7.01 (m, 1H, *p*-C₆H₅), 2.79 (s, 9H, CH₃), 2.19–2.18 (m, 6H, BCH₂).

¹³C NMR (CD₂Cl₂): δ 223.32 (bs, CO), 160.24–158.15 (q, BC_q), 131.21 (s, *m*-C₆H₅), 127.80 (s, *o*-C₆H₅), 125.01 (s, *p*-C₆H₅), 32.50–30.93 (q, ¹J_{BC} = 39.8 Hz, BCH₂), 26.03 (s, CH₃).

IR (cm⁻¹): ν (C≡O): 2026 (s), 1940 (s), 1908 (s).

Anal. Calcd. for C₁₅H₂₀BBrO₃S₃W (619.07): C, 29.10; H, 3.26, S, 15.54. **Found:** C, 29.13; H, 3.15; S, 15.19.

[W(CO)₂(η^2 -CH₂SCH₃)(PhTt)] (12)

In a 25 mL Schlenk flask, 98 mg [WBr₂(CO)₃(NCMe)₂] (**7**) (1 equiv., 0.19 mmol) and 128 mg [Bu₄N][PhTt] (1.3 equiv., 0.25 mmol) were dissolved in 5 mL MeCN. The resulting green-brown solution was allowed to stir for five hours, whereupon the

reaction was terminated by evaporation. The dark brown, sticky residue was dissolved in 7 mL CH₂Cl₂, and the solution was overlaid with 7 mL heptane. Upon slow evaporation, a brown, sticky solid was precipitated. The supernatant solution was isolated by filtration and subsequently evaporated to dryness to give **12** as yellow powder. Crystallization from acetonitrile gave the product as orange crystals suitable for X-ray diffraction analysis.

Yield: < 20 % (< 20 mg, < 0.03 mmol)

¹H NMR (CD₂Cl₂): δ 7.20 (m, 2H, *o*-C₆H₅), 7.15–7.10 (t, 2H, *m*-C₆H₅), 7.00–6.96 (tt, 1H, *p*-C₆H₅), 3.31–3.29 (d, 1H, WCH₂), 3.01–2.98 (d, 1H, WCH₂), 2.66 (bs, 9H, CH₃), 2.39 (s, 3H, CH₃), 2.20 (m, 3H, BCH₂), 1.95 (m, 3H, BCH₂).

IR (cm⁻¹): ν (C≡O): 1925 (s), 1810 (s).

[W(CO)₂(mt)(PhTt)] (13)

A solution of 242 mg Na(mt) (**4**) (1.1 equiv., 1.78 mmol) in 10 mL THF was added dropwise to a stirred solution of 1.00 g [WBr(CO)₃(PhTt)] (**11**) (1 equiv., 1.62 mmol) in 15 mL THF. The flask was equipped with a bubbler and the dark orange reaction mixture was allowed to stir for one hour, whereupon the solvent was evaporated *in vacuo*. Subsequently, the solid was suspended in 20 mL MeCN and filtrated through Celite which was washed with 10 mL THF afterwards. The desired product was crystallized by slow evaporation and washed with MeCN (2x 5 mL) to give **13** as dark orange microcrystalline powder.

Yield: 51 % (0.52 g, 0.83 mmol).

¹H NMR (CD₂Cl₂): δ 7.23 (m, 2H, *o*-C₆H₅), 7.18–7.17 (d, 1H, CH), 7.17–7.13 (m, 2H, *m*-C₆H₅), 7.03–6.99 (tt, 1H, *p*-C₆H₅), 6.60 (d, 1H, CH), 3.34 (s, 3H, NCH₃), 2.46 (s, 9H, SCH₃), 2.17 (bm, 6H, BCH₂).

¹³C NMR (CD₂Cl₂): δ 161.56–159.46 (q, BC_q), 152.43 (s, C=S), 131.35 (s, *o*-C₆H₅), 127.62 (s, *m*-C₆H₅), 126.22 (s, CH), 124.63 (s, *p*-C₆H₅), 120.09 (s, CH), 33.29–31.71 (q, BCH₂), 30.87 (s, NCH₃), 25.44 (s, SCH₃).

IR (cm⁻¹): ν (C≡O): 1922 (s), 1826 (s).

[WBr(CO)(η^2 -C₂Me₂)₂(PhTt-S,S')] (14)

A solution of 267 mg Cs[PhTt] (**1**) (1.1 equiv., 0.66 mmol) in 8 mL MeCN was added dropwise to a stirred solution of 312 mg [WBr₂(CO)(η^2 -C₂Me₂)₂(NCMe)] (**9**) (1 equiv., 0.60 mmol) in 8 mL MeCN. After addition, the resulting yellow-green mixture was allowed to stir for 30 min at -15 °C. Then, the solvent was removed *in vacuo*. The dark yellow solid was subsequently suspended in 20 mL CH₂Cl₂ at -15 °C and filtrated through Celite. The solvent was evaporated *in vacuo* giving a yellow ocher solid as crude product. Yellow crystals suitable for X-ray diffraction analysis were obtained by crystallization from CH₂Cl₂/heptane at -35 °C.

Yield: 50 % (202 mg, 0.30 mmol).

¹H NMR (CD₂Cl₂, 14a): δ 7.37–7.35 (m, 2H, *o*-C₆H₅), 7.19–7.14 (t, 2H, *m*-C₆H₅), 7.06–7.01 (tt, 1H, *p*-C₆H₅), 3.10 (s, 3H, \equiv -CH₃), 3.10 (s, 3H, \equiv -CH₃), 2.89 (s, 3H, \equiv -CH₃), 2.89 (s, 3H, \equiv -CH₃), 2.27 (m, 4H, CH₂), 1.94 (s, 6H, SCH₃), 1.90 (s, 3H, SCH₃), 1.59–1.58 (d, 2H, CH₂).

¹H NMR (CD₂Cl₂, 14b): δ 7.25–7.24 (m, 2H, *o*-C₆H₅), 7.11–7.06 (t, 2H, *m*-C₆H₅), 6.98–6.93 (tt, 1H, *p*-C₆H₅), 3.13 (s, 3H, \equiv -CH₃), 3.13 (s, 3H, \equiv -CH₃), 3.00 (s, 3H, \equiv -CH₃), 3.00 (s, 3H, \equiv -CH₃), 2.25 (m, 2H, CH₂), 2.21 (m, 2H, CH₂), 1.90 (s, 3H, SCH₃), 1.90 (s, 6H, SCH₃), 1.80–1.79 (d, 2H, CH₂).

¹³C NMR (CD₂Cl₂, 14a): δ 208.74 (s, C=O), 179.83 (s, C \equiv C), 161.81 (s, C \equiv C), 132.82 (s, *o*-C₆H₅), 127.02 (s, *m*-C₆H₅), 124.29 (s, *p*-C₆H₅), 36.77–34.78 (m, CH₂), 26.53 (s, SCH₃), 20.08–2.05 (d, SCH₃), 18.92 (s, \equiv -CH₃), 18.31 (s, \equiv -CH₃).

¹³C NMR (CD₂Cl₂, 14b): δ 208.71 (s, C=O), 179.55 (s, C \equiv C), 161.81 (s, C \equiv C), 131.97 (s, *o*-C₆H₅), 127.15 (s, *m*-C₆H₅), 124.23 (s, *p*-C₆H₅), 36.77–34.78 (m, CH₂), 26.53 (s, SCH₃), 20.47–2.43 (d, SCH₃), 18.98 (s, \equiv -CH₃), 18.34 (s, \equiv -CH₃).

IR (cm⁻¹): ν (C \equiv O): 2038 (s).

V REFERENCES

- (1) Ljungdahl, L. G.; Andreesen, J. R. *FEBS Letters* **1975**, *54*, 279–282.
- (2) Kletzin, A.; Adams, M. W. W. *FEMS Microbiol. Rev.* **1996**, *18*, 5–63.
- (3) Yamamoto, I.; Saiki, T.; Liu, S.-M.; Ljungdahl, L. G. *J. Biol. Chem.* **1983**, *258*, 1826–1832.
- (4) *Biological Inorganic Chemistry: Structure and Reactivity*; Bertini, I.; Gray, H. B.; Stiefel, E. I.; Valentine, J. S., Eds.; University Science Books, 2006.
- (5) Rajagopalan, K. V.; Johnson, J. L. *J. Biol. Chem.* **1992**, *267*, 10199–10202.
- (6) Holder, A. A. *Annu. Rep. Prog. Chem., Sect. A: Inorg. Chem.* **2013**, *109*, 119.
- (7) Barabanov, V. F. *Int. Geol. Rev.* **1971**, *13*, 332–344.
- (8) Johnson, M. K.; Rees, D. C.; Adams, M. W. W. *Chem. Rev.* **1996**, *96*, 2817–2839.
- (9) Hille, R. *Trends in Biochem. Sci.* **2002**, *27*, 360–367.
- (10) Carpenter, L. G.; Garrett, D. E. *Min. Eng.* **1959**, *11*, 301–303.
- (11) Basu, P.; Burgmayer, S. J. N. *Coord. Chem. Rev.* **2011**, *255*, 1016–1038.
- (12) Pushie, M. J.; Cotelesage, J. J.; George, G. N. *Metallomics* **2014**, *6*, 15–24.
- (13) *Molybdenum and Tungsten Enzymes*; Hille, R.; Schulzke, C.; Kirk, M. L., Eds.; Royal Society of Chemistry: Cambridge, 2017.
- (14) Boll, M.; Einsle, O.; Ermler, U.; Kroneck, P. M. H.; Ullmann, G. M. *J. Mol. Microbiol. Biotechnol.* **2016**, *26*, 119–137.
- (15) McEwan, A. G.; Ridge, J. P.; McDevitt, C. A.; Hugenholtz, P. *Geomicrobiol. J.* **2010**, *19*, 3–21.
- (16) Scott, I. M.; Rubinstein, G. M.; Lipscomb, G. L.; Basen, M.; Schut, G. J.; Rhaesa, A. M.; Lancaster, W. A.; Poole, F. L.; Kelly, R. M.; Adams, M. W. W. *Appl. Environ. Microbiol.* **2015**, *81*, 7339–7347.
- (17) Weinert, T.; Huwiler, S. G.; Kung, J. W.; Weidenweber, S.; Hellwig, P.; Stärk, H.-J.; Biskup, T.; Weber, S.; Cotelesage, J. J. H.; George, G. N. *et al. Nat. Chem. Biol.* **2015**, *11*, 586–591.
- (18) Bertram, P. A.; Schmitz, R. A.; Linder, D.; Thauer, R. K. *Arch. Microbiol.* **1994**, *161*, 220–222.
- (19) Rosner, B. M.; Schink, B. *J. Bacteriol.* **1995**, *177*, 5767–5772.
- (20) Schink, B. *Arch. Microbiol.* **1985**, *142*, 295–301.
- (21) Boll, M.; Schink, B.; Messerschmidt, A.; Kroneck, P. M. H. *Biol. Chem.* **2005**, *386*, 999–1006.

- (22) Abbasian, F.; Lockington, R.; Mallavarapu, M.; Naidu, R. *Appl. Biochem. Biotechnol.* **2015**, *176*, 670–699.
- (23) Kroneck, P. M. H. *J. Biol. Inorg. Chem.* **2016**, *21*, 29–38.
- (24) tenBrink, F. *Met. Ions Life Sci.* **2014**, *14*, 15–35.
- (25) Zahnle, K. J. *J. Geophys. Res.* **1986**, *91*, 2819.
- (26) Meckenstock, R. U.; Krieger, R. R.; Ensign, S.; Kroneck, P. M. H.; Schink, B. *Eur. J. Biochem.* **1999**, *264*, 176–182.
- (27) tenBrink, F.; Schink, B.; Kroneck, P. M. H. *J. Bacteriol.* **2011**, *193*, 1229–1236.
- (28) Yadav, J.; Das, S. K.; Sarkar, S. *J. Am. Chem. Soc.* **1997**, *119*, 4315–4316.
- (29) Einsle, O.; Niessen, H.; Abt, D. J.; Seiffert, G.; Schink, B.; Huber, R.; Messerschmidt, A.; Kroneck, P. M. H. *Acta Crystallogr. Sect. F Struct. Biol. Cryst. Commun.* **2005**, *61*, 299–301.
- (30) Seiffert, G. B.; Ullmann, G. M.; Messerschmidt, A.; Schink, B.; Kroneck, P. M. H.; Einsle, O. *Proc. Natl. Acad. Sci. U.S.A.* **2007**, *104*, 3073–3077.
- (31) Burger, E.-M.; Andrade, S. L. A.; Einsle, O. *Curr. Opin. Struct. Biol.* **2015**, *35*, 32–40.
- (32) Antony, S.; Bayse, C. A. *Organometallics* **2009**, *28*, 4938–4944.
- (33) Vincent, M. A.; Hillier, I. H.; Periyasamy, G.; Burton, N. A. *Dalton Trans.* **2010**, *39*, 3816–3822.
- (34) Liao, R.-Z.; Yu, J.-G.; Himo, F. *Proc. Natl. Acad. Sci. U.S.A.* **2010**, *107*, 22523–22527.
- (35) Liao, R.-Z.; Thiel, W. *J. Chem. Theory Comput.* **2012**, *8*, 3793–3803.
- (36) Liao, R.-Z.; Thiel, W. *J. Phys. Chem. B* **2013**, *117*, 3954–3961.
- (37) Liao, R.-Z.; Himo, F. *ACS Catal.* **2011**, *1*, 937–944.
- (38) Liu, Y.-F.; Liao, R.-Z.; Ding, W.-J.; Yu, J.-G.; Liu, R.-Z. *J. Biol. Inorg. Chem.* **2011**, *16*, 745–752.
- (39) Templeton, J. L.; Winston, P. B.; Ward, B. C. *J. Am. Chem. Soc.* **1981**, *103*, 7713–7721.
- (40) Majumdar, A.; Sarkar, S. *Coord. Chem. Rev.* **2011**, *255*, 1039–1054.
- (41) Majumdar, A. *Dalton Trans.* **2014**, *43*, 8990–9003.
- (42) *Dithiolene Chemistry: Synthesis, Properties, and Applications*; Stiefel, E. I., Ed.; Progress in Inorganic Chemistry Volume 52; John Wiley & Sons, Inc.: Hoboken, New Jersey, 2004.

- (43) Burgmayer, S. J. N.; Kim, M.; Petit, R.; Rothkopf, A.; Kim, A.; BelHamdounia, S.; Hou, Y.; Somogyi, A.; Habel-Rodriguez, D.; Williams, A. *et al. J. Inorg. Biochem.* **2007**, *101*, 1601–1616.
- (44) Bhuiyan, M. A. I.; Hargrove, W. R.; Metz, C. R.; White, P. S.; Sendlinger, S. C. *Trans. Met. Chem.* **2015**, *40*, 613–621.
- (45) Das, S. K.; Biswas, D.; Maiti, R.; Sarkar, S. *J. Am. Chem. Soc.* **1996**, *118*, 1387–1397.
- (46) Wallace, D.; Gibson, L. T.; Reglinski, J.; Spicer, M. D. *Inorg. Chem.* **2007**, *46*, 3804–3806.
- (47) Trofimenko, S. *Chem. Rev.* **1993**, *93*, 943–980.
- (48) *Scorpionates: Polypyrazolylborate Ligands and Their Coordination Chemistry*; Trofimenko, S., Ed.; Imperial College Press, 1999.
- (49) Trofimenko, S. *J. Am. Chem. Soc.* **1966**, *88*, 1842–1844.
- (50) Serpas, L.; Baum, R. R.; McGhee, A.; Nieto, I.; Jernigan, K. L.; Zeller, M.; Ferrence, G. M.; Tierney, D. L.; Papish, E. T. *Polyhedron* **2016**, *114*, 62–71.
- (51) Ge, P.; Haggerty, B. S.; Rheingold, A. L.; Riordan, C. G. *J. Am. Chem. Soc.* **1994**, *116*, 8406–8407.
- (52) Garner, M.; Reglinski, J.; Cassidy, I.; Spicer, M. D.; Kennedy, A. R. *Chem. Commun.* **1996**, 1975–1976.
- (53) Holler, S.; Tüchler, M.; Belaj, F.; Veiros, L. F.; Kirchner, K.; Mösch-Zanetti, N. C. *Inorg. Chem.* **2016**, *55*, 4980–4991.
- (54) Imran, M.; Neumann, B.; Stammler, H.-G.; Monkowius, U.; Ertl, M.; Mitzel, N. W. *Dalton Trans.* **2013**, *42*, 15785–15795.
- (55) Baker, P. K.; Muldoon, D. J.; Lavery, A. J.; Shawcross, A. *Polyhedron* **1994**, *13*, 2915–2921.
- (56) Hill, A. F.; Tshabang, N.; Willis, A. C. *Eur. J. Inorg. Chem.* **2007**, 3781–3785.
- (57) Gerber, D.; Chongsawangvirod, P.; Leung, A. K.; Ochrymowycz, L. A. *J. Org. Chem.* **1977**, *42*, 2644–2645.
- (58) Kueppers, H. J.; Wieghardt, K.; Nuber, B.; Weiss, J. W.; Bill, E.; Trautwein, A. X. *Inorg. Chem.* **1987**, *26*, 3762–3769.
- (59) Groot, B. de; Loeb, S. J. *Inorg. Chem.* **1990**, *29*, 4084–4090.
- (60) Baker, P. K.; Coles, S. J.; Durrant, M. C.; Harris, S. D.; Hughes, D. L.; Hursthouse, M. B.; Richards, R. L. *J. Chem. Soc., Dalton Trans.* **1996**, 4003–4010.

- (61) Baker, P. K.; Harris, S. D.; Durrant, M. C.; Hughes, D. L.; Richards, R. L. *J. Chem. Soc., Dalton Trans.* **1994**, 1401–1407.
- (62) Baker, P. K.; Clark, A. I.; Drew, M. G. B.; Durrant, M. C.; Richards, R. L. *Polyhedron* **1998**, *9*, 1407–1413.
- (63) Baker, P. K.; Clark, A. I.; Coles, S. J.; Hursthouse, M. B.; Richards, R. L. *J. Organomet. Chem.* **1996**, *518*, 235–237.
- (64) Davis, M. F.; Levason, W.; Light, M. E.; Ratnani, R.; Reid, G.; Saraswat, K.; Webster, M. *Eur. J. Inorg. Chem.* **2007**, *2007*, 1903–1910.
- (65) Levason, W.; Ollivere, L. P.; Reid, G.; Tsoureas, N.; Webster, M. *J. Organomet. Chem.* **2009**, *694*, 2299–2308.
- (66) Barton, A. J.; Connolly, J.; Levason, W.; Mendia-Jalon, A.; Orchard, S. D.; Reid, G. *Polyhedron* **2000**, *19*, 1373–1379.
- (67) Baker, P. K.; Clark, A. I.; Coles, S. J.; Drew, M. G. B.; Durrant, M. C.; Hursthouse, M. B.; Richards, R. L. *J. Chem. Soc., Dalton Trans.* **1998**, 1281–1287.
- (68) Ohrenberg, C.; Ge, P.; Schebler, P.; Riordan, C. G.; Yap, G. P. A.; Rheingold, A. L. *Inorg. Chem.* **1996**, *35*, 749–754.
- (69) Riordan, C. G. *Coord. Chem. Rev.* **2010**, *254*, 1815–1825.
- (70) Ohrenberg, C.; Saleem, M. M.; Riordan, C. G.; Yap, G. P. A.; Verma, A. K.; Rheingold, A. L. *Chem. Commun.* **1996**, 1081–1082.
- (71) Ohrenberg, C.; Riordan, C. G.; Liable-Sands, L. M.; Rheingold, A. L. *Coord. Chem. Rev.* **1998**, *174*, 301–311.
- (72) Schebler, P. J.; Riordan, C. G.; Guzei, I. A.; Rheingold, A. L. *Inorg. Chem.* **1998**, *37*, 4754–4755.
- (73) Ohrenberg, C.; Liable-Sands, L. M.; Rheingold, A. L.; Riordan, C. G. *Inorg. Chem.* **2001**, *40*, 4276–4283.
- (74) Fujita, K.; Rheingold, A. L.; Riordan, C. G. *Dalton Trans.* **2003**, *33*, 2004–2008.
- (75) Mock, M. T.; Popescu, C. V.; Yap, G. P. A.; Dougherty, W. G.; Riordan, C. G. *Inorg. Chem.* **2008**, *47*, 1889–1891.
- (76) Wang, P.; Yap, G. P. A.; Riordan, C. G. *Chem. Commun.* **2014**, *50*, 5871–5873.
- (77) Brückner, R. *Reaktionsmechanismen: Organische Reaktionen, Stereochemie, moderne Synthesemethoden*, 3. Auflage; Spektrum Akad. Verlag: Heidelberg, 2004.
- (78) Ricard, L.; Weiss, R.; Newton, W. E.; Chen, G. J.-J.; McDonald, J. W. *J. Am. Chem. Soc.* **1978**, *100*, 1318–1320.

- (79) Peschel, L. M.; Belaj, F.; Mösch-Zanetti, N. C. *Angew. Chem. Int. Ed.* **2015**, *54*, 13018–13021.
- (80) Beattie, R. J.; White, P. S.; Templeton, J. L. *Organometallics* **2016**, *35*, 32–38.
- (81) Alt, H. G. *J. Organomet. Chem.* **1977**, *127*, 349–356.
- (82) Ward, B. C.; Templeton, J. L. *J. Am. Chem. Soc.* **1980**, *102*, 1532–1538.
- (83) Umland, P.; Vahrenkamp, H. *Chem. Ber.* **1982**, *115*, 3580–3586.
- (84) Alt, H. G. *J. Organomet. Chem.* **1983**, *256*, C12-C14.
- (85) Alt, H. G. *J. Organomet. Chem.* **1985**, *288*, 149–163.
- (86) Morrow, J. R.; Tonker, T. L.; Templeton, J. L.; Kenan, W. R. *J. Am. Chem. Soc.* **1985**, *107*, 6956–6963.
- (87) Alt, H. G.; Han, J. S.; Maisel, H. E. *J. Organomet. Chem.* **1991**, *409*, 197–205.
- (88) Alt, H. G.; Han, J. S. *J. Organomet. Chem.* **1993**, *459*, 209–217.
- (89) Wells, M. B.; White, P. S.; Templeton, J. L. *Organometallics* **1997**, *16*, 1857–1864.
- (90) Frohnepfel, D. S.; Reinartz, S.; White, P. S.; Templeton, J. L. *Organometallics* **1998**, *17*, 3759–3769.
- (91) Templeton, J. L.; Ward, B. C.; Chen, G. J.-J.; McDonald, J. W.; Newton, W. E. *Inorg. Chem.* **1981**, *20*, 1248–1253.
- (92) Alt, H. G.; Hayen, H. I. *J. Organomet. Chem.* **1986**, *316*, 105–119.
- (93) Kersting, M.; El-Kholi, A.; Müller, U.; Dehnicke, K. *Chem. Ber.* **1989**, *122*, 279–285.
- (94) Williams, D. S.; Schofield, M. H.; Schrock, R. R. *Organometallics* **1993**, *12*, 4560–4571.
- (95) Crane, T. W.; White, P. S.; Templeton, J. L. *Organometallics* **1999**, *18*, 1897–1903.
- (96) Crane, T. W.; White, P. S.; Templeton, J. L. *Inorg. Chem.* **2000**, *39*, 1081–1091.
- (97) Tillmann, J.; Lerner, H.-W.; Bolte, M. *Acta Crystallogr. Sect. E, Struct. Rep. Online* **2009**, *66*, o203.
- (98) Baker, P. K.; Drew, M. G. B.; Meehan, M. M.; Szewczyk, J. *J. Organomet. Chem.* **1999**, *580*, 265–272.
- (99) Peschel, L. M.; Unpublished results.
- (100) Peterson, D. J. *J. Org. Chem.* **1967**, *32*, 1717–1720.

- (101) Ruth, K. Entwicklung und Darstellung von Monooxygenase-Modellsystemen auf der Basis neuartiger schwefelhaltiger Skorpionatliganden. PhD thesis, University Frankfurt/Main, Frankfurt/Main, 2008.
- (102) Ruth, K.; Dinnebier, R. E.; Tönnes, S. W.; Alig, E.; Sängler, I.; Lerner, H.-W.; Wagner, M. *Chem. Commun.* **2005**, 3442–3444.
- (103) Peschel, L. M.; Schachner, J. A.; Sala, C. H.; Belaj, F.; Mösch-Zanetti, N. C. Z. *anorg. allg. Chem.* **2013**, 639, 1559–1567.
- (104) Vidovič, C. Active Site Modeling of Acetylene Hydratase: Studies towards tungsten-hydrotris(methimazolyl)borate complexes. Master thesis, KFU Graz, Graz, 2016.
- (105) Chen, G.-J.; Yelton, R. O.; McDonald, J. W. *Inorg. Chim. Acta* **1977**, 22, 249–252.
- (106) Johnson, C. K. *ORTEP: Report ORNL-3794*; Oak Ridge National Laboratory, Tennessee, USA, 1965.
- (107) Dreisch, K.; Andersson, C.; Stalhandske, C. *Polyhedron* **1992**, 11, 2143–2150.
- (108) Peschel, L. M.; Čorovič, M.; Unpublished results.
- (109) Crabtree, R. H. *The Organometallic Chemistry of the Transition Metals*, 4th; John Wiley & Sons, Inc.: Hoboken, New Jersey, 2005.
- (110) Davidson, J. L.; Vasapollo, G. *J. Chem. Soc., Dalton Trans.* **1988**, 2855–2863.
- (111) Armstrong, E. M.; Baker, P. K.; Flower, K. R. *J. Chem. Soc., Dalton Trans.* **1990**, 2535–2541.
- (112) Wrighton, M. *Chem. Rev.* **1974**, 74, 401–430.
- (113) Sheldrick, G. M. *Acta crystallogr. A* **2008**, 64, 112–122.
- (114) Snyder, D. M. Isoxanthate salts and dithiocarbonate diesters.

VI APPENDIX

Table 13: Crystal data and structure refinement for [WBr(CO)₃(PhTt)] (**11**) and [W(CO)₂(η²-CH₂SCH₃)(PhTt)] (**12**).

Crystal data	[WBr(CO) ₃ (PhTt)] (11)	[W(CO) ₂ (η ² -CH ₂ SCH ₃)(PhTt)] (12)
Empirical formula	C ₁₅ H ₂₀ BBrO ₃ S ₃ W	C ₁₆ H ₂₅ BO ₂ S ₄ W
Formula weight	619.06	572.26
Crystal description	needle, orange	plate, orange
Crystal size	0.15 x 0.10 x 0.06mm	0.18 x 0.13 x 0.11mm
Crystal system, space group	monoclinic, P 2 ₁ /c	triclinic, P -1
Unit cell dimensions:	a = 9.3551(7)Å b = 13.0767(9)Å c = 16.4959(11)Å β = 93.200(4)°	a = 8.9219(4)Å b = 9.5091(4)Å c = 12.1788(5)Å α = 85.2924(15)° β = 85.2924(15)° γ = 87.8416(14)°
Volume	2014.9(2)Å ³	1004.42(7)Å ³
Z	4	2
Calculated density	2.041Mg/m ³	1.892Mg/m ³
F(000)	1184	560
Linear absorption coefficient μ	8.037mm ⁻¹	6.173mm ⁻¹
Absorption correction	semi-empirical from equivalents	semi-empirical from equivalents
Max. and min. transmission	1.000 and 0.702	1.000 and 0.526
Unit cell determination	2.47° < Θ < 34.40° 9962 reflections used at 100K	2.85° < Θ < 45.94° 9842 reflections used at 100K
Data collection		
Scan type	φ and ω scans	φ and ω scans
Θ range for data collection	1.99 to 35.00°	1.72 to 44.99°
Reflections collected / unique	47418 / 8861	99607 / 16572
Significant unique reflections	7463 with I > 2σ(I)	15167 with I > 2σ(I)
R(int), R(sigma)	0.0512, 0.0397	0.0611, 0.0357
Completeness to Θ = 35.00°/44.99°	100.0%	100.0%
Refinement		
Data / parameters / restraints	8861 / 227 / 0	16572 / 244 / 5
Goodness-of-fit on F ²	1.050	1.063
Final R indices [I > 2σ(I)]	R1 = 0.0278, wR2 = 0.0506	R1 = 0.0255, wR2 = 0.0541
R indices (all data)	R1 = 0.0396, wR2 = 0.0533	R1 = 0.0310, wR2 = 0.0564
Extinction expression	none	none
Weighting scheme	w = 1/[σ ² (F _o ²)+(aP) ² +bP] where P = (F _o ² +2F _c ²)/3	w = 1/[σ ² (F _o ²)+(aP) ² +bP] where P = (F _o ² +2F _c ²)/3
Weighting scheme parameters a, b	0.0140, 2.1992	0.0127, 1.2164
Largest Δ/σ in last cycle	0.002	0.003
Largest difference peak and hole	2.093 and -1.658e/Å ³	3.582 and -2.917e/Å ³

Table 14: Crystal data and structure refinement for [WBr(CO)(η^2 -C₂Me₂)₂(PhTt-S,S')] (14a and 14b).

Crystal data	[WBr(CO)(η^2 -C ₂ Me ₂) ₂ (PhTt-S,S')] (14a)	[WBr(CO)(η^2 -C ₂ Me ₂) ₂ (PhTt-S,S')] (14b)
Empirical formula	C ₂₁ H ₃₂ BBrOS ₃ W · CH ₂ Cl ₂	C ₂₁ H ₃₂ BBrOS ₃ W
Formula weight	756.14	671.21
Crystal description	block, yellow	rhombic, yellow
Crystal size	0.28 x 0.23 x 0.21mm	0.25 x 0.13 x 0.12mm
Crystal system, space group	monoclinic, P 2 ₁ /n	smonoclinic, P 2 ₁ /n
Unit cell dimensions:	a = 18.2193(15)Å b = 8.1853(7)Å c = 19.4059(16)Å β = 90.420(3)°	a = 8.2035(6)Å b = 15.7902(13)Å c = 18.9901(16)Å β = 93.809(4)°
Volume	2893.9(4)Å ³	2454.4(3)Å ³
Z	4	4
Calculated density	1.735Mg/m ³	1.816Mg/m ³
F(000)	1480	1312
Linear absorption coefficient μ	5.787mm ⁻¹	6.600mm ⁻¹
Absorption correction	semi-empirical from equivalents	semi-empirical from equivalents
Max. and min. transmission	1.000 and 0.773	1.000 and 0.696
Unit cell determination	2.70° < Θ < 35.68° 9843 reflections used at 100K	2.58° < Θ < 35.87° 9961 reflections used at 100K
Data collection		
Scan type	ϕ and ω scans	ϕ and ω scans
Θ range for data collection	2.10 to 35.00°	1.68 to 35.00°
Reflections collected / unique	45008 / 12732	28517 / 10816
Significant unique reflections	9923 with $I > 2\sigma(I)$	8633 with $I > 2\sigma(I)$
R(int), R(sigma)	0.0453, 0.0511	0.0437, 0.0521
Completeness to $\Theta = 35.0^\circ$	100.0%	99.9%
Refinement		
Data / parameters / restraints	12732 / 299 / 0	10816 / 271 / 0
Goodness-of-fit on F ²	1.026	1.024
Final R indices [$I > 2\sigma(I)$]	R1 = 0.0348, wR2 = 0.0751	R1 = 0.0308, wR2 = 0.0667
R indices (all data)	R1 = 0.0531, wR2 = 0.0812	R1 = 0.0484, wR2 = 0.0732
Extinction expression	none	none
Weighting scheme	w = 1/[$\sigma^2(F_o^2)+(aP)^2+bP$] where P = (F _o ² +2F _c ²)/3	w = 1/[$\sigma^2(F_o^2)+(aP)^2+bP$] where P = (F _o ² +2F _c ²)/3
Weighting scheme parameters a, b	0.0305, 3.9576	0.0306, 1.3114
Largest Δ/σ in last cycle	0.002	0.001
Largest difference peak and hole	2.338 and -1.367e/Å ³	2.258 and -2.238e/Å ³

Table 15: Crystal data and structure refinement for [W(CO)₂(mt)(PhTt)] (13) and [WBr(CO)(η²-C₂Ph₂)(PhTt-S,S')] (15).

Crystal data	[W(CO) ₂ (mt)(PhTt)] (13)	[WBr(CO)(η ² -C ₂ Ph ₂) ₂ (PhTt-S,S')] (15)
Empirical formula	C ₁₈ H ₂₅ BN ₂ O ₂ S ₄ W	2C ₄₁ H ₄₀ BBrOS ₃ W · 2C ₇ H ₁₆ · CH ₂ Cl ₂
Formula weight	624.30	2124.28
Crystal description	board, orange	needle, yellow
Crystal size	0.27 x 0.14 x 0.07mm	0.21 x 0.20 x 0.18mm
Crystal system, space group	triclinic, P -1	triclinic, P -1
Unit cell dimensions:	a = 9.2614(10)Å b = 11.1329(12)Å c = 11.3930(12)Å α = 101.568(4)° β = 95.532(4)° γ = 100.068(5)°	a = 13.9791(16)Å b = 14.1887(18)Å c = 14.8499(19)Å α = 64.406(4)° β = 74.075(3)° γ = 61.542(3)°
Volume	1122.5(2)Å ³	2326.7(5)Å ³
Z	2	1
Calculated density	1.847Mg/m ³	1.516Mg/m ³
F(000)	612	1070
Linear absorption coefficient μ	5.534mm ⁻¹	3.568mm ⁻¹
Absorption correction	semi-empirical from equivalents	semi-empirical from equivalents
Max. and min. transmission	1.000 and 0.613	1.000 and 0.660
Unit cell determination	2.71° < Θ < 40.89° 9906 reflections used at 100K	2.35° < Θ < 29.17° 9894 reflections used at 100K
Data collection		
Scan type	φ and ω scans	φ and ω scans
Θ range for data collection	2.25 to 40.00°	1.75 to 30.00°
Reflections collected / unique	35889 / 13896	54851 / 13571
Significant unique reflections	12285 with I > 2σ(I)	10711 with I > 2σ(I)
R(int), R(sigma)	0.0609, 0.0629	0.0782, 0.0804
Completeness to Θ = 40.0°	99.9%	99.9%
Refinement		
Data / parameters / restraints	13896 / 266 / 0	13571 / 524 / 24
Goodness-of-fit on F ²	1.042	1.049
Final R indices [I > 2σ(I)]	R1 = 0.0307, wR2 = 0.0716	R1 = 0.0459, wR2 = 0.1089
R indices (all data)	R1 = 0.0385, wR2 = 0.0756	R1 = 0.0686, wR2 = 0.1194
Extinction expression	none	none
Weighting scheme	w = 1/[σ ² (F _o ²)+(aP) ² +bP] where P = (F _o ² +2F _c ²)/3	w = 1/[σ ² (F _o ²)+(aP) ² +bP] where P = (F _o ² +2F _c ²)/3
Weighting scheme parameters a, b	0.0151, 0.4128	0.0567, 1.7370
Largest Δ/σ in last cycle	0.004	0.001
Largest difference peak and hole	2.127 and -2.370e/Å ³	2.290 and -2.442e/Å ³

Table 16: Full list of bond lengths (Å) and angles (°) for [WBr(CO)₃(PhTt)] (11).

W(1)-C(1)	1.972(3)	C(12)-S(1)-W(1)	114.89(9)
W(1)-C(2)	2.001(2)	S(1)-C(12)-H(121)	109.5
W(1)-C(3)	2.009(3)	S(1)-C(12)-H(122)	109.5
W(1)-S(1)	2.5420(6)	H(121)-C(12)-H(122)	109.5
W(1)-S(2)	2.5654(5)	S(1)-C(12)-H(123)	109.5
W(1)-S(3)	2.5526(6)	H(121)-C(12)-H(123)	109.5
W(1)-Br(1)	2.6517(3)	H(122)-C(12)-H(123)	109.5
C(1)-O(1)	1.153(3)	B(1)-C(21)-S(2)	112.90(15)
C(2)-O(2)	1.147(3)	B(1)-C(21)-H(211)	109.0
C(3)-O(3)	1.141(3)	S(2)-C(21)-H(211)	109.0
B(1)-C(41)	1.633(3)	B(1)-C(21)-H(212)	109.0
B(1)-C(21)	1.649(3)	S(2)-C(21)-H(212)	109.0
B(1)-C(11)	1.652(4)	H(211)-C(21)-H(212)	107.8
B(1)-C(31)	1.658(3)	C(22)-S(2)-C(21)	101.87(11)
C(11)-S(1)	1.809(2)	C(21)-S(2)-W(1)	115.41(8)
C(11)-H(111)	0.99	C(22)-S(2)-W(1)	110.98(9)
C(11)-H(112)	0.99	S(2)-C(22)-H(221)	109.5
S(1)-C(12)	1.805(3)	S(2)-C(22)-H(222)	109.5
C(12)-H(121)	0.98	H(221)-C(22)-H(222)	109.5
C(12)-H(122)	0.98	S(2)-C(22)-H(223)	109.5
C(12)-H(123)	0.98	H(221)-C(22)-H(223)	109.5
C(21)-S(2)	1.815(2)	H(222)-C(22)-H(223)	109.5
C(21)-H(211)	0.99	B(1)-C(31)-S(3)	111.62(16)
C(21)-H(212)	0.99	B(1)-C(31)-H(311)	109.3
S(2)-C(22)	1.806(2)	S(3)-C(31)-H(311)	109.3
C(22)-H(221)	0.98	B(1)-C(31)-H(312)	109.3
C(22)-H(222)	0.98	S(3)-C(31)-H(312)	109.3
C(22)-H(223)	0.98	H(311)-C(31)-H(312)	108.0
C(31)-S(3)	1.807(2)	C(32)-S(3)-C(31)	102.87(12)
C(31)-H(311)	0.99	C(31)-S(3)-W(1)	108.71(8)
C(31)-H(312)	0.99	C(32)-S(3)-W(1)	112.11(9)
S(3)-C(32)	1.800(3)	S(3)-C(32)-H(321)	109.5
C(32)-H(321)	0.98	S(3)-C(32)-H(322)	109.5
C(32)-H(322)	0.98	H(321)-C(32)-H(322)	109.5
C(32)-H(323)	0.98	S(3)-C(32)-H(323)	109.5
C(41)-C(42)	1.401(3)	H(321)-C(32)-H(323)	109.5
C(41)-C(46)	1.403(4)	H(322)-C(32)-H(323)	109.5
C(42)-C(43)	1.401(3)	C(42)-C(41)-C(46)	116.2(2)
C(42)-H(42)	0.95	C(42)-C(41)-B(1)	123.6(2)
C(43)-C(44)	1.383(4)	C(46)-C(41)-B(1)	120.1(2)
C(43)-H(43)	0.95	C(43)-C(42)-C(41)	122.0(2)
C(44)-C(45)	1.395(4)	C(43)-C(42)-H(42)	119.0
C(44)-H(44)	0.95	C(41)-C(42)-H(42)	119.0
C(45)-C(46)	1.393(4)	C(44)-C(43)-C(42)	120.3(2)
C(45)-H(45)	0.95	C(44)-C(43)-H(43)	119.9
C(46)-H(46)	0.95	C(42)-C(43)-H(43)	119.9
		C(43)-C(44)-C(45)	119.2(2)
S(1)-W(1)-Br(1)	154.752(14)	C(43)-C(44)-H(44)	120.4
S(3)-W(1)-Br(1)	91.442(15)	C(45)-C(44)-H(44)	120.4
S(2)-W(1)-Br(1)	80.125(15)	C(46)-C(45)-C(44)	119.9(3)
C(1)-W(1)-Br(1)	128.79(8)	C(46)-C(45)-H(45)	120.0
C(2)-W(1)-Br(1)	76.56(7)	C(44)-C(45)-H(45)	120.0
C(3)-W(1)-Br(1)	77.33(8)	C(45)-C(46)-C(41)	122.4(2)
C(1)-W(1)-C(2)	71.51(11)	C(45)-C(46)-H(46)	118.8
C(1)-W(1)-C(3)	73.47(11)	C(41)-C(46)-H(46)	118.8
C(2)-W(1)-C(3)	104.66(10)		
C(1)-W(1)-S(1)	75.35(8)	C(41)-B(1)-C(11)-S(1)	-155.54(16)
C(2)-W(1)-S(1)	123.90(7)	C(21)-B(1)-C(11)-S(1)	-36.3(2)
C(3)-W(1)-S(1)	107.57(8)	C(31)-B(1)-C(11)-S(1)	85.8(2)
C(1)-W(1)-S(2)	135.95(8)	B(1)-C(11)-S(1)-C(12)	-170.83(17)
C(2)-W(1)-S(2)	152.26(8)	B(1)-C(11)-S(1)-W(1)	-48.07(17)
C(3)-W(1)-S(2)	84.43(7)	C(41)-B(1)-C(21)-S(2)	-155.29(17)
S(1)-W(1)-S(2)	75.837(18)	C(11)-B(1)-C(21)-S(2)	85.0(2)
S(3)-W(1)-S(2)	87.232(19)	C(31)-B(1)-C(21)-S(2)	-36.4(2)
C(1)-W(1)-S(3)	119.22(8)	B(1)-C(21)-S(2)-C(22)	-156.51(18)

C(2)-W(1)-S(3)	78.60(7)	B(1)-C(21)-S(2)-W(1)	-36.2(2)
C(3)-W(1)-S(3)	167.00(8)	C(41)-B(1)-C(31)-S(3)	-143.67(16)
S(1)-W(1)-S(3)	79.888(19)	C(21)-B(1)-C(31)-S(3)	96.3(2)
O(1)-C(1)-W(1)	175.6(2)	C(11)-B(1)-C(31)-S(3)	-23.3(2)
O(2)-C(2)-W(1)	178.3(2)	B(1)-C(31)-S(3)-C(32)	-176.18(17)
O(3)-C(3)-W(1)	177.8(3)	B(1)-C(31)-S(3)-W(1)	-57.16(16)
C(41)-B(1)-C(21)	109.49(18)	C(21)-B(1)-C(41)-C(42)	-129.8(2)
C(41)-B(1)-C(11)	110.20(19)	C(11)-B(1)-C(41)-C(42)	-11.8(3)
C(21)-B(1)-C(11)	107.4(2)	C(31)-B(1)-C(41)-C(42)	108.8(3)
C(41)-B(1)-C(31)	107.44(19)	C(21)-B(1)-C(41)-C(46)	52.0(3)
C(21)-B(1)-C(31)	111.66(19)	C(11)-B(1)-C(41)-C(46)	170.0(2)
C(11)-B(1)-C(31)	110.61(18)	C(31)-B(1)-C(41)-C(46)	-69.5(3)
B(1)-C(11)-S(1)	112.60(15)	C(46)-C(41)-C(42)-C(43)	-0.7(4)
B(1)-C(11)-H(111)	109.1	B(1)-C(41)-C(42)-C(43)	-179.0(2)
S(1)-C(11)-H(111)	109.1	C(41)-C(42)-C(43)-C(44)	0.5(4)
B(1)-C(11)-H(112)	109.1	C(42)-C(43)-C(44)-C(45)	-0.3(5)
S(1)-C(11)-H(112)	109.1	C(43)-C(44)-C(45)-C(46)	0.4(5)
H(111)-C(11)-H(112)	107.8	C(44)-C(45)-C(46)-C(41)	-0.7(5)
C(12)-S(1)-C(11)	100.87(12)	C(42)-C(41)-C(46)-C(45)	0.8(4)
C(11)-S(1)-W(1)	112.18(8)	B(1)-C(41)-C(46)-C(45)	179.2(3)

Table 17: Full list of bond lengths (Å) and angles (°) for [WBr(CO)₂(η²-CH₂SCH₃)(PhTi)] (12).

W(1)-C(1)	1.9824(14)	S(1)-C(11)-H(111)	108.9
W(1)-C(2)	1.9267(14)	B(1)-C(11)-H(112)	108.9
W(1)-S(1)	2.5528(3)	S(1)-C(11)-H(112)	108.9
W(1)-S(2)	2.5804(3)	H(111)-C(11)-H(112)	107.7
W(1)-S(3)	2.4999(3)	C(12)-S(1)-C(11)	101.84(7)
W(1)-C(41)	2.2184(14)	C(12)-S(1)-W(1)	109.50(5)
W(1)-S(4)	2.4561(4)	C(11)-S(1)-W(1)	112.23(4)
C(1)-O(1)	1.1576(18)	S(1)-C(12)-H(121)	109.5
C(2)-O(2)	1.1731(18)	S(1)-C(12)-H(122)	109.5
B(1)-C(101)	1.634(2)	H(121)-C(12)-H(122)	109.5
B(1)-C(11)	1.6517(19)	S(1)-C(12)-H(123)	109.5
B(1)-C(21)	1.661(2)	H(121)-C(12)-H(123)	109.5
B(1)-C(31)	1.670(2)	H(122)-C(12)-H(123)	109.5
C(101)-C(102)	1.4057(19)	B(1)-C(21)-S(2)	111.66(9)
C(101)-C(106)	1.410(2)	B(1)-C(21)-H(211)	109.3
C(102)-C(103)	1.396(2)	S(2)-C(21)-H(211)	109.3
C(102)-H(102)	0.95	B(1)-C(21)-H(212)	109.3
C(103)-C(104)	1.395(2)	S(2)-C(21)-H(212)	109.3
C(103)-H(103)	0.95	H(211)-C(21)-H(212)	108.0
C(104)-C(105)	1.391(2)	C(22)-S(2)-C(21)	102.06(7)
C(104)-H(104)	0.95	C(22)-S(2)-W(1)	114.25(5)
C(105)-C(106)	1.397(2)	C(21)-S(2)-W(1)	110.57(5)
C(105)-H(105)	0.95	S(2)-C(22)-H(221)	109.5
C(106)-H(106)	0.95	S(2)-C(22)-H(222)	109.5
C(11)-S(1)	1.8153(14)	H(221)-C(22)-H(222)	109.5
C(11)-H(111)	0.98	S(2)-C(22)-H(223)	109.5
C(11)-H(112)	0.98	H(221)-C(22)-H(223)	109.5
S(1)-C(12)	1.8046(15)	H(222)-C(22)-H(223)	109.5
C(12)-H(121)	0.98	B(1)-C(31)-S(3)	110.87(8)
C(12)-H(122)	0.98	B(1)-C(31)-H(311)	109.5
C(12)-H(123)	0.98	S(3)-C(31)-H(311)	109.5
C(21)-S(2)	1.8140(14)	B(1)-C(31)-H(312)	109.5
C(21)-H(211)	0.98	S(3)-C(31)-H(312)	109.5
C(21)-H(212)	0.98	H(311)-C(31)-H(312)	108.1
S(2)-C(22)	1.8070(15)	C(32)-S(3)-C(31)	102.75(7)
C(22)-H(221)	0.98	C(32)-S(3)-W(1)	113.99(6)
C(22)-H(222)	0.98	C(31)-S(3)-W(1)	110.71(4)
C(22)-H(223)	0.98	S(3)-C(32)-H(321)	109.5
C(31)-S(3)	1.8043(13)	S(3)-C(32)-H(322)	109.5
C(31)-H(311)	0.98	H(321)-C(32)-H(322)	109.5
C(31)-H(312)	0.98	S(3)-C(32)-H(323)	109.5
S(3)-C(32)	1.8027(16)	H(321)-C(32)-H(323)	109.5

C(32)-H(321)	0.98	H(322)-C(32)-H(323)	109.5
C(32)-H(322)	0.98	S(4)-C(41)-W(1)	75.24(5)
C(32)-H(323)	0.98	S(4)-C(41)-H(411)	112.6(11)
C(41)-S(4)	1.7611(15)	W(1)-C(41)-H(411)	120.3(5)
C(41)-H(411)	0.98	S(4)-C(41)-H(412)	110.4(5)
C(41)-H(412)	0.98	W(1)-C(41)-H(412)	116.1(15)
S(4)-C(42)	1.8080(16)	H(411)-C(41)-H(412)	115.1(14)
C(42)-H(421)	0.98	C(41)-S(4)-C(42)	105.72(8)
C(42)-H(422)	0.98	C(41)-S(4)-W(1)	60.86(5)
C(42)-H(423)	0.98	C(42)-S(4)-W(1)	111.47(5)
		S(4)-C(42)-H(421)	106.5(5)
C(1)-W(1)-S(1)	161.30(4)	S(4)-C(42)-H(422)	110.2(6)
C(2)-W(1)-S(2)	175.03(4)	H(421)-C(42)-H(422)	107.4(11)
S(3)-W(1)-S(4)	162.318(12)	S(4)-C(42)-H(423)	111.4(13)
S(3)-W(1)-C(41)	150.47(4)	H(421)-C(42)-H(423)	112(2)
C(2)-W(1)-C(1)	82.46(6)	H(422)-C(42)-H(423)	108.9(14)
C(2)-W(1)-C(41)	98.53(5)		
C(1)-W(1)-C(41)	71.47(6)	B(1)-C(11)-S(1)-W(1)	41.91(10)
C(2)-W(1)-S(4)	92.17(4)	B(1)-C(21)-S(2)-W(1)	48.28(10)
C(1)-W(1)-S(4)	113.62(4)	B(1)-C(31)-S(3)-W(1)	53.76(9)
C(41)-W(1)-S(4)	43.90(4)	B(1)-C(11)-S(1)-C(12)	158.91(10)
C(2)-W(1)-S(3)	93.68(4)	B(1)-C(21)-S(2)-C(22)	170.20(10)
C(1)-W(1)-S(3)	83.71(4)	B(1)-C(31)-S(3)-C(32)	175.85(10)
C(2)-W(1)-S(1)	91.52(4)	S(2)-W(1)-S(1)-C(12)	-172.67(6)
C(41)-W(1)-S(1)	127.09(4)	S(3)-W(1)-S(2)-C(22)	-177.37(8)
S(4)-W(1)-S(1)	84.174(12)	S(1)-W(1)-S(3)-C(32)	173.18(7)
S(3)-W(1)-S(1)	79.005(11)	W(1)-C(41)-S(4)-C(42)	-106.16(6)
C(1)-W(1)-S(2)	101.33(4)	C(1)-W(1)-S(4)-C(41)	-17.33(7)
C(41)-W(1)-S(2)	85.79(4)	C(2)-W(1)-S(4)-C(42)	-3.51(7)
S(4)-W(1)-S(2)	89.237(12)	C(11)-B(1)-C(101)-C(102)	-168.67(13)
S(3)-W(1)-S(2)	83.625(10)	C(21)-B(1)-C(101)-C(102)	-46.83(17)
S(1)-W(1)-S(2)	83.876(11)	C(31)-B(1)-C(101)-C(102)	72.71(15)
O(1)-C(1)-W(1)	175.58(13)	C(11)-B(1)-C(101)-C(106)	16.72(18)
O(2)-C(2)-W(1)	179.60(14)	C(21)-B(1)-C(101)-C(106)	138.55(14)
C(101)-B(1)-C(11)	109.46(10)	C(31)-B(1)-C(101)-C(106)	-101.91(15)
C(101)-B(1)-C(21)	110.65(11)	C(106)-C(101)-C(102)-C(103)	-1.0(2)
C(11)-B(1)-C(21)	110.36(11)	B(1)-C(101)-C(102)-C(103)	-175.98(14)
C(101)-B(1)-C(31)	106.05(10)	C(101)-C(102)-C(103)-C(104)	0.6(2)
C(11)-B(1)-C(31)	110.00(11)	C(102)-C(103)-C(104)-C(105)	0.2(3)
C(21)-B(1)-C(31)	110.23(10)	C(103)-C(104)-C(105)-C(106)	-0.5(3)
C(102)-C(101)-C(106)	116.01(12)	C(104)-C(105)-C(106)-C(101)	0.1(3)
C(102)-C(101)-B(1)	121.58(11)	C(102)-C(101)-C(106)-C(105)	0.7(2)
C(106)-C(101)-B(1)	122.21(12)	B(1)-C(101)-C(106)-C(105)	175.58(15)
C(103)-C(102)-C(101)	122.42(13)	C(101)-B(1)-C(11)-S(1)	158.53(9)
C(103)-C(102)-H(102)	118.8	C(21)-B(1)-C(11)-S(1)	36.52(14)
C(101)-C(102)-H(102)	118.8	C(31)-B(1)-C(11)-S(1)	-85.32(12)
C(104)-C(103)-C(102)	120.05(14)	B(1)-C(11)-S(1)-C(12)	158.91(10)
C(104)-C(103)-H(103)	120.0	B(1)-C(11)-S(1)-W(1)	41.91(11)
C(102)-C(103)-H(103)	120.0	C(101)-B(1)-C(21)-S(2)	146.00(9)
C(105)-C(104)-C(103)	119.12(14)	C(11)-B(1)-C(21)-S(2)	-92.69(11)
C(105)-C(104)-H(104)	120.4	C(31)-B(1)-C(21)-S(2)	29.01(13)
C(103)-C(104)-H(104)	120.4	B(1)-C(21)-S(2)-C(22)	170.20(10)
C(104)-C(105)-C(106)	120.22(14)	B(1)-C(21)-S(2)-W(1)	48.28(10)
C(104)-C(105)-H(105)	119.9	C(101)-B(1)-C(31)-S(3)	147.45(9)
C(106)-C(105)-H(105)	119.9	C(11)-B(1)-C(31)-S(3)	29.18(13)
C(105)-C(106)-C(101)	122.17(14)	C(21)-B(1)-C(31)-S(3)	-92.74(11)
C(105)-C(106)-H(106)	118.9	B(1)-C(31)-S(3)-C(32)	175.85(10)
C(101)-C(106)-H(106)	118.9	B(1)-C(31)-S(3)-W(1)	53.76(9)
B(1)-C(11)-S(1)	113.43(9)	W(1)-C(41)-S(4)-C(42)	-106.16(6)
B(1)-C(11)-H(111)	108.9		

Table 18: Full list of bond lengths (Å) and angles (°) for [WBr(CO)(η^2 -C₂Me₂)₂(PhTt-S,S')] (**14a**).

W(1)-C(1)	2.064(3)	C(4)-C(3)-W(1)	74.04(18)
W(1)-C(2)	2.110(3)	C(30)-C(3)-W(1)	142.2(2)
W(1)-C(3)	2.069(3)	C(3)-C(4)-C(40)	145.5(3)

W(1)-C(4)	2.114(3)	C(3)-C(4)-W(1)	70.28(17)
W(1)-C(5)	2.019(3)	C(40)-C(4)-W(1)	144.2(2)
W(1)-Br(1)	2.6073(4)	C(4)-C(40)-H(401)	109.5
W(1)-S(1)	2.6500(7)	C(4)-C(40)-H(402)	109.5
W(1)-S(2)	2.6533(7)	H(401)-C(40)-H(402)	109.5
C(10)-C(1)	1.488(4)	C(4)-C(40)-H(403)	109.5
C(10)-H(101)	0.98	H(401)-C(40)-H(403)	109.5
C(10)-H(102)	0.98	H(402)-C(40)-H(403)	109.5
C(10)-H(103)	0.98	O(5)-C(5)-W(1)	177.1(3)
C(1)-C(2)	1.281(4)	C(41)-B(1)-C(21)	105.7(2)
C(2)-C(20)	1.482(5)	C(41)-B(1)-C(11)	109.4(3)
C(20)-H(201)	0.98	C(21)-B(1)-C(11)	108.9(2)
C(20)-H(202)	0.98	C(41)-B(1)-C(31)	110.5(3)
C(20)-H(203)	0.98	C(21)-B(1)-C(31)	109.9(3)
C(30)-C(3)	1.479(4)	C(11)-B(1)-C(31)	112.1(2)
C(30)-H(301)	0.98	B(1)-C(11)-S(1)	115.4(2)
C(30)-H(302)	0.98	B(1)-C(11)-H(111)	108.4
C(30)-H(303)	0.98	S(1)-C(11)-H(111)	108.4
C(3)-C(4)	1.282(4)	B(1)-C(11)-H(112)	108.4
C(4)-C(40)	1.484(4)	S(1)-C(11)-H(112)	108.4
C(40)-H(401)	0.98	H(111)-C(11)-H(112)	107.5
C(40)-H(402)	0.98	C(11)-S(1)-C(12)	101.19(15)
C(40)-H(403)	0.98	C(11)-S(1)-W(1)	114.76(9)
C(5)-O(5)	1.133(4)	C(12)-S(1)-W(1)	104.38(10)
B(1)-C(41)	1.626(5)	S(1)-C(12)-H(121)	109.5
B(1)-C(21)	1.649(4)	S(1)-C(12)-H(122)	109.5
B(1)-C(11)	1.649(5)	H(121)-C(12)-H(122)	109.5
B(1)-C(31)	1.651(5)	S(1)-C(12)-H(123)	109.5
C(11)-S(1)	1.800(3)	H(121)-C(12)-H(123)	109.5
C(11)-H(111)	0.99	H(122)-C(12)-H(123)	109.5
C(11)-H(112)	0.99	B(1)-C(21)-S(2)	115.0(2)
S(1)-C(12)	1.806(3)	B(1)-C(21)-H(211)	108.5
C(12)-H(121)	0.98	S(2)-C(21)-H(211)	108.5
C(12)-H(122)	0.98	B(1)-C(21)-H(212)	108.5
C(12)-H(123)	0.98	S(2)-C(21)-H(212)	108.5
C(21)-S(2)	1.812(3)	H(211)-C(21)-H(212)	107.5
C(21)-H(211)	0.99	C(22)-S(2)-C(21)	100.28(15)
C(21)-H(212)	0.99	C(22)-S(2)-W(1)	104.39(11)
S(2)-C(22)	1.806(3)	C(21)-S(2)-W(1)	116.14(10)
C(22)-H(221)	0.98	S(2)-C(22)-H(221)	109.5
C(22)-H(222)	0.98	S(2)-C(22)-H(222)	109.5
C(22)-H(223)	0.98	H(221)-C(22)-H(222)	109.5
C(31)-S(3)	1.798(3)	S(2)-C(22)-H(223)	109.5
C(31)-H(311)	0.99	H(221)-C(22)-H(223)	109.5
C(31)-H(312)	0.99	H(222)-C(22)-H(223)	109.5
S(3)-C(32)	1.781(5)	B(1)-C(31)-S(3)	112.7(2)
C(32)-H(321)	0.98	B(1)-C(31)-H(311)	109.0
C(32)-H(322)	0.98	S(3)-C(31)-H(311)	109.0
C(32)-H(323)	0.98	B(1)-C(31)-H(312)	109.0
C(41)-C(46)	1.373(5)	S(3)-C(31)-H(312)	109.0
C(41)-C(42)	1.408(5)	H(311)-C(31)-H(312)	107.8
C(42)-C(43)	1.391(5)	C(32)-S(3)-C(31)	102.36(19)
C(42)-H(42)	0.95	S(3)-C(32)-H(321)	109.5
C(43)-C(44)	1.393(6)	S(3)-C(32)-H(322)	109.5
C(43)-H(43)	0.95	H(321)-C(32)-H(322)	109.5
C(44)-C(45)	1.376(6)	S(3)-C(32)-H(323)	109.5
C(44)-H(44)	0.95	H(321)-C(32)-H(323)	109.5
C(45)-C(46)	1.405(5)	H(322)-C(32)-H(323)	109.5
C(45)-H(45)	0.95	C(46)-C(41)-C(42)	114.7(3)
C(46)-H(46)	0.95	C(46)-C(41)-B(1)	124.5(3)
C(6)-Cl(1)	1.710(5)	C(42)-C(41)-B(1)	120.8(3)
C(6)-Cl(2)	1.790(5)	C(43)-C(42)-C(41)	123.6(4)
C(6)-H(61)	0.99	C(43)-C(42)-H(42)	118.2
C(6)-H(62)	0.99	C(41)-C(42)-H(42)	118.2
		C(42)-C(43)-C(44)	119.2(4)
C(5)-W(1)-C(1)	110.23(12)	C(42)-C(43)-H(43)	120.4
C(5)-W(1)-C(3)	109.37(11)	C(44)-C(43)-H(43)	120.4
C(1)-W(1)-C(3)	92.05(11)	C(45)-C(44)-C(43)	119.0(3)

C(5)-W(1)-C(2)	74.58(12)	C(45)-C(44)-H(44)	120.5
C(1)-W(1)-C(2)	35.72(12)	C(43)-C(44)-H(44)	120.5
C(3)-W(1)-C(2)	106.11(11)	C(44)-C(45)-C(46)	119.9(4)
C(5)-W(1)-C(4)	73.72(12)	C(44)-C(45)-H(45)	120.0
C(1)-W(1)-C(4)	105.85(11)	C(46)-C(45)-H(45)	120.0
C(3)-W(1)-C(4)	35.68(11)	C(41)-C(46)-C(45)	123.5(4)
C(2)-W(1)-C(4)	98.14(11)	C(41)-C(46)-H(46)	118.2
C(5)-W(1)-Br(1)	157.99(8)	C(45)-C(46)-H(46)	118.2
C(1)-W(1)-Br(1)	85.11(8)	Cl(1)-C(6)-Cl(2)	114.9(3)
C(3)-W(1)-Br(1)	84.90(8)	Cl(1)-C(6)-H(61)	108.5
C(2)-W(1)-Br(1)	118.54(8)	Cl(2)-C(6)-H(61)	108.5
C(4)-W(1)-Br(1)	118.35(8)	Cl(1)-C(6)-H(62)	108.5
C(5)-W(1)-S(1)	79.75(8)	Cl(2)-C(6)-H(62)	108.5
C(1)-W(1)-S(1)	168.33(8)	H(61)-C(6)-H(62)	107.5
C(3)-W(1)-S(1)	90.11(8)		
C(2)-W(1)-S(1)	152.98(9)	C(10)-C(1)-C(2)-C(20)	-3.4(9)
C(4)-W(1)-S(1)	82.39(8)	W(1)-C(1)-C(2)-C(20)	177.9(5)
Br(1)-W(1)-S(1)	83.670(17)	C(10)-C(1)-C(2)-W(1)	178.6(5)
C(5)-W(1)-S(2)	80.75(8)	C(30)-C(3)-C(4)-C(40)	1.8(8)
C(1)-W(1)-S(2)	89.64(8)	W(1)-C(3)-C(4)-C(40)	-179.3(5)
C(3)-W(1)-S(2)	168.35(8)	C(30)-C(3)-C(4)-W(1)	-178.9(5)
C(2)-W(1)-S(2)	81.77(8)	C(41)-B(1)-C(11)-S(1)	163.2(2)
C(4)-W(1)-S(2)	153.43(8)	C(21)-B(1)-C(11)-S(1)	-81.6(3)
Br(1)-W(1)-S(2)	83.763(19)	C(31)-B(1)-C(11)-S(1)	40.2(3)
S(1)-W(1)-S(2)	86.00(2)	B(1)-C(11)-S(1)-C(12)	174.4(2)
C(1)-C(10)-H(101)	109.5	B(1)-C(11)-S(1)-W(1)	62.6(2)
C(1)-C(10)-H(102)	109.5	C(41)-B(1)-C(21)-S(2)	-163.6(2)
H(101)-C(10)-H(102)	109.5	C(11)-B(1)-C(21)-S(2)	78.9(3)
C(1)-C(10)-H(103)	109.5	C(31)-B(1)-C(21)-S(2)	-44.3(3)
H(101)-C(10)-H(103)	109.5	B(1)-C(21)-S(2)-C(22)	-171.1(2)
H(102)-C(10)-H(103)	109.5	B(1)-C(21)-S(2)-W(1)	-59.3(3)
C(2)-C(1)-C(10)	143.2(3)	C(41)-B(1)-C(31)-S(3)	-61.9(3)
C(2)-C(1)-W(1)	74.12(19)	C(21)-B(1)-C(31)-S(3)	-178.23(19)
C(10)-C(1)-W(1)	142.7(2)	C(11)-B(1)-C(31)-S(3)	60.5(3)
C(1)-C(2)-C(20)	145.0(3)	B(1)-C(31)-S(3)-C(32)	-179.9(3)
C(1)-C(2)-W(1)	70.16(19)	C(21)-B(1)-C(41)-C(46)	-105.1(4)
C(20)-C(2)-W(1)	144.8(2)	C(11)-B(1)-C(41)-C(46)	12.1(4)
C(2)-C(20)-H(201)	109.5	C(31)-B(1)-C(41)-C(46)	136.0(3)
C(2)-C(20)-H(202)	109.5	C(21)-B(1)-C(41)-C(42)	73.6(4)
H(201)-C(20)-H(202)	109.5	C(11)-B(1)-C(41)-C(42)	-169.2(3)
C(2)-C(20)-H(203)	109.5	C(31)-B(1)-C(41)-C(42)	-45.2(4)
H(201)-C(20)-H(203)	109.5	C(46)-C(41)-C(42)-C(43)	-1.0(5)
H(202)-C(20)-H(203)	109.5	B(1)-C(41)-C(42)-C(43)	-179.8(3)
C(3)-C(30)-H(301)	109.5	C(41)-C(42)-C(43)-C(44)	1.0(6)
C(3)-C(30)-H(302)	109.5	C(42)-C(43)-C(44)-C(45)	-0.8(6)
H(301)-C(30)-H(302)	109.5	C(43)-C(44)-C(45)-C(46)	0.7(6)
C(3)-C(30)-H(303)	109.5	C(42)-C(41)-C(46)-C(45)	0.9(5)
H(301)-C(30)-H(303)	109.5	B(1)-C(41)-C(46)-C(45)	179.7(3)
H(302)-C(30)-H(303)	109.5	C(44)-C(45)-C(46)-C(41)	-0.8(6)
C(4)-C(3)-C(30)	143.8(3)		

Table 19: Full list of bond lengths (Å) and angles (°) for [WBr(CO)(η^2 -C₂Me₂)₂(PhTt-S,S')] (**14b**).

W(1)-C(1)	2.058(3)	C(4)-C(3)-C(30)	143.8(3)
W(1)-C(2)	2.102(3)	C(4)-C(3)-W(1)	73.68(18)
W(1)-C(3)	2.080(3)	C(30)-C(3)-W(1)	142.5(2)
W(1)-C(4)	2.115(2)	C(3)-C(4)-C(40)	145.7(3)
W(1)-C(5)	2.004(3)	C(3)-C(4)-W(1)	70.71(16)
W(1)-Br(1)	2.6391(3)	C(40)-C(4)-W(1)	143.6(3)
W(1)-S(1)	2.6334(6)	C(4)-C(40)-H(401)	109.5
W(1)-S(2)	2.6473(6)	C(4)-C(40)-H(402)	109.5
C(10)-C(1)	1.484(4)	H(401)-C(40)-H(402)	109.5
C(10)-H(101)	0.98	C(4)-C(40)-H(403)	109.5
C(10)-H(102)	0.98	H(401)-C(40)-H(403)	109.5
C(10)-H(103)	0.98	H(402)-C(40)-H(403)	109.5

C(1)-C(2)	1.292(4)	O(5)-C(5)-W(1)	177.7(3)
C(2)-C(20)	1.486(4)	C(41)-B(1)-C(11)	110.9(2)
C(20)-H(201)	0.98	C(41)-B(1)-C(31)	112.3(2)
C(20)-H(202)	0.98	C(11)-B(1)-C(31)	102.1(2)
C(20)-H(203)	0.98	C(41)-B(1)-C(21)	110.3(2)
C(30)-C(3)	1.480(5)	C(11)-B(1)-C(21)	112.0(2)
C(30)-H(301)	0.98	C(31)-B(1)-C(21)	109.0(2)
C(30)-H(302)	0.98	B(1)-C(11)-S(1)	112.96(17)
C(30)-H(303)	0.98	B(1)-C(11)-H(111)	109.0
C(3)-C(4)	1.283(4)	S(1)-C(11)-H(111)	109.0
C(4)-C(40)	1.488(4)	B(1)-C(11)-H(112)	109.0
C(40)-H(401)	0.98	S(1)-C(11)-H(112)	109.0
C(40)-H(402)	0.98	H(111)-C(11)-H(112)	107.8
C(40)-H(403)	0.98	C(11)-S(1)-C(12)	102.74(13)
C(5)-O(5)	1.136(4)	C(11)-S(1)-W(1)	111.92(9)
B(1)-C(41)	1.632(4)	C(12)-S(1)-W(1)	105.44(11)
B(1)-C(11)	1.651(4)	S(1)-C(12)-H(121)	109.5
B(1)-C(31)	1.653(4)	S(1)-C(12)-H(122)	109.5
B(1)-C(21)	1.664(4)	H(121)-C(12)-H(122)	109.5
C(11)-S(1)	1.800(2)	S(1)-C(12)-H(123)	109.5
C(11)-H(111)	0.99	H(121)-C(12)-H(123)	109.5
C(11)-H(112)	0.99	H(122)-C(12)-H(123)	109.5
S(1)-C(12)	1.807(3)	B(1)-C(21)-S(2)	111.47(19)
C(12)-H(121)	0.98	B(1)-C(21)-H(211)	109.3
C(12)-H(122)	0.98	S(2)-C(21)-H(211)	109.3
C(12)-H(123)	0.98	B(1)-C(21)-H(212)	109.3
C(21)-S(2)	1.811(3)	S(2)-C(21)-H(212)	109.3
C(21)-H(211)	0.99	H(211)-C(21)-H(212)	108.0
C(21)-H(212)	0.99	C(22)-S(2)-C(21)	102.37(15)
S(2)-C(22)	1.805(3)	C(22)-S(2)-W(1)	104.22(9)
C(22)-H(221)	0.98	C(21)-S(2)-W(1)	110.00(9)
C(22)-H(222)	0.98	S(2)-C(22)-H(221)	109.5
C(22)-H(223)	0.98	S(2)-C(22)-H(222)	109.5
C(31)-S(3)	1.808(3)	H(221)-C(22)-H(222)	109.5
C(31)-H(311)	0.99	S(2)-C(22)-H(223)	109.5
C(31)-H(312)	0.99	H(221)-C(22)-H(223)	109.5
S(3)-C(32)	1.810(3)	H(222)-C(22)-H(223)	109.5
C(32)-H(321)	0.98	B(1)-C(31)-S(3)	115.84(19)
C(32)-H(322)	0.98	B(1)-C(31)-H(311)	108.3
C(32)-H(323)	0.98	S(3)-C(31)-H(311)	108.3
C(41)-C(42)	1.399(4)	B(1)-C(31)-H(312)	108.3
C(41)-C(46)	1.404(4)	S(3)-C(31)-H(312)	108.3
C(42)-C(43)	1.389(5)	H(311)-C(31)-H(312)	107.4
C(42)-H(42)	0.95	C(31)-S(3)-C(32)	99.81(14)
C(43)-C(44)	1.387(5)	S(3)-C(32)-H(321)	109.5
C(43)-H(43)	0.95	S(3)-C(32)-H(322)	109.5
C(44)-C(45)	1.387(5)	H(321)-C(32)-H(322)	109.5
C(44)-H(44)	0.95	S(3)-C(32)-H(323)	109.5
C(45)-C(46)	1.394(4)	H(321)-C(32)-H(323)	109.5
C(45)-H(45)	0.95	H(322)-C(32)-H(323)	109.5
C(46)-H(46)	0.95	C(42)-C(41)-C(46)	114.7(3)
C(5)-W(1)-C(1)	108.70(12)	C(42)-C(41)-B(1)	123.5(3)
C(5)-W(1)-C(3)	109.27(12)	C(46)-C(41)-B(1)	121.8(3)
C(1)-W(1)-C(3)	96.88(11)	C(43)-C(42)-C(41)	122.9(3)
C(5)-W(1)-C(2)	72.71(12)	C(43)-C(42)-H(42)	118.5
C(1)-W(1)-C(2)	36.16(12)	C(41)-C(42)-H(42)	118.5
C(3)-W(1)-C(2)	105.73(11)	C(44)-C(43)-C(42)	120.7(3)
C(5)-W(1)-C(4)	73.66(12)	C(44)-C(43)-H(43)	119.6
C(1)-W(1)-C(4)	108.50(10)	C(42)-C(43)-H(43)	119.6
C(3)-W(1)-C(4)	35.61(12)	C(45)-C(44)-C(43)	118.3(3)
C(2)-W(1)-C(4)	95.17(10)	C(45)-C(44)-H(44)	120.8
C(5)-W(1)-Br(1)	160.01(8)	C(43)-C(44)-H(44)	120.8
C(1)-W(1)-Br(1)	84.29(8)	C(44)-C(45)-C(46)	120.0(3)
C(3)-W(1)-Br(1)	83.31(8)	C(44)-C(45)-H(45)	120.0
C(2)-W(1)-Br(1)	119.87(8)	C(46)-C(45)-H(45)	120.0
C(4)-W(1)-Br(1)	117.50(9)	C(45)-C(46)-C(41)	123.2(3)
S(1)-W(1)-Br(1)	86.113(16)	C(45)-C(46)-H(46)	118.4
		C(41)-C(46)-H(46)	118.4

C(5)-W(1)-S(1)	78.94(8)	C(10)-C(1)-C(2)-C(20)	1.7(8)
C(1)-W(1)-S(1)	168.33(7)	W(1)-C(1)-C(2)-C(20)	-179.6(5)
C(3)-W(1)-S(1)	88.57(8)	C(10)-C(1)-C(2)-W(1)	-178.7(4)
C(2)-W(1)-S(1)	151.12(9)	C(30)-C(3)-C(4)-C(40)	0.8(8)
C(4)-W(1)-S(1)	81.87(7)	W(1)-C(3)-C(4)-C(40)	-177.3(5)
C(5)-W(1)-S(2)	86.78(8)	C(30)-C(3)-C(4)-W(1)	178.1(5)
C(1)-W(1)-S(2)	92.24(7)	C(41)-B(1)-C(11)-S(1)	62.3(2)
C(3)-W(1)-S(2)	157.67(7)	C(31)-B(1)-C(11)-S(1)	-177.86(18)
C(2)-W(1)-S(2)	93.64(7)	C(21)-B(1)-C(11)-S(1)	-61.4(3)
C(4)-W(1)-S(2)	155.00(9)	B(1)-C(11)-S(1)-C(12)	-169.1(2)
S(1)-W(1)-S(2)	79.16(2)	B(1)-C(11)-S(1)-W(1)	78.3(2)
Br(1)-W(1)-S(2)	77.355(17)	C(41)-B(1)-C(21)-S(2)	-146.19(19)
C(1)-C(10)-H(101)	109.5	C(11)-B(1)-C(21)-S(2)	-22.1(3)
C(1)-C(10)-H(102)	109.5	C(31)-B(1)-C(21)-S(2)	90.1(2)
H(101)-C(10)-H(102)	109.5	B(1)-C(21)-S(2)-C(22)	-168.11(18)
C(1)-C(10)-H(103)	109.5	B(1)-C(21)-S(2)-W(1)	81.56(17)
H(101)-C(10)-H(103)	109.5	C(41)-B(1)-C(31)-S(3)	-60.4(3)
H(102)-C(10)-H(103)	109.5	C(11)-B(1)-C(31)-S(3)	-179.29(18)
C(2)-C(1)-C(10)	142.6(3)	C(21)-B(1)-C(31)-S(3)	62.1(3)
C(2)-C(1)-W(1)	73.77(17)	B(1)-C(31)-S(3)-C(32)	-167.5(2)
C(10)-C(1)-W(1)	143.6(2)	C(11)-B(1)-C(41)-C(42)	-143.9(3)
C(1)-C(2)-C(20)	145.0(3)	C(31)-B(1)-C(41)-C(42)	102.5(3)
C(1)-C(2)-W(1)	70.07(17)	C(21)-B(1)-C(41)-C(42)	-19.3(3)
C(20)-C(2)-W(1)	144.9(2)	C(11)-B(1)-C(41)-C(46)	36.5(3)
C(2)-C(20)-H(201)	109.5	C(31)-B(1)-C(41)-C(46)	-77.0(3)
C(2)-C(20)-H(202)	109.5	C(21)-B(1)-C(41)-C(46)	161.2(2)
H(201)-C(20)-H(202)	109.5	C(46)-C(41)-C(42)-C(43)	1.4(4)
C(2)-C(20)-H(203)	109.5	B(1)-C(41)-C(42)-C(43)	-178.1(3)
H(201)-C(20)-H(203)	109.5	C(41)-C(42)-C(43)-C(44)	-0.3(5)
H(202)-C(20)-H(203)	109.5	C(42)-C(43)-C(44)-C(45)	-1.3(5)
C(3)-C(30)-H(301)	109.5	C(43)-C(44)-C(45)-C(46)	1.6(5)
C(3)-C(30)-H(302)	109.5	C(44)-C(45)-C(46)-C(41)	-0.3(5)
H(301)-C(30)-H(302)	109.5	C(42)-C(41)-C(46)-C(45)	-1.1(4)
C(3)-C(30)-H(303)	109.5	B(1)-C(41)-C(46)-C(45)	178.4(3)
H(301)-C(30)-H(303)	109.5		
H(302)-C(30)-H(303)	109.5		

Table 20: Full list of bond lengths (Å) and angles (°) for [W(CO)₂(mt)(PhTt)] (13).

W(1)-C(1)	1.934(2)	C(22)-S(2)-W(1)	116.60(9)
W(1)-C(2)	1.967(2)	C(21)-S(2)-W(1)	110.42(7)
W(1)-N(53)	2.1862(18)	S(2)-C(22)-H(221)	109.5
W(1)-S(1)	2.5920(5)	S(2)-C(22)-H(222)	109.5
W(1)-S(2)	2.5279(5)	H(221)-C(22)-H(222)	109.5
W(1)-S(3)	2.5068(5)	S(2)-C(22)-H(223)	109.5
W(1)-S(5)	2.6098(6)	H(221)-C(22)-H(223)	109.5
C(1)-O(1)	1.176(3)	H(222)-C(22)-H(223)	109.5
C(2)-O(2)	1.160(3)	B(1)-C(31)-S(3)	113.04(13)
B(1)-C(41)	1.640(3)	B(1)-C(31)-H(311)	109.0
B(1)-C(11)	1.653(3)	S(3)-C(31)-H(311)	109.0
B(1)-C(31)	1.656(3)	B(1)-C(31)-H(312)	109.0
B(1)-C(21)	1.665(3)	S(3)-C(31)-H(312)	109.0
C(11)-S(1)	1.818(2)	H(311)-C(31)-H(312)	107.8
C(11)-H(111)	0.99	C(32)-S(3)-C(31)	101.96(11)
C(11)-H(112)	0.99	C(32)-S(3)-W(1)	111.31(8)
S(1)-C(12)	1.811(2)	C(31)-S(3)-W(1)	116.72(6)
C(12)-H(121)	0.98	S(3)-C(32)-H(321)	109.5
C(12)-H(122)	0.98	S(3)-C(32)-H(322)	109.5
C(12)-H(123)	0.98	H(321)-C(32)-H(322)	109.5
C(21)-S(2)	1.8137(19)	S(3)-C(32)-H(323)	109.5
C(21)-H(211)	0.99	H(321)-C(32)-H(323)	109.5
C(21)-H(212)	0.99	H(322)-C(32)-H(323)	109.5
S(2)-C(22)	1.811(2)	C(46)-C(41)-C(42)	115.59(19)
C(22)-H(221)	0.98	C(46)-C(41)-B(1)	120.55(17)
C(22)-H(222)	0.98	C(42)-C(41)-B(1)	123.76(19)

C(22)-H(223)	0.98	C(43)-C(42)-C(41)	122.2(2)
C(31)-S(3)	1.820(2)	C(43)-C(42)-H(42)	118.9
C(31)-H(311)	0.99	C(41)-C(42)-H(42)	118.9
C(31)-H(312)	0.99	C(44)-C(43)-C(42)	120.6(2)
S(3)-C(32)	1.804(2)	C(44)-C(43)-H(43)	119.7
C(32)-H(321)	0.98	C(42)-C(43)-H(43)	119.7
C(32)-H(322)	0.98	C(43)-C(44)-C(45)	118.7(2)
C(32)-H(323)	0.98	C(43)-C(44)-H(44)	120.6
C(41)-C(46)	1.409(3)	C(45)-C(44)-H(44)	120.6
C(41)-C(42)	1.412(3)	C(46)-C(45)-C(44)	120.2(2)
C(42)-C(43)	1.400(3)	C(46)-C(45)-H(45)	119.9
C(42)-H(42)	0.95	C(44)-C(45)-H(45)	119.9
C(43)-C(44)	1.387(4)	C(45)-C(46)-C(41)	122.7(2)
C(43)-H(43)	0.95	C(45)-C(46)-H(46)	118.7
C(44)-C(45)	1.399(3)	C(41)-C(46)-H(46)	118.7
C(44)-H(44)	0.95	C(52)-S(5)-W(1)	77.79(7)
C(45)-C(46)	1.393(3)	C(52)-N(51)-C(55)	106.66(18)
C(45)-H(45)	0.95	C(52)-N(51)-C(56)	126.24(19)
C(46)-H(46)	0.95	C(55)-N(51)-C(56)	127.07(19)
S(5)-C(52)	1.727(2)	N(53)-C(52)-N(51)	110.80(18)
N(51)-C(52)	1.351(3)	N(53)-C(52)-S(5)	114.33(15)
N(51)-C(55)	1.391(3)	N(51)-C(52)-S(5)	134.85(16)
N(51)-C(56)	1.462(3)	C(52)-N(53)-C(54)	107.27(18)
C(52)-N(53)	1.329(3)	C(52)-N(53)-W(1)	103.35(13)
N(53)-C(54)	1.383(3)	C(54)-N(53)-W(1)	148.92(15)
C(54)-C(55)	1.366(3)	C(55)-C(54)-N(53)	108.03(19)
C(54)-H(54)	0.95	C(55)-C(54)-H(54)	126.0
C(55)-H(55)	0.95	N(53)-C(54)-H(54)	126.0
C(56)-H(561)	0.98	C(54)-C(55)-N(51)	107.23(19)
C(56)-H(562)	0.98	C(54)-C(55)-H(55)	126.4
C(56)-H(563)	0.98	N(51)-C(55)-H(55)	126.4
		N(51)-C(56)-H(561)	109.5
C(1)-W(1)-C(2)	73.14(11)	N(51)-C(56)-H(562)	109.5
C(1)-W(1)-N(53)	84.18(8)	H(561)-C(56)-H(562)	109.5
C(2)-W(1)-N(53)	125.91(8)	N(51)-C(56)-H(563)	109.5
C(1)-W(1)-S(3)	86.49(7)	H(561)-C(56)-H(563)	109.5
C(2)-W(1)-S(3)	140.49(7)	H(562)-C(56)-H(563)	109.5
N(53)-W(1)-S(3)	83.67(5)		
C(1)-W(1)-S(2)	103.00(7)	C(41)-B(1)-C(11)-S(1)	-146.09(13)
C(2)-W(1)-S(2)	76.41(7)	C(31)-B(1)-C(11)-S(1)	94.17(16)
N(53)-W(1)-S(2)	157.60(5)	C(21)-B(1)-C(11)-S(1)	-27.04(19)
S(3)-W(1)-S(2)	75.746(16)	B(1)-C(11)-S(1)-C(12)	-165.56(14)
C(1)-W(1)-S(1)	167.11(7)	B(1)-C(11)-S(1)-W(1)	-48.89(14)
C(2)-W(1)-S(1)	119.26(8)	C(41)-B(1)-C(21)-S(2)	-147.47(13)
N(53)-W(1)-S(1)	85.19(5)	C(11)-B(1)-C(21)-S(2)	90.59(16)
S(3)-W(1)-S(1)	85.107(17)	C(31)-B(1)-C(21)-S(2)	-30.7(2)
S(2)-W(1)-S(1)	84.366(17)	B(1)-C(21)-S(2)-C(22)	-177.22(15)
C(1)-W(1)-S(5)	102.33(7)	B(1)-C(21)-S(2)-W(1)	-53.10(14)
C(2)-W(1)-S(5)	73.47(7)	C(41)-B(1)-C(31)-S(3)	-164.12(14)
N(53)-W(1)-S(5)	64.28(5)	C(11)-B(1)-C(31)-S(3)	-42.42(19)
S(3)-W(1)-S(5)	145.264(17)	C(21)-B(1)-C(31)-S(3)	80.25(18)
S(2)-W(1)-S(5)	132.492(16)	B(1)-C(31)-S(3)-C(32)	-155.41(15)
S(1)-W(1)-S(5)	79.461(17)	B(1)-C(31)-S(3)-W(1)	-33.91(16)
O(1)-C(1)-W(1)	176.0(2)	C(11)-B(1)-C(41)-C(46)	-158.17(19)
O(2)-C(2)-W(1)	175.2(3)	C(31)-B(1)-C(41)-C(46)	-37.7(3)
C(41)-B(1)-C(11)	111.46(16)	C(21)-B(1)-C(41)-C(46)	79.7(2)
C(41)-B(1)-C(31)	108.25(16)	C(11)-B(1)-C(41)-C(42)	25.7(3)
C(11)-B(1)-C(31)	109.50(16)	C(31)-B(1)-C(41)-C(42)	146.16(19)
C(41)-B(1)-C(21)	106.52(16)	C(21)-B(1)-C(41)-C(42)	-96.4(2)
C(11)-B(1)-C(21)	111.73(16)	C(46)-C(41)-C(42)-C(43)	-1.3(3)
C(31)-B(1)-C(21)	109.27(15)	B(1)-C(41)-C(42)-C(43)	175.01(19)
B(1)-C(11)-S(1)	112.88(13)	C(41)-C(42)-C(43)-C(44)	0.6(3)
B(1)-C(11)-H(111)	109.0	C(42)-C(43)-C(44)-C(45)	1.0(3)
S(1)-C(11)-H(111)	109.0	C(43)-C(44)-C(45)-C(46)	-1.8(4)
B(1)-C(11)-H(112)	109.0	C(44)-C(45)-C(46)-C(41)	1.0(4)
S(1)-C(11)-H(112)	109.0	C(42)-C(41)-C(46)-C(45)	0.5(3)
H(111)-C(11)-H(112)	107.8	B(1)-C(41)-C(46)-C(45)	-175.9(2)
C(12)-S(1)-C(11)	99.55(10)	C(55)-N(51)-C(52)-N(53)	-1.1(2)

C(12)-S(1)-W(1)	111.02(7)	C(56)-N(51)-C(52)-N(53)	-179.2(2)
C(11)-S(1)-W(1)	110.07(6)	C(55)-N(51)-C(52)-S(5)	-179.67(18)
S(1)-C(12)-H(121)	109.5	C(56)-N(51)-C(52)-S(5)	2.2(4)
S(1)-C(12)-H(122)	109.5	W(1)-S(5)-C(52)-N(53)	-4.20(13)
H(121)-C(12)-H(122)	109.5	W(1)-S(5)-C(52)-N(51)	174.3(2)
S(1)-C(12)-H(123)	109.5	N(51)-C(52)-N(53)-C(54)	0.8(2)
H(121)-C(12)-H(123)	109.5	S(5)-C(52)-N(53)-C(54)	179.65(14)
H(122)-C(12)-H(123)	109.5	N(51)-C(52)-N(53)-W(1)	-173.84(13)
B(1)-C(21)-S(2)	111.86(12)	S(5)-C(52)-N(53)-W(1)	5.04(16)
B(1)-C(21)-H(211)	109.2	C(52)-N(53)-C(54)-C(55)	-0.1(2)
S(2)-C(21)-H(211)	109.2	W(1)-N(53)-C(54)-C(55)	169.7(2)
B(1)-C(21)-H(212)	109.2	N(53)-C(54)-C(55)-N(51)	-0.6(2)
S(2)-C(21)-H(212)	109.2	C(52)-N(51)-C(55)-C(54)	1.0(2)
H(211)-C(21)-H(212)	107.9	C(56)-N(51)-C(55)-C(54)	179.1(2)
C(22)-S(2)-C(21)	101.23(11)		

Table 21: Selected bond lengths (Å) and angles (°) for [WBr(CO)(η^2 -C₂Ph₂)₂(PhTt-S,S')] (15).

W(1)-C(1)	2.077(4)	C(5)-W(1)-Br(1)	151.99(12)
W(1)-C(2)	2.111(4)	S(1)-W(1)-S(2)	83.15(3)
W(1)-C(3)	2.080(4)	C(2)-W(1)-S(1)	152.65(11)
W(1)-C(4)	2.091(4)	C(3)-W(1)-S(2)	169.36(12)
W(1)-C(5)	2.035(5)	C(4)-W(1)-S(2)	148.45(12)
W(1)-Br(1)	2.6047(5)	C(2)-C(1)-C(101)	140.8(5)
W(1)-S(1)	2.6532(12)	C(1)-C(2)-C(201)	142.0(4)
W(1)-S(2)	2.6501(10)	C(4)-C(3)-C(301)	137.0(4)
C(1)-C(2)	1.303(6)	C(3)-C(4)-C(401)	144.5(4)
C(3)-C(4)	1.313(6)	C(12)-S(1)-C(11)	99.8(2)
C(5)-O(5)	1.135(6)	C(12)-S(1)-W(1)	104.46(16)
C(11)-S(1)	1.811(4)	C(11)-S(1)-W(1)	114.69(14)
S(1)-C(12)	1.810(5)	C(22)-S(2)-C(21)	100.8(2)
C(21)-S(2)	1.815(5)	C(22)-S(2)-W(1)	103.53(16)
S(2)-C(22)	1.810(5)	C(21)-S(2)-W(1)	116.12(15)
C(31)-S(3)	1.815(5)	C(32)-S(3)-C(31)	101.4(2)
S(3)-C(32)	1.810(5)		